INVESTIGATIONS OF DESCRIBING FUNCTION TECHNIQUE

DUNSTAN GRAHAM
LEE GREGOR HOFMANN

SYSTEMS TECHNOLOGY, INC.

FOREWORD

This report was prepared by Systems Technology, Inc., Hawthorne, California under U. S. Air Force Contract AF 33(615)-1474 for the "Investigation and Extension of Describing Function Technique." The work was monitored by the Flight Dynamics Laboratory on Task 821904, "Systems Analysis and Optimization." Mr. David K. Bowser was the technical monitor for the Laboratory.

The studies presented here began 15 January 1964 and were concluded in November 1964. Mr. Dunstan Graham of the Princeton Branch of Systems Technology, Inc. was the project engineer for the Company and a majority of the work was accomplished by the Company's staff in Princeton, New Jersey. Some of the developments in Chapters II and III, however, were carried out by members of the staff in California under the general supervision of Mr. Duane McRuer. Mr. Graham and Mr. McRuer shared responsibility as principal investigators for the planning and execution of the technical aspects of the project.

The authors here gratefully acknowledge the technical contributions to this work of Mr. I. L. Ashkenas, Mr. Charles P. Shortwell, Mr. David H. Weir, Mr. Robert L. Stapleford, Mr. Daniel B. McElwain, and Mr. John J. Best, all of Systems Technology, Inc. Their individual contributions are noted at appropriate points in the text. The typescript was painstakingly composed by Miss Helen Perna.

This report is the final report and concludes the work on Contract No. AF 33(615)-1474.

The manuscript was released by the authors in April 1965 for publication as an RTD Technical Report.

This technical report has been reviewed and is approved.

Charles B. Westbrook

CHARLES B. WESTBROOK
Chief, Control Criteria Branch
Air Force Flight Dynamics Laboratory

ABSTRACT

Three problems were chosen so as to explore some of the apparent limitations of describing function technique for the analysis of nonlinear systems, and to show how the technique might be extended so as to overcome the indicated deficiencies. The problems were a) the effects of stick and valve friction in fully powered, manual aircraft control systems, b) limit cycles in satellite attitude control with off-on jets, and c) the effects of aerodynamic hysteresis in the stability derivatives of tilt-wing VTOL aircraft.

The results indicate that new describing functions can be developed as closed-loop functions provided that specific restrictions are met, that non-sinusoidal, Fourier series describing functions or a generalized periodic input describing function can be successful, but that they are extraordinarily difficult to apply, and that the aerodynamic nonlinearities which were considered are of small practical importance.

CONTENTS

LIST OF ILLUSTRATIONS

CHAPTER I

INTRODUCTION AND SUMMARY

The theory of linear control system analysis is a beautiful structure, both elaborate and complete. Unfortunately, however, many engineering problems must be stated so as to account for nonlinear phenomena. In these cases, there is no workable general theory. Nevertheless, there are a very large number of "methods" which allow more or less approximate answers to the most pressing questions of design. But the bewildering variety of methods makes it difficult to select the one or two most likely to yield useful results and to distinguish that which is important from that which is merely interesting.

Confusion is compounded when several approximate methods give quite different answers to the same problem or, equally, when there is no alternative to a single method which might serve as a basis for comparison. With an embarrassment of riches, or dirt-poor, the analyst is in the uncomfortable position of being unable to satisfy himself that he understands the dynamic behavior of the system. Since any failure on his part to discover the secrets of the mechanism can lead to the most unpleasant surprises for its builders or users, it is a matter of surpassing importance to know where and how to use the several methods.

While there have been a number of earnest attempts to describe and compare the various engineering methods of nonlinear control system analysis (Refs. 1, 2, 3 among others), both the study and physical synthesis of nonlinear control systems are still in a distressingly unsatisfactory state. This is in spite of a large amount of applied research accomplished each year and the continuing development of new methods. One still promising concept, however, is the general idea of quasi-linearization (Refs. 1, 2, 3, 4, 5, 6). Quasi-linearization leads directly to the development of describing functions, and these have repeatedly been shown to have an outstanding utilitarian value in the analysis of nonlinear systems.

In order to characterize a system element in terms of cause and effect relationships, the analyst requires a "mathematical model" which responds to a given input in a fashion which closely approximates the response of the actual physical element. It is, of course, well known that for systems or elements described by linear, constant-coefficient equations, the weighting

function or its Laplace transform, the transfer function, allows the analyst to predict the response to any input. The system or element is thus described mathematically as an entity which is independent of both the input and response.

In a nonlinear system, on the other hand, some of the system parameters depend upon the values of the dependent variables which define the system's response. In this case, the system cannot be characterized as a separate entity and the behavior of the system is a function of particular inputs and initial conditions. In spite of this, in a great many nonlinear systems of interest, specific input-response pairs appear to be similar to input-response pairs for linear systems. This similarity most strongly suggests that the performance of nonlinear elements, for certain inputs, can be divided into two parts:

1. The response of a linear element driven by the particular input.

2. An additional quantity called the remnant.

This general idea leads to the concept of quasi-linearization, which emphasizes the similarities, rather than the differences, between linear and nonlinear systems. A quasi-linear system is one in which the relationships between pertinent measures of system input and output signals are linear in spite of the existence of nonlinear elements. The quasi-linear system is an exact representation of the nonlinear system for specific inputs.

A particular quasi-linear system is found from the actual nonlinear input-system combination by replacing the nonlinear elements with "equivalent" linear elements characterized mathematically by describing functions and remnants. Each equivalent linear element is derived from consideration of the response of the corresponding nonlinear element to a specific input. The new linear system has the same response to the input in question as the original nonlinear system. If only an appropriate quasi-linear system can be found, the analysis problem is easily solved.

Describing Function Technique

In principle, the partition of an output response into two components, one linearly connected with the input and the other a remnant, can be accomplished for almost any combination of nonlinear elements and inputs. In actual systems,

however, interest is centered upon the system as a whole, and not on its constituent elements. Consequently, the fact that a quasi-linear equivalent can be found for a particular nonlinear element is of very little value unless this knowledge can be converted into a precise, or usefully approximate, quasi-linear system model. The difficulties encountered here stem from the presence of feedback loops within the system. The actual input signal to a particular nonlinear element is required in order to construct the quasi-linear representation for the element. Because of the feedbacks, the input to the nonlinear element can only be found by solving for the system response. Since this was the problem in the first place, little would appear to be gained by knowing the quasi-linear description of a given nonlinear element excited by a particular input signal.

In some cases, however, the signals existing within the system at the inputs to the nonlinearities are, in fact, exactly the ones for which quasi-linear element representations are easily found. In these fortunate circumstances, the quasi-linear representation for the nonlinear elements can be substituted for the actual elements to obtain an exact linear representation of the nonlinear input-system combination. In many other cases, the signals at the inputs to the nonlinearities are quite similar to the ones for which describing functions and remnants are known or can be found. Then the quasi-linear representations of the nonlinear elements are substituted for the actual nonlinearities in order to obtain a close first approximation to the quasi-linear system. This process is often identified as the describing function technique, but a more sophisticated view is that describing function technique is the means of developing a quasi-linear system at any suitable level of approximation.

Describing function technique becomes useful when:

1. It can be generalized for a whole category or class of inputs.
2. When it can be shown that the describing function of a given nonlinear element is unique, i.e. the describing function does not depend on the system of which the nonlinearity is a part.
3. When it can be shown, or at least believed, that the effect of the remnant on the input to the nonlinear element is negligible.

Under these circumstances, it is possible to develop a practical catalog of nonlinear element, input-response pairs in terms of describing functions, and

the describing functions act as linear operators. Then, by means of linear analysis, the performance of an approximate (or very rarely an accurate) quasi-linear system may be quickly found, and the analyst can expect congratulations.

Varieties of Describing Functions

In the light of the discussion above, it may be readily appreciated that there is a tremendous variety of potentially useful describing functions. Since, for any given nonlinearity, there is a describing function appropriate to each input, and since, in a feedback system, the input to the nonlinearity depends both on the input to the system and the action of the entire system in producing the response, so that the input to the nonlinearity depends on its place in and function with respect to the system; while, in addition, it is possible to define the "equivalent linear element" in several suitable ways; there is something like a triple infinity of all possible describing functions. Only a very few of these have been developed to any extent whatever. Naturally, the ones which have received the most attention are the ones which lead most rapidly and easily to practical quasi-linear systems.

Corresponding to the three main categories of test input functions which are employed in linear analysis, there are three main types of describing functions:

1. Transient (actually step) input describing functions.
2. Periodic (usually sinusoidal) input describing functions.
3. Stationary random input describing functions.

Transient input describing functions are of more conceptual than practical interest. They cannot be developed in as general and as satisfactory a form as the others. In truth, consideration of Chen's paper (Ref. 4) shows how quickly the analyst is confounded by the fact that both describing function and remnant are determined to a large extent by the system rather than by the nonlinearity itself. Thus, while it may well be advantageous to use Chen's methods to construct a quasi-linear system for a transient input problem, the result cannot be generalized and it is impossible to tabulate transient input describing functions for particular nonlinearities.

Sinusoidal input describing functions have been quite thoroughly explored for many, but by no means all, interesting definitions of equivalence and

nonlinearities (Vide Refs. 1 and 3.) They have a surpassing importance in the analysis of nonlinear control systems because they are particularly amenable to the determination of oscillatory stability. It has been repeatedly shown that their use often produces good results with a modicum of effort. Furthermore, the use of sinusoidal input describing functions permits the extension to nonlinear control systems of the well-known harmonic or frequency response method of designing equalizing or compensating networks. This is a tremendous and almost unique advantage. Remnant data, however, are notably lacking in many cases. Only Graham and McRuer (Ref. 1) and Ogata (Ref. 5) seem to have concerned themselves specifically with the use of the remnant to construct second or higher approximation quasi-linear systems.

Finally, the stationary random input describing functions can be developed in a fairly general way if the input has a Gaussian amplitude distribution and the effect of the nonlinear element on the performance of the system is not too large. The real significance of random input describing function analysis where these conditions are not met is not well understood. In particular, the effect of the remnant on the performance of the system has not been thoroughly evaluated. Under favorable circumstances, when the describing functions have been formulated analytically, or measured experimentally, the Gaussian, random input describing function may be employed to predict the response and accuracy of the system under dynamic conditions, but examples of such calculations are comparatively rare.

Extension of Describing Function Technique

With the view that describing function technique is the means of developing a quasi-linear system at a suitable level of approximation, and recognizing that, as in all nonlinear analysis, the choice of the best means depends on the particular problem, it was thought that the most profitable extensions of describing function technique would derive from realistic endeavors to develop new or more accurate quasi-linear systems.

The research reported here revolved around an attempt to formulate and analyze selected quasi-linear systems. Preference was accorded to two types of problems.

1. Systems with periodic outputs in which it was known or suspected that conventional first approximation sinusoidal describing function analysis had failed.
2. Systems with random inputs.

The choices were made so as to have direct relevance to flight control problems of modern aerospace vehicles.

Summary of the Report

There is explored, in Chapter II, a technique for building new sinusoidal describing functions for system elements with internal feedback paths. A manual control system for a high performance airplane is used as an example. It is shown that the technique may work, but that the restriction that the effect of the remnant be negligible at the input to the nonlinearity must be observed. This analysis sharpens our understanding of the use of sinusoidal input describing functions.

Consideration of reaction jet control of satellite attitude suggests a means of developing a generalized describing function for system with periodic outputs. We attempted to apply the generalized describing function concept to this problem. Because of the peculiar nature of the problem, however, the results were less than completely satisfactory, but it may very well be that the method will enjoy more success in connection with more tractable systems. A discussion of the method together with suggestions for its use is contained in Chapter III.

A mathematical study of pilot control of a VTOL aircraft configuration with prominent aerodynamic nonlinearities is set forth in Chapter IV. The study illustrates the use of the random input describing function for hysteresis, but the results were not very dramatic. It turned out that pilot control of the vehicle motions suppressed the effect of the nonlinearities and that such effect as they did have was, on the whole beneficial. This result was somewhat surprising.

CHAPTER II

BUILDING SINUSOIDAL DESCRIBING FUNCTIONS

Describing function technique is most often an approximate method of analysis. It is, therefore, important to explore the limitations on its use. The analysis of particular nonlinear flight control systems, with careful attention to the processes of quasi-linearization and the effect of the remnant, would seem likely to indicate techniques which might find more general application. This would be especially true in those cases where the results of the describing function analysis could be compared to other analytical or experimental results. Among the problems selected for detailed study, with these objectives in mind, were the effects of Coulomb friction in the manually controlled valve of a fully powered aircraft surface actuator, and the effects of Coulomb friction in a non-compliant aircraft control system linkage. The generally deleterious effects of valve and control system friction are described in the survey article by Glenn (Ref. 7). Our interest, however, and the motivation for applying describing function technique lies in the fact that control system nonlinearities may play a surpassingly important role in the development and sustentation of pilot induced oscillations (Refs. 8 and 9). These oscillations typically are, in fact, limit cycles of the pilot vehicle system, and as such they may be amenable to analysis by means of quasi-linearization about a condition of periodic oscillation.

The describing functions chosen for study, besides being of practical importance in themselves, illustrate a technique for building up the describing functions of complex system elements, by means of block diagram algebra, from the describing functions of simple elements. This technique is obviously capable of handling problems other than the ones to which it has been applied.

Valve and Stick Friction

Figure 2-1 shows schematically a typical aircraft control system including a fully powered hydraulic actuator. Friction, of course, acts in the bearings of the control linkage and may also act at points such as fairleads which are not illustrated. In addition to friction in the linkage; friction acts to restrain the valve. (The friction here is primarily generated at the seal

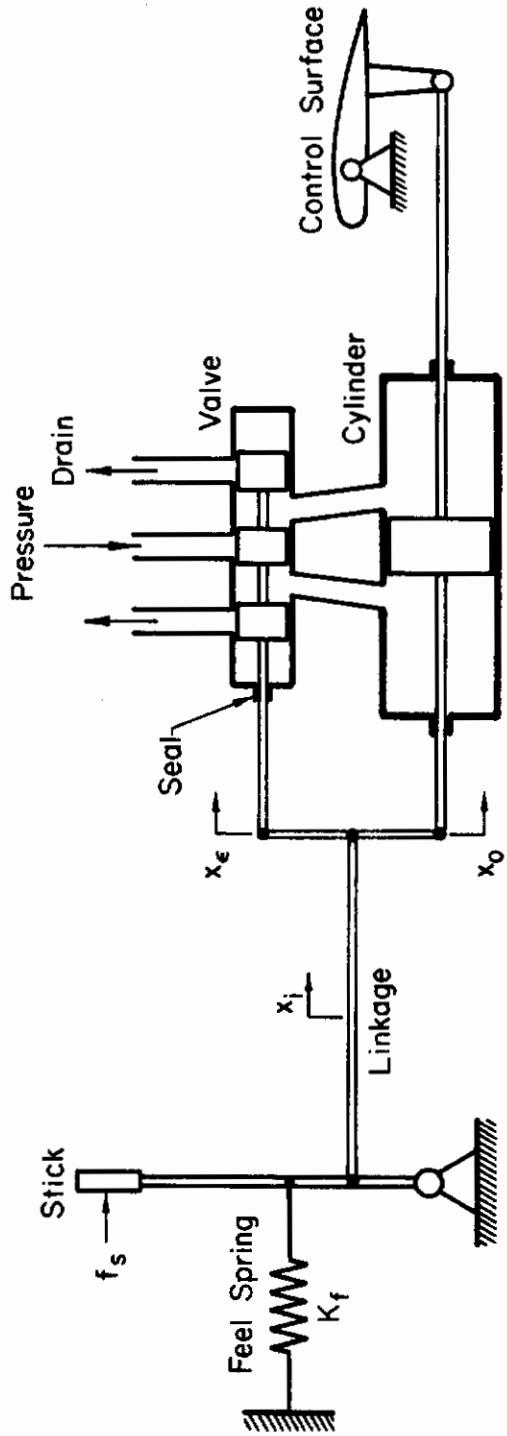

Figure 2-1. Aircraft Control System Schematic

rather than, for example, between the lands of the spool and the valve housing.)

We assume in both cases that the friction is Coulomb friction, i.e. the friction opposes velocity and is independent of speed as long as a motion exists. When there is no motion, it should be apparent from physical considerations that the friction force must exactly oppose and balance the applied force. This characteristic is illustrated in Figure 2-2. We neglect the well

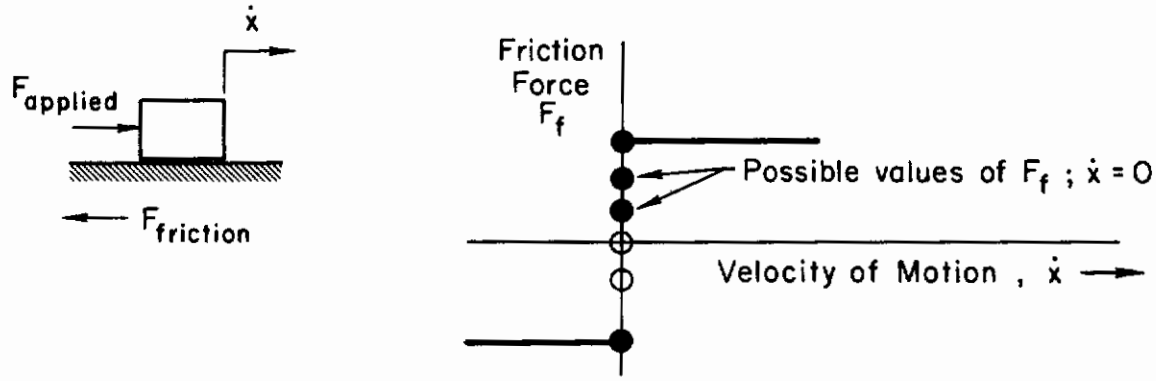

Figure 2-2. Coulomb Friction

known fact that the starting friction (stiction) may exceed the running friction and we assume, in this case, that starting and running friction have the same value.

For the purposes of the analysis we shall consider first valve friction acting alone, and then stick friction acting alone.

Ashkenas (Ref. 10) carried out the particular approximate analysis of the effect of valve friction which follows. It was not published partly because of some skepticism (even on the part of the author) concerning the validity of the assumption on which the analysis was based, but, at the same time, it was always considered to be an intriguing example of a technique for building complex describing functions from simple ones. We shall see later that the questionable assumptions can be justified in this case. The same type of analysis, however, is inappropriate and misleading in the seemingly closely related problem of stick or linkage friction. Understanding of the careful distinction which must be drawn between these two cases is helpful in es-

tablishing some of the limits on the validity of sinusoidal describing functions in general, and of the "building" technique in particular.

Approximate Analysis of Valve Friction

Assume the system to be represented by the schematic diagram of Figure 1. Under suitable assumptions (Ref. 11), the actuator can be considered to be a first order servomechanism whose actuating signal x_ϵ, is (proportional to) the difference between the control linkage displacement, x_i, and the actuator output, x_o. The inertial reaction and any viscous friction forces in the control linkage are assumed negligible compared to the applied stick force, f_s, and the force supplied by the feel spring, $K_f\ x_i$. Then, with all the forces reflected to the stick, the system may be represented by the block diagram of Figure 2-3. The effect of valve friction is included by assuming that a Coulomb friction force F_f sgn $\dot{x}_\epsilon$ is reflected at the stick grip. Note that in the block diagram this requires a differentiator acting on the difference between the servo input and output signals, followed by a sgn function nonlinear block. (Note further that the gains inherent in the adding linkage have been taken to be unity.)

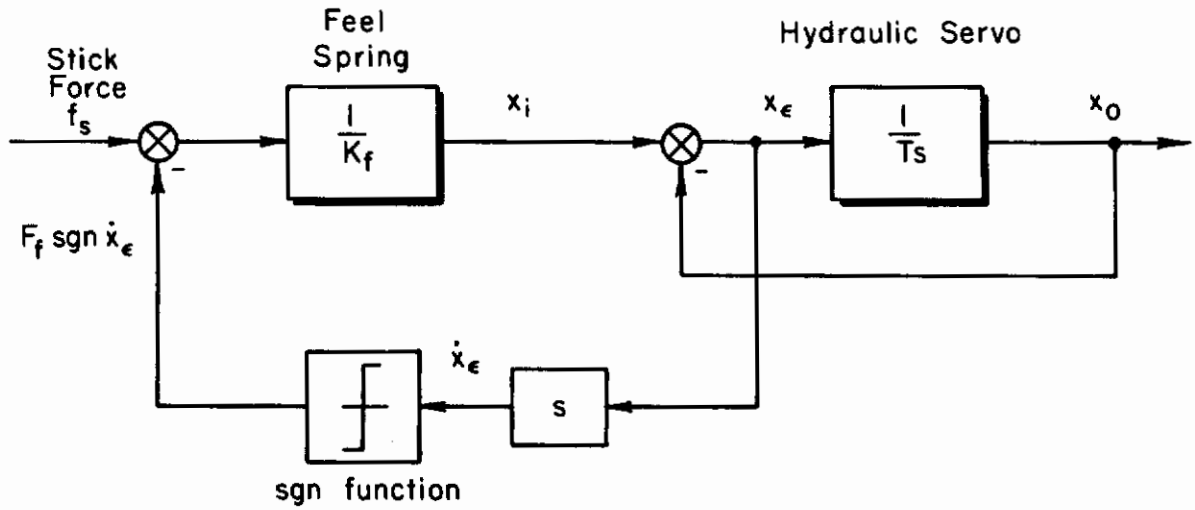

Figure 2-3. Block Diagram — Aircraft Control System with Valve Friction

Summing the forces acting on the stick:

$$+ f_s - K_f x_i - F_f \operatorname{sgn} \dot{x}_\epsilon = 0 \qquad (2\text{-}1)$$

We are interested in the case in which $f_s(t) = F_s \sin \omega_s t$ and the system is undergoing a periodic oscillation. In this case, representation of Coulomb friction by an "equivalent" viscous friction has a history which antedates describing function analysis as such (Ref. 12). Nevertheless, since we have been taught that the success of describing function analysis is likely to be dependent on the attenuation of the remnant (higher harmonics) by integrations in the control loop, we perhaps should be uneasy about applying describing function analysis here where we have a differentiator in the loop. (The differentiator certainly will accentuate the higher harmonics.) If, however, we overcome our reluctance and barge ahead, we may assume that x_ϵ is a sinusoidal signal and that $F_f \operatorname{sgn} \dot{x}_\epsilon$ can be adequately approximated by the first harmonic component of the Fourier series for the square wave which is the friction force. A sinusoidal $\dot{x}_\epsilon$, and the friction force are illustrated in Figure 2-4. The coefficient for the first term of the Fourier series for the square wave,

$F_f \operatorname{sgn} \dot{x}_\epsilon = \frac{4F_f}{\pi}\left[\sin \omega t + \frac{\sin 3\omega t}{3} + \ldots\right]$, is $4F_f/\pi$, and the amplitude ratio or

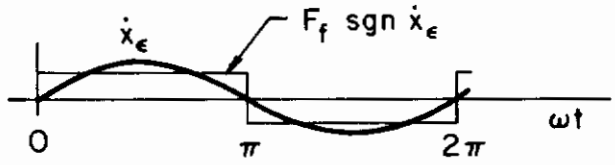

Figure 2-4. Assumed Waveforms

equivalent gain of linearity is $4F_f/\pi(\dot{x}_\epsilon)_{max}$. From the block diagram of Figure 2-3, replacing the nonlinear block by its equivalent gain

$$\left[F_s - \frac{4F_f}{\pi(\dot{x}_\epsilon)_{max}} s(X_i - X_0)\right] = K_f X_i \qquad (2\text{-}2)$$

or

$$F_s = K_f X_i + \frac{4F_f}{\pi(\dot{x}_\epsilon)_{max}} s(X_i - X_0)$$

but

$$\frac{X_0}{X_i} = \frac{1/Ts}{1+1/Ts} = \frac{1}{Ts+1} \tag{2-3}$$

or

$$X_i = (Ts + 1)\, X_0$$

therefore

$$F_s = \left[K_f(Ts + 1) + \frac{4F_f}{\pi(\dot{x}_\epsilon)_{max}}\, s(Ts + 1 - 1) \right] X_0$$

or

$$\frac{X_0}{F_s} = \frac{1}{K_f\left[\left(\frac{4F_fT}{K_f\pi(\dot{x}_\epsilon)_{max}}\right) s^2 + Ts + 1\right]} \tag{2-4}$$

$$= \frac{1/K_f}{\frac{s^2}{\omega_a^2} + Ts + 1}$$

where

$$\omega_a^2 = \frac{K_f\pi(\dot{x}_\epsilon)_{max}}{4F_fT}$$

Now for $f_s(t) = F_s \sin \omega t$, $F_s(s) = \frac{F_s\, \omega_s}{s^2+\omega_s^2}$

then

$$X_0(s) = \frac{F_s\omega_s}{K_f} \frac{1}{(s^2+\omega_s^2)\left(\frac{s^2}{\omega_a^2} + Ts + 1\right)}$$

and

$$X_\epsilon(s) = X_i(s) - X_0(s) = (Ts + 1 - 1)\, X_0(s)$$

$$= \frac{F_s \omega_s \omega_a^2 Ts}{K_f(s^2+\omega_s^2)\ (s^2+\omega_a^2\ Ts + \omega_a^2)} \qquad (2\text{-}5)$$

Inverse transforming, using pair 1.359 of the table in Ref. 13, retaining only the steady state component

$$x_\epsilon(t) = \frac{F_s \omega_s \omega_a^2 T}{K_f}\ \frac{1}{\omega_s}\left[\frac{\omega_s^2}{(\omega_a^2 - \omega_s^2)^2 + \omega_s^2 T^2 \omega_a^4}\right]^{1/2} \sin(\omega_s t + \psi_1) \qquad (2\text{-}6)$$

so that

$$(\dot{x}_\epsilon)_{max} = \frac{F_s \omega_s^2 \omega_a^2 T}{K_f \sqrt{(\omega_a^2 - \omega_s^2)^2 + \omega_s^2 T^2 \omega_a^4}} \qquad (2\text{-}7)$$

but

$$\omega_a^2 = \frac{\pi K_f}{4TF_f}\ (\dot{x}_\epsilon)_{max} = \frac{\pi F_s \omega_s^2 \omega_a^2}{4F_f \omega_a^2 \sqrt{\left[1 - \left(\frac{\omega_s}{\omega_a}\right)^2\right]^2 + T^2\omega_s^2}} \qquad (2\text{-}8)$$

or:

$$\omega_a^4 \left\{\left[1 - \left(\frac{\omega_s}{\omega_a}\right)^2\right]^2 + T^2\omega_s^2\right\} = \left(\frac{\pi}{4}\frac{F_s}{F_f}\right)^2 \omega_s^4 \qquad (2\text{-}9)$$

Expanding the left hand side

$$\omega_a^4 - 2\omega_a^2\omega_s^2 + \omega_s^4 + T^2\omega_s^2\omega_a^4 = \left(\frac{\pi}{4}\frac{F_s}{F_f}\right)^2 \omega_s^4$$

and rearranging terms:

$$\omega_a^4(1 + T^2\omega_s^2) - 2\omega_a^2\omega_s^2 + \omega_s^4\left[1 - \left(\frac{\pi}{4}\frac{F_s}{F_f}\right)^2\right] = 0 \qquad (2\text{-}10)$$

Now for modern flight control system actuators, typically $T \leq 0.05$ secs., and considering pilot induced oscillations, $\omega_s \leq 2\pi \text{ sec}^{-1}$, so $T^2\omega_s^2 \ll 1$.* Then:

$$\omega_s^2 \doteq \frac{2\omega_a^2 \pm \sqrt{4\omega_a^4 - 4\omega_a^4\left[1 - \left(\frac{\pi}{4}\frac{F_s}{F_f}\right)^2\right]}}{2\left[1 - \left(\frac{\pi}{4}\frac{F_s}{F_f}\right)^2\right]}$$

$$= \frac{\omega_a^2 \pm \omega_a^2\sqrt{1 - 1 + \left(\frac{\pi}{4}\frac{F_s}{F_f}\right)^2}}{1 - \left(\frac{\pi}{4}\frac{F_s}{F_f}\right)^2} = \frac{\omega_a^2\left(1 \pm \frac{\pi F_s}{4F_f}\right)}{1 - \left(\frac{\pi}{4}\frac{F_s}{F_f}\right)^2} \qquad (2\text{-}11)$$

$$= \frac{\omega_a^2}{1 \mp \left(\frac{\pi}{4}\frac{F_s}{F_f}\right)}$$

Now since $(\pi F_s/4F_f)$ can be greater than 1, but ω_s^2 must be positive we retain only the positive sign.

Substituting the expression

$$\omega_a^2 = \omega_s^2\left[1 + \frac{\pi}{4}\frac{F_s}{F_f}\right]$$

in Eq. 2-4:

$$\frac{X_0}{F_s} = \frac{1/K_f}{\frac{s^2}{\omega_s^2\left[1 + \frac{\pi}{4}\frac{F_s}{F_f}\right]} + Ts + 1} \qquad (2\text{-}12)$$

*This assumption is not necessary and is made only for convenience in carrying out the algebra. We may still solve for the describing function without it, but the expressions are messy and less instructive.

and evaluating the describing function at the frequency $\omega = \omega_s$, so that $s = j\omega_s$, $s^2 = -\omega_s^2$

$$\frac{X_0}{F_s} = \frac{1/K_f}{T j\omega_s + 1 - \dfrac{1}{1 + \left(\dfrac{\pi}{4}\dfrac{F_s}{F_f}\right)}} = \frac{1/K_f}{T j\omega_s + \dfrac{\left(\dfrac{\pi}{4}\dfrac{F_s}{F_f}\right)}{1 + \left(\dfrac{\pi}{4}\dfrac{F_s}{F_f}\right)}}$$

$$\frac{X_0}{F_s} = \frac{1}{K_f} \frac{1 + \left(\dfrac{\pi}{4}\dfrac{F_s}{F_f}\right)}{\left(\dfrac{\pi}{4}\dfrac{F_s}{F_f}\right)} \frac{1}{\dfrac{1 + \left(\dfrac{\pi}{4}\dfrac{F_s}{F_f}\right)}{\left(\dfrac{\pi}{4}\dfrac{F_s}{F_f}\right)} T j\omega_s + 1}$$

$$= \frac{1}{K_f}\left\{1 + \left(\frac{4}{\pi}\frac{F_f}{F_s}\right)\right\} \frac{1}{\left(1 + \dfrac{4}{\pi}\dfrac{F_f}{F_s}\right) T j\omega_s + 1} \qquad (2\text{-}13)$$

or, with $T^2\omega_s^2 \ll 1$ and also $\dfrac{F_f}{F_s} < 1$ (or there would be no motion):

$$\left|\frac{X_0}{F_s}\right| \doteq \frac{1}{K_f}\left(1 + \frac{4}{\pi}\frac{F_f}{F_s}\right) ; \angle\left(\frac{X_0}{F_s}\right) \doteq -\tan^{-1}\omega_s T\left(1 + \frac{4}{\pi}\frac{F_f}{F_s}\right)$$

The closed loop sinusoidal describing function for the manual control system with valve friction shows that both gain and time constant (phase lag) are augmented by the factor $\left(1 + \dfrac{4}{\pi}\dfrac{F_f}{F_s}\right)$. The effect of friction on the performance of the system in both respects is destabilizing. We might therefore expect this describing function to be of some usefulness and importance in establishing the conditions for a pilot-vehicle oscillation.

It is worth remarking that this describing function is one of very few interesting, frequency-dependent, describing functions. Others, obtained in the same way, would not have sine wave inputs in most practical cases.

Extension to the Case of Stick Friction

Emboldened by the possible success of the analysis given above, it is tempting to apply the same technique to the calculation of a describing function for the case of stick friction acting alone and to the calculation of a describing function for valve and stick friction acting together. There is no impediment to doing this, although as it turns out there may be no very good reason for doing so.

Consider the situation in which stick friction acts alone. Again it is assumed that inertial reaction and viscous friction forces in the control system are negligible compared to the applied force and the feel spring force. The control system is assumed to have no compliance. Then the portion of the system of concern can be represented by the block diagram of Figure 2-5.

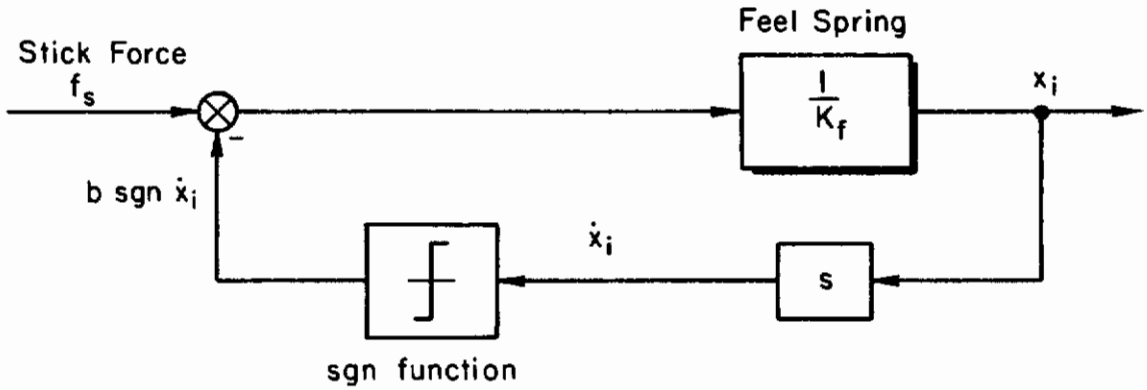

Figure 2-5. Block Diagram — Control Stick with Linkage Bearing Friction

Again, assuming the signal $\dot{x}_i$ to be sinusoidal, and replacing the nonlinear Coulomb friction block by an "equivalent" gain $4b/\pi(\dot{x}_i)_{max}$, the closed loop describing function can be written by inspection:

$$\frac{X_i}{F_s} = \frac{1/K_f}{1 + \frac{1}{K_f}\frac{4}{\pi}\frac{b}{(\dot{x}_i)_{max}}\,s} \qquad (2\text{-}14)$$

Let $\tau = \frac{1}{K_f} \frac{4}{\pi} \frac{b}{(\dot{x}_i)_{max}}$, then

$$\frac{\dot{X}_i}{F_s} = \frac{1}{K_f} \frac{s}{1 + \tau s}$$

and evaluating this describing function at $s = j\omega_s$

$$\frac{\dot{X}_i}{F_s} (j\omega_s) = \frac{1}{K_f} \frac{j\omega_s}{1 + \tau j\omega_s}$$

and

$$\left|\dot{X}_i(j\omega_s)\right| = (\dot{x}_i)_{max} = \frac{F_s}{K_f} \left[\frac{\omega_s}{\sqrt{1 + \tau^2 \omega_s^2}} \right]$$

$$(\dot{x}_i)^2_{max} (1 + \tau^2 \omega_s^2) = \left(\frac{F_s}{K_f} \omega_s \right)^2$$

$$(\dot{x}_i)^2_{max} + \left(\frac{4b}{K_f \pi}\right)^2 \omega_s^2 = \left(\frac{F_s \omega_s}{K_f} \right)^2$$

Therefore

$$(\dot{x}_i)_{max} = \frac{F_s \omega_s}{K_f} \sqrt{1 - \left(\frac{4b}{\pi F_s} \right)^2} \qquad (2\text{-}15)$$

Substituting this result in Eq. 2-14:

$$\frac{X_i}{F_s} = \frac{1/K_f}{1 + \left(\frac{4}{\pi} \frac{b}{F_s \omega_s} \right) \frac{1}{\sqrt{1 - \left(\frac{4b}{\pi F_s} \right)^2}} s}$$

$$\frac{X_i}{F_s} = \frac{1/K_f}{1 + \frac{s}{\omega_s}\frac{1}{\sqrt{\left(\frac{\pi F_s}{4b}\right)^2 - 1}}} \tag{2-16}$$

Then evaluating this closed loop describing function at $s = j\omega_s$:

$$\frac{X_i}{F_s} = \frac{1/K_f}{1 + j\frac{1}{\sqrt{\left(\frac{\pi F_s}{4b}\right)^2 - 1}}} \tag{2-17}$$

or

$$\left|\frac{X_i}{F_s}\right| = \frac{1}{K_f}\sqrt{1 - \left(\frac{4b}{\pi F_s}\right)^2}$$

$$\measuredangle\left(\frac{X_i}{F_s}\right) = -\tan^{-1}\frac{\left(\frac{4b}{\pi F_s}\right)}{\sqrt{1 - \left(\frac{4b}{\pi F_s}\right)^2}}$$

A Contradiction

The describing function for stick friction (Eq. 2-17) can be compared to the describing function for mechanical hysteresis which represents the "actual" case. Consider the abstraction of Figure 2-6.

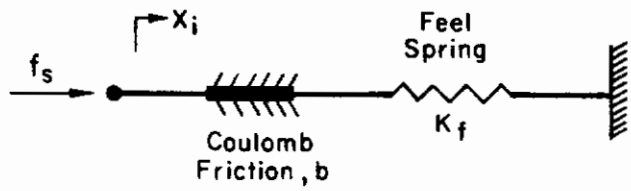

Figure 2-6. Abstraction of Control System with Linkage Bearing Friction

If a sinusoidal force, f_s, is applied: the linkage will not begin to move until $f_s > b$, the Coulomb friction force. Then the deflection of the feel spring will be $(f_s - b)/K_f$. After f_s reaches its maximum value and begins to decrease, the linkage will stand still while the friction force builds up in the opposite direction until the magnitude of the spring force, $K_f\, x_{i_{max}}$, exceeds $f_s + b$. With f_s now decreasing further, the linkage will move in the negative x_i direction until f_s reaches its maximum negative value. The linkage will then "stick" again. The process then repeats itself with alternate negative and positive half cycles. The first two half-cycles of the motion are shown in Figure 2-7. The wave form of $\dot{x}_i$ is also shown.

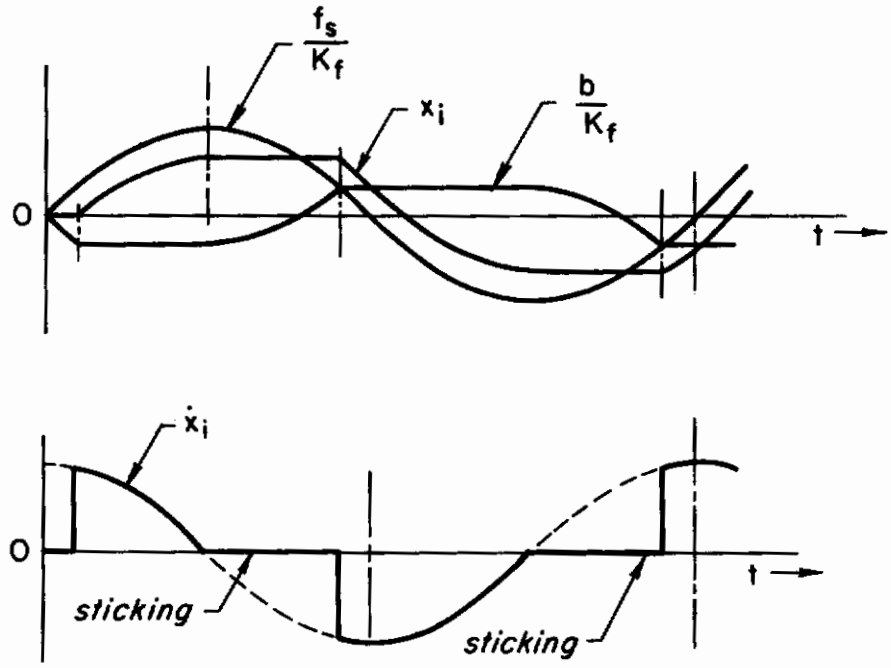

Figure 2-7. Waveforms in Linkage with Bearing Friction

$\dot{x}_i = \frac{d}{dt}\left[(f_s - b)/K_f\right]$ and the condition $\dot{x}_i = 0$ defines the "sticking."

Now the sinusoidal describing function between f_s and X_i, in this case, is well known. It is given, for example, by Ref. 1 and with suitable changes in notation it can be expressed:

$$\left|\frac{X_i}{F_s}\right| = \frac{1}{K_f \pi}\sqrt{1 - u^2 + \left(\frac{3\pi}{2} - \sin^{-1}u\right)^2 + 2u\left(\frac{3\pi}{2} - \sin^{-1}u\right)\sqrt{1 - u^2}}$$

$$\measuredangle\left(\frac{X_i}{F_s}\right) = \tan^{-1}\frac{u^2 - 1}{\left[\frac{3\pi}{2} - \sin^{-1}u + u\sqrt{1 - u^2}\right]} \qquad (2\text{-}18)$$

where

$$u = 1 - 2\left(\frac{b}{F_s}\right) \text{ ; when } u = 0 \text{ take } \sin^{-1} u = \pi$$

A graphical comparison of the describing functions of Eqs. 2-17 and 2-18 is presented on the gain-phase plane in Figure 2-8. It may be seen there that the approximate analysis does not compare very favorably with the describing function for mechanical hysteresis. The approximation over-estimates the lagging phase angle and underestimates the attenuation provided by Coulomb friction in the control system linkage. It might be argued, however, that the approximation is "conservative" in that it will tend to show the onset of instability sooner than would "actually" be the case. A typical airplane short period transfer function for the loop closure between pitch angle, θ, and elevator deflection, δ_e, is also shown in Figure 2-8. An intersection of this "locus of linear elements," for the value of gain which is illustrated, with the approximate describing function indicates a limit cycle (Ref. 1). In "actuality" there is not much danger that it will occur. This is all the more the case since it is common practice to preload the control system so as to mask the effect of friction and to provide for a return of the stick to the trim position in spite of the effect of Coulomb friction in the control linkage. A very marked attenuation of the describing function for preload with friction makes a pilot-vehicle oscillation, from this cause, quite improbable. (The describing function for preload and friction is also illustrated on the gain-phase plane in Figure 2-8.) It can, therefore, be appreciated that the preload is not only useful for the purpose of returning the stick to the trim position, which is an advantage in maintaining equilibrium flight, but also that the preload is beneficial in terms of the dynamic stability of the pilot-vehicle system. This favorable effect of preload was noted, in other terms, in Ref. 9.

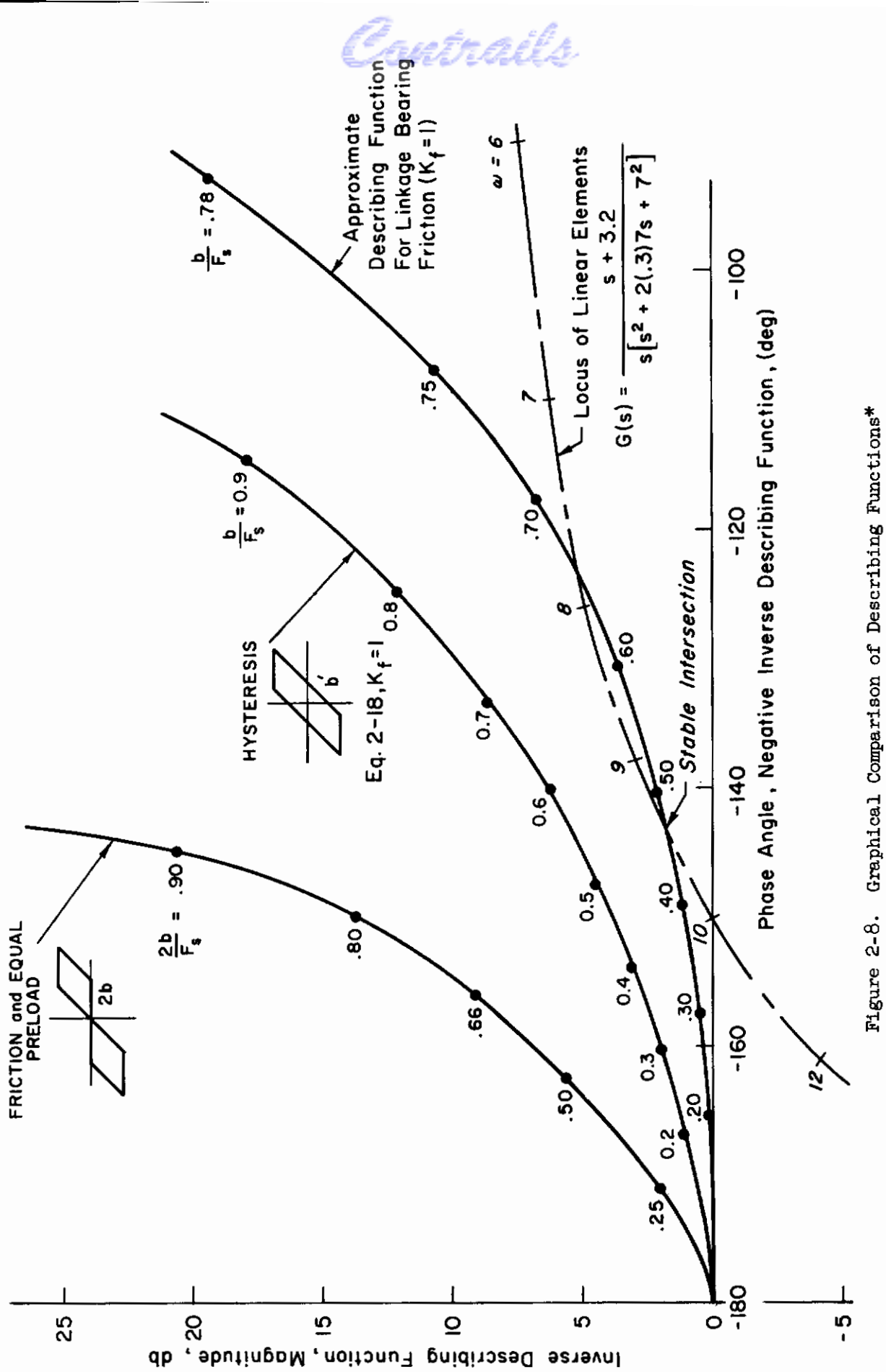

Figure 2-8. Graphical Comparison of Describing Functions*

*Computed by C. P. Shortwell and D. B. McElwain.

Consideration of the Remnant

It might seem, in the light of the immediately fore-going argument, that the attempt to develop sinusoidal describing functions for complex nonlinearities by finding closed-loop describing functions for loops containing simple nonlinearities is doomed to failure. In particular it may seem that considerable doubt is cast on the validity of the describing function for a control system with Coulomb friction in the valve which was developed previously.

There is, however, an essential difference between the analysis including valve friction and the analysis including linkage bearing friction. This difference, as we might expect, is revealed by considering the "remnant" portion of the quasi-linear system and its transmission around the loop. Actually it is perhaps easier, in these instances, to consider the actual waveforms rather than to view them as being composed of a fundamental and higher harmonics.

The validity of sinusoidal describing function analysis is founded on the assumption of a waveform at the input to the nonlinearity which is closely approximated by a single sine wave component. If, in particular, it can be shown that the transmission of the harmonics, generated in the nonlinearity, around the loop has a negligible effect on the relationship between the fundamental component of the input and the fundamental component of the output, then the analysis is justified. It is precisely in situations where these circumstances do not obtain, that second approximation describing functions find their usefulness.

It should be apparent from the diagrams of Figure 2-7 that the waveform of $\dot{x}_i$, which is the input to the nonlinearity in the case of linkage bearing friction, is typically very far from sinusoidal. This is a direct result of the "sticking" of the motion. With 20/20 hindsight we might say that the attempt to develop a complex closed loop describing function from the simple describing function for Coulomb friction was, in this case, wrong-headed. Fortunately, since the sinusoidal describing function for mechanical hysteresis is known, it is not necessary to attempt the development of second, or higher, approximation describing functions from detailed consideration of the waveforms.

The case of the describing function for the control system with valve friction is quite another matter. Here, as we shall presently see, the valve does not "stick," and the input to the nonlinearity is substantially sinusoidal. Not only is this the case, but also the fundamental component of the output of the nonlinearity is unaltered in magnitude and phase angle when the remnant is taken into account. It is on this basis that we may claim that the analysis is justified!

Figure 2-9 shows typical waveforms in the loop illustrated in Figure 2-3.

Starting with an applied force $f_s = F_s \sin \omega_s t$ at $t = 0$, the effect of friction in the valve is similar to the effect of friction in linkage bearings - initially. The friction force builds up so as to oppose the applied force. Then when the applied force reaches the level of the sliding friction, the linkage begins to move, and $\dot{x}_i$ jumps to a positive finite value. Thereafter $\dot{x}_i$ is the same as $\frac{d}{dt}\left(\frac{f_s}{K_f}\right)$ except for momentary intervals of infinitesimal duration.

According to the block diagram of Figure 2-3, the relationship between the valve displacement, x_ϵ, and the linkage displacement, x_i, is such that x_ϵ lags $\dot{x}_i$ and is attenuated.

$$X_\epsilon(s) = \frac{T}{Ts + 1} \dot{X}_i(s) \qquad (2\text{-}19)$$

In the drawing of Figure 2-9 the magnitude of x_ϵ has been exaggerated for clarity. (For a typical actuator time constant $T = 0.05$ sec and oscillation frequency $\omega_s = 2\pi$ rad/sec = 1 cps, the maximum value of x_ϵ would be approximately $.05\ \dot{x}_{i_{max}}$ and the phase angle would be very small indeed.)

We may now invoke superposition and consider separately the response of the system to the applied sinusoidal force and to the superposed square wave which arises from the friction force. The continuing response to the sinusoidal component only is indicated in Figure 2-9 by the dashed lines.

Note that when $\dot{x}_\epsilon = 0$, x_ϵ has a large value and this implies that the output of the actuator continues its motion even in the absence of any change

in the input, x_i. Not only is this the case but also $\frac{d}{dt}\left(\frac{f_s}{K_f}\right)$ is not zero here. It is thus clear that the valve does not "stick," and the distortion of the waveform typical of the case of linkage bearing friction does not occur in this case.

As $\dot{x}_\epsilon$ tends to pass through zero the friction force will change sign, and (still assuming a rigid, massless linkage) the signal x_i will contain a step function component. The response of x_ϵ to this step function will be the well known response of a washout to a step function of input; and its derivative $\dot{x}_\epsilon$ will have an infinite spike and an exponential decay of opposite sign. When these transient responses are superposed on the sine wave responses of Figure 2-9, the solid line responses are the result. The effect of the remnant transmission around the loop is observed only in the infinite spike (of zero width) and the very, very small exponential decay in $\dot{x}_\epsilon$.

For the reason that the spike is theoretically infinite, the method of harmonic balance is not suited to this problem, and it is not possible to develop second, or higher, approximation describing functions in terms of Fourier series for the waveforms.

Otherwise it is clear that the axis crossings of the signal $\dot{x}_\epsilon$ are unaltered by the inclusion of the remnant, and therefore, in this case, the output waveform is unaltered.

At the output of the servomechanism, the third and higher harmonics of the superposed square wave will have been attenuated and the description of the waveform of x_0 in terms of its first Fourier component will thus have a practical validity which cannot be gainsaid. The waveform of a typical x_0 wave is also shown in Figure 2-9. This wave, representing elevator deflection, illustrates the increase in gain and phase angle which is the result, under the original assumptions, of hydraulic surface actuator valve friction. Since its corners would be further smoothed by the filtering action of the airplane transfer function, in the case of a pilot-vehicle oscillation, the describing function developed here, considering its fundamental component only, may be deemed to be substantially correct.

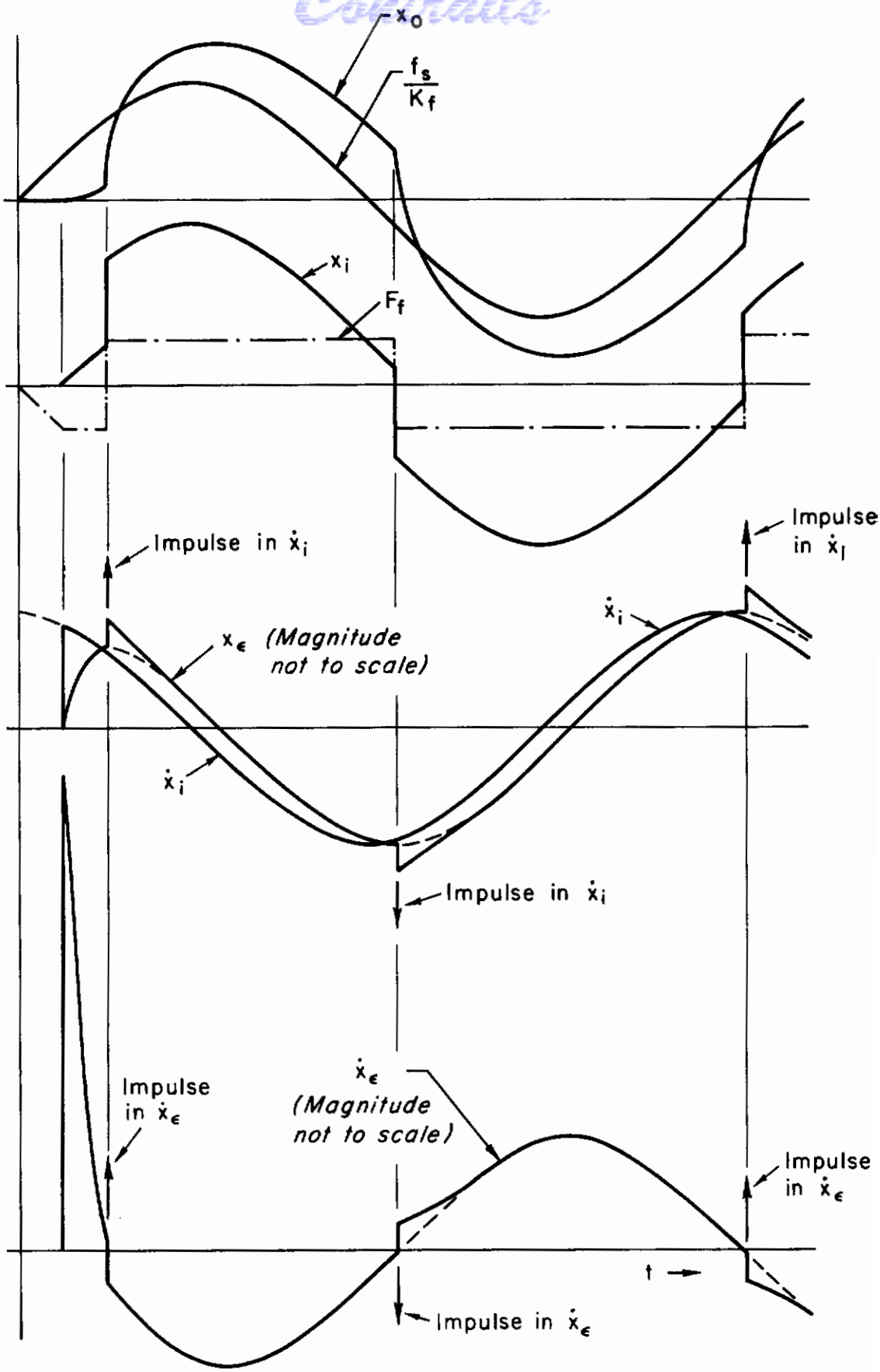

Figure 2-9. Waveforms in Control System with Valve Friction

The new frequency-dependent describing function for a control system with valve friction is illustrated in Figure 2-10. It can be appreciated by comparison with the airplane locus of Figure 2-8, that the nonlinearity represented by this type of describing function is indeed very inimical to stability. This would be especially true in manual control systems with relatively long actuator lag time constants.

It may be concluded that it is entirely possible to develop new describing functions for complex nonlinearities by combining the describing functions of simple nonlinearities with transfer functions of linear elements, provided the basic assumption of sinusoidal describing analysis is not violated. This is that the input to the nonlinearity is substantially sinusoidal, and that the output waveform is not altered by including the effect of the remnant at the input to the nonlinearity. These conditions may be met even when there are differentiators in the loop.

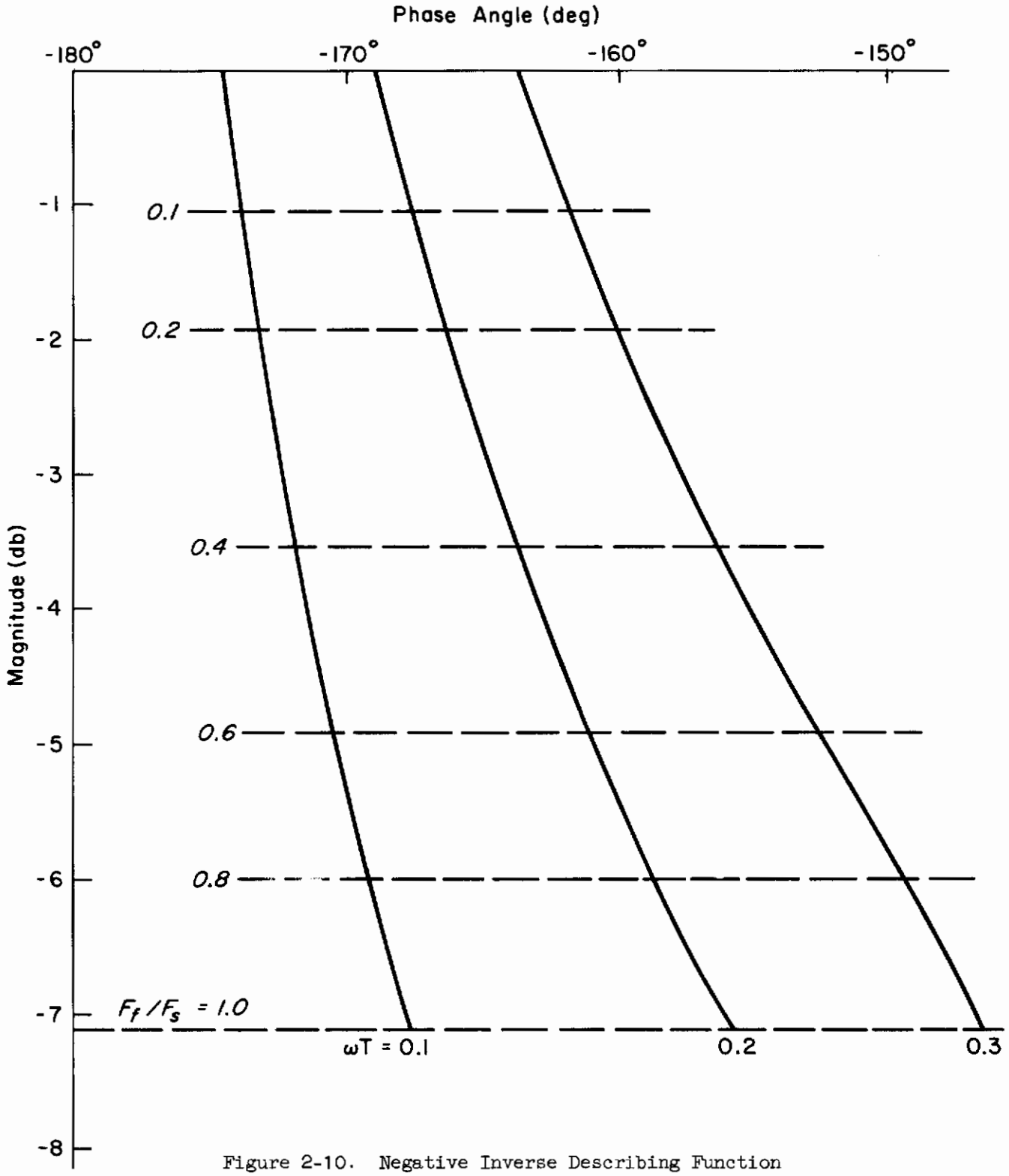

Figure 2-10. Negative Inverse Describing Function for a Control System with Valve Friction*
K_f = 1

*Computed by C. P. Shortwe..

CHAPTER III

A GENERALIZED PERIODIC INPUT DESCRIBING FUNCTION

A most welcome addition to the stable of engineering techniques would be a generalized periodic input describing function. Broadly speaking, attempts to develop such a technique for determining self-sustained oscillations in closed-loop systems containing a single, nonlinear element have, in the past, been discouraging. Recently, it became apparent how two familiar devices might be combined in a new assault on the problem. These devices are:

1. The introduction of an arbitrary perturbation (in phase in this instance) to obtain initial or first order solutions to problems where such an initial solution would not ordinarily exist. In some cases, as higher order solutions are obtained using the initial solution, the arbitrary perturbation can, in the end, be removed without "removing" the solution.

2. The use of steep descent methods to solve a set of nonlinear algebraic equations.

Much of the impetus to pursue such an approach is due to West (Ref. 15) who observed in connection with the dual-input describing function, "...it may be possible for a phase change to occur in the fundamental ... term in passing through the nonlinearity (due to the presence of higher harmonics)."

We shall illustrate how a higher harmonic can induce a significant phase shift in the describing function for the fundamental. Figure 3-1 shows two different input waveforms and the corresponding output waveforms for a relay-with-deadzone nonlinearity. The inputs consist of:

1. A single sinusoid -- corresponding to the fundamental.

2. A single sinusoid summed with a third harmonic which is out of phase with the first sinusoid.

Clearly, the third harmonic in the input to the nonlinearity induces a substantial phase lag in the fundamental component of the output waveform (shown dashed). An effect such as this can substantially influence the limit cycle parameters and the prediction of limit cycle existence as discussed previously. This effect of higher harmonics is really no surprise in view of engineering experience [Graham and McRuer (Ref. 1) showed this phenomenon]

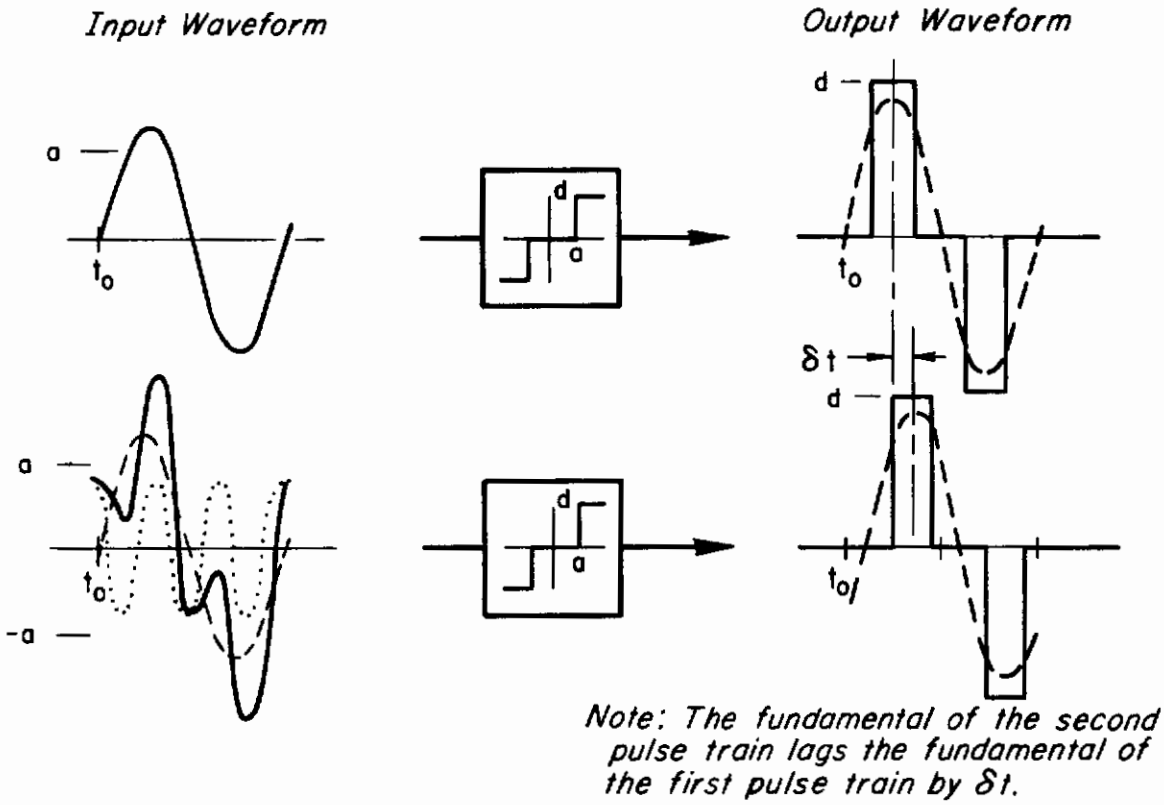

Figure 3-1. Higher Harmonic Influence Upon the Describing Function for the Fundamental

but it did lead West to formulate the dual-input describing function. West computed and tabulated the dual-input describing function for a saturation nonlinearity and applied it to at least one example. The results were very laboriously obtained and were unexciting by West's account because the first approximation sinusoidal describing function produced good answers in the case studied.

Despite West's lack of enthusiasm for the technique (mostly because of the labor involved), his work suggested a fruitful approach to take when dealing with systems for which the loci of $-1/N_1$ and $G(j\omega)$ made glancing intersections or perhaps only approached one another closely but did not intersect. In such cases, even small phase shifts in the fundamental wave which may be induced, so to speak, by the higher harmonics could be of crucial importance to the prediction of limit cycles.

Broadly, the condition for a limit cycle which must be satisfied is one of harmonic balance. That is, each harmonic component of the periodic limit cycle waveform must be sustained in its trip around the closed loop. (Notice that, as in the case of the first approximation sinusoidal describing function, no distinction is made between stable and unstable limit cycles.) The equation expressing this condition is:

$$-1/N_n = G(jn\omega) \; ; \; n = 1,2,3, \; \ldots \; , N \; ; \text{ in the limit as } N \to \infty \qquad (3\text{-}1)$$

It is reasonable to expect that fairly accurate approximations to the limit cycle may be obtained by finding those values of the limit cycle variables which produce solutions to a truncated set of the above equations for some small number of higher harmonics. The limit cycle variables are taken to be the fundamental frequency and amplitude, as well as the amplitudes and phases, relative to the fundamental, of the higher harmonics which are included.

We will now sketch the means for calculating these values of the limit cycle variables.

Assume that for a particular problem of interest the first approximation sinusoidal describing function indicates that $-1/N_1 = G(j\omega)$ is not satisified for any combination of fundamental wave amplitude and frequency (e.g., the satellite attitude control problem discussed below.) This first obstacle to obtaining an initial solution is overcome by introducing an arbitrary phase shift, Δ, into the open-loop in a manner which allows $-1/N_1 = G(j\omega)\, e^{j\Delta}$ to be satisfied for at least one combination of fundamental wave amplitude and frequency of the input to the nonlinear element. This provides the initial, albeit artificial, first solution to the problem.

It is easy to visualize at this point how a computational procedure might utilize steep descent to arrive at this first solution once Δ and the other system parameters have been specified. For instance, working in terms of amplitude ratio versus phase coordinates, we might define a positive definite criterion function to minimize consisting of the square of the difference between $|-1/N_1|^2$ and $|G(j\omega)|^2$ plus the square of difference between $\angle - 1/N_1$ and $\angle G(j\omega_1) + \Delta$. To converge to a solution of $-1/N_1 = G(j\omega)\, e^{j\Delta}$, we minimize the criterion function with respect to the amplitude and frequency of the fundamental wave at the input to the nonlinear element. The values of the amplitude

and frequency which reduce the criterion function to an absolute minimum of zero are the answers we seek. A summary of equations necessary to carry out this procedure for a broad selection of system configurations is included as Appendix A to this report.

While the above exercise might seem to be of small value in the sense that the same result can be achieved more efficiently by graphical methods without resorting to a computer and descent methods, it is actually extremely important because it provides a conceptually lucid description of an alternative method for discovering those values of the waveform variables which satisfy $-1/N_1 = G(j\omega)\, e^{j\Delta}$. And notably, this alternative method lends itself to generalization for treating multiple harmonically related sine wave input describing function calculations. It is a matter of plain fact that the graphical approach is not amenable to similar generalization for almost all cases of interest. [The cases where the Tsypkin locus (Ref. 18) is applicable may be considered to constitute the exceptions.]

In generalization of the graphical methods the basic difficulty is that of trying to find those values of the 2N waveform parameters which satisfy the N equations given by Eq. 3-1 simultaneously. The job of finding these 2N parameter values is all the more difficult because the terms in Eq. 3-1 are complicated functions of the 2N parameters.

Now, consider a generalization using the steep descent method. Let us assume that the artificial initial solution has been found by one means or another. Next, the third harmonic component of the nonlinearity output must be considered. At this point, terms are added to the criterion function expressing the cost of errors arising from failure to satisfy $-1/N_3 = G(j3\omega)\, e^{j\Delta}$ exactly. These terms are the square of the difference between $|-1/N_3|^2$ and $|G(j3\omega)|^2$, and the square of the difference between $\angle -1/N_3$ and $\angle G(j3\omega) + \Delta$. The amplitudes of the fundamental and third harmonic sine wave inputs to the nonlinearity, the phase of the third harmonic relative to the fundamental and the fundamental frequency are then adjusted to cause reduction of the criterion function. This is accomplished by computing a steep descent path with respect to the above variables. Having arrived at a solution including the fundamental and third harmonic waves which is again artificial, we desire to eliminate the arbitrary phase

shift, Δ, so that the system corresponds to that which is actually of interest. The process for eliminating Δ involves reducing Δ in small increments while adjusting the nonlinearity input waveform variables, previously discovered by the steep descent method, in a way which keeps the criterion function arbitrarily small as Δ is incremented to zero.

Two alternative end results are possible:

1. A two harmonic approximation to a limit cycle waveform is obtained. (The criterion function can be brought arbitrarily close to zero.) This approximation may be refined further by adding higher harmonics.
2. No nontrivial solutions to $-1/N_n = G(jn\omega)$ $n = 1,3$ are found. Then the possibilities are:
   a. No nontrivial solutions exist.
   b. The existence of a nontrivial solution will only be exposed upon the addition of more harmonics. Each of these harmonics may be added in a manner completely analogous to that by which the third harmonic was added. (It is necessary to proceed using an artificial solution including the fundamental and third harmonic as the initial solution, of course.)

After a reasonable number of harmonics have been included, the results, no matter which of the above situations exists, should be relatively conclusive. By conclusive we mean that an engineer's confidence in the results will increase greatly with the number of harmonics included.

However, as a word of caution we must realize that the presence of a limit cycle can still only be determined absolutely in the limit as an infinite number of harmonics are included in the analysis.

This generalized describing function is used essentially as an approximate numerical technique although the theoretical development is made in literal form without approximation. Because of this fact the generalized describing function is best compared with other methods of analysis in the context of an example. The particular example we have chosen as the vehicle for comparison is the single-axis attitude control system for a satellite shown in Figure 3-2. This example is extremely suitable to our purpose for several reasons:

1. Exact answers are available from rate diagram analysis and from phase plane analysis. Existence of a limit cycle is insured for $0 < \tau < T_E$ for reasonable values of the linear element gain.
2. Several analytical techniques are applicable to this problem for comparative purposes. These are summarized in Appendix C.
3. Some methods of (approximate) analysis say "yes" there is a limit cycle while others say "no" there is not a limit cycle. Notably, curves representing the first-approximation sinusoidal input describing function and frequency response function do not intersect but are tangent on the gain-phase plane at zero frequency for values of the linear element gain which are of practical interest, i.e. low values. Therefore, no periodic solution (limit cycle) is predicted. (Vide Appendix C.)

Thus we shall be able to examine the absolute accuracy of the generalized describing function method and its efficacy relative to other approximate analysis methods.

Application of the Generalized Describing Function to the Satellite Attitude Control Problem

Consider the single-axis attitude control system for a satellite illustrated in Figure 3-2. Attitude and rate feedbacks are employed to provide both stability and control. Control of the rockets is by switching, but there are some actuation and ignition delays. These are represented in non-dimensional form by the transfer function G(s). The torque applied by the jets accelerates the vehicle in attitude, and the transfer function of the vehicle is represented by a double integrator.

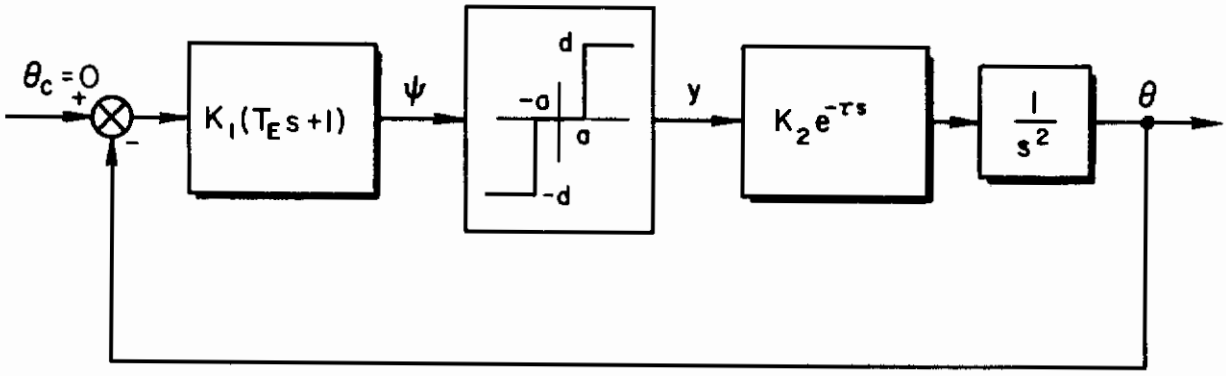

Figure 3-2. Single-Axis Attitude Control System for a Satellite

The question of the lifetime of the control system and indeed whether or not an auxiliary inertia wheel control system is required may be determined by whether or not the system of Figure 3-2 is susceptible to a limit cycle, a continuous oscillation of fixed frequency and amplitude.

Parenthetically we may remark that the answer as to whether a limit cycle exists is also almost unbelievably sensitive to the particular choice of usually equivalent representations for the actuator and ignition delays. The use of a deadtime, $e^{-\tau s}$, to represent delays is heuristically, but quite plausibly, justified in Appendix A of Ref. 16.

We will now apply the generalized describing function technique to the satellite attitude control problem. The pertinent equations are summarized in general form in Appendix A. We noted previously in the introductory remarks that the curves representing the negative inverse first approximation sinusoidal input describing function and the frequency response function were tangent on the gain-phase plane at zero frequency and that for "reasonable" values of the linear element gain, K_1K_2, no other intersections exist. Furthermore, the phase plane analysis predicts the existence of a limit cycle with finite frequency for $0 < \tau < T_E$ which indicates that the answer obtained from a generalized describing function should have a low, but non-zero frequency intersection with the frequency response function for the fundamental component of the limit cycle waveform. Since this does not occur naturally when only the fundamental of the waveform is considered, we will force the condition by introducing an appropriate artificial phase shift, Δ, into the frequency response function. In this case, the appropriate Δ would be any small negative phase shift.

The limit cycle frequency so indicated need not be an approximation to the one which actually exists, the only matter of importance is that its frequency be finite and non-zero. A typical choice for Δ is shown in Figure 3-3.

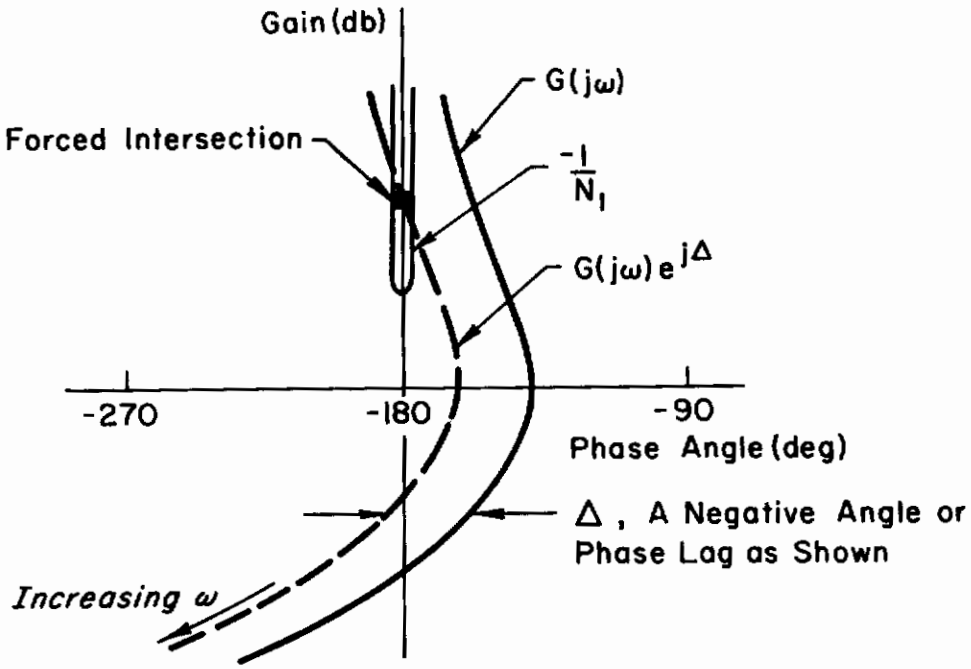

Figure 3-3. Obtaining an Artificial First Solution

The limit cycle parameters existing at the indicated intersection may be obtained by the steep descent method described at the beginning of this Chapter. Utilization of this method requires that an initial guess for the fundamental component amplitude and frequency be made. From these values, corresponding values of $|-1/N_1|^2$, $|G(j\omega)|^2$, $\angle(-1/N_1)$, and $\angle G(j\omega) + \Delta$ are determined.

Next, the error between $-1/N_1$ and $G(j\omega)\ e^{j\Delta}$ is defined as:

$$e = \left[|-1/N_1|^2 - |G(j\omega)|^2\right]^2 + K^2\left[\angle -1/N_1 - (\angle G(j\omega) + \Delta)\right]^2 \qquad (3\text{-}2)$$

At an intersection of $-1/N_1$ and $G(j\omega)\ e^{j\Delta}$, this error vanishes; elsewhere it is greater than zero. Physically, the error is the square of the distance between $-1/N_1$ and $G(j\omega)\ e^{j\Delta}$ for particular values of amplitude and frequency of the fundamental when plotted on the $(\text{gain})^2$ versus K(phase) plane.*

*The use of $(\text{gain})^2$ and K(phase) coordinates is unorthodox and somewhat arbitrary. They have been used here because it appeared that digital computation using an error which is the square of a distance in these coordinates would be most economical and most easily interpreted.

By making the error arbitrarily close to zero, we can approach an intersection with arbitrary closeness.

Reducing the error involves computing the first partial derivatives of the error with respect to the amplitude and frequency of the fundamental, and incrementing the amplitude and frequency in such a way that the product of each first partial with the appropriate incremental quantity is negative. This procedure is repeated until the error is brought arbitrarily close to zero as in Figure 3-4. If the curves shown in Figure 3-4 are plotted on the $(\text{gain})^2$ and K(phase) coordinates, the length squared of arrow (1) would equal the error for our initial guess at the limit cycle parameters. Subsequent stages in the descent to the intersection are indicated by the arrows in order of increasing number. The limiting point of the descent (intersection) is indicated by the shaded square. Note that it is inappropriate to reduce Δ to zero at this stage when only the fundamental has been included because the solution for the intersection would disappear for this example.

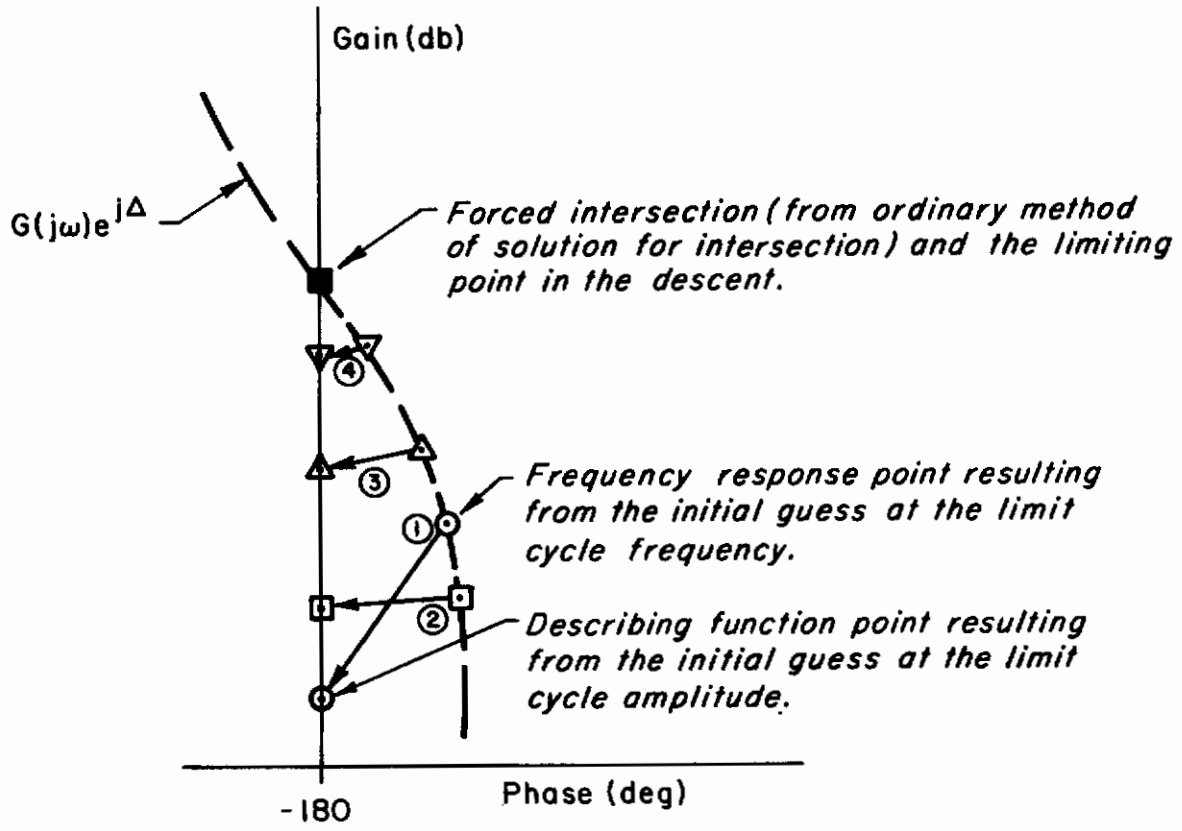

Figure 3-4. Several Steps in a Steep Descent to an Intersection

We interrupt the main argument to present two additional considerations which are best discussed before adding the effect of the third harmonic.

It should be noted that several intersections or identical intersections for different limit cycle parameters are often possible. It is evident that the latter case prevails for the problem we are considering. In connection with this point, let us note that selection of the "initial guess" limit cycle parameters in effect selects the intersection to which the solution will ultimately converge. The analyst can control this selection through his knowledge of first approximation sinusoidal input describing functions. This situation is analogous to the one encountered in locating a particular root of a polynomial using an analog computer; in that with each case, the initial point must be chosen in the region of influence of the solution to which we desire to converge.

It is also possible to encounter locally minimum values of the error which are greater than zero. The manner in which to treat these minimum points is not always clear. However, a conservative viewpoint is to treat them analogously to the absolute minimum points indicating intersections (where the error becomes zero). Such a treatment could allow us to dispense with the phase shifting technique for certain cases of the satellite attitude control problem. Figure 3-5 shows the basis for this approach. Clearly, such a minimum will

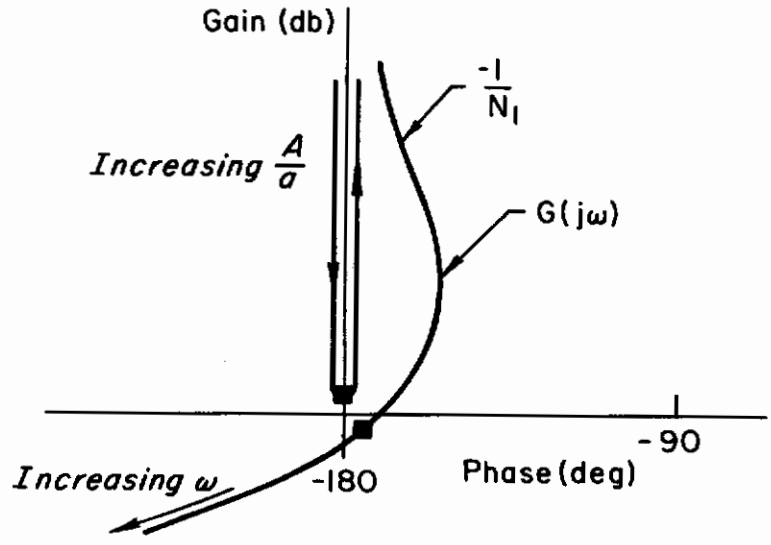

Figure 3-5. A Situation Where a Local (Nonzero) Minimum of the Error Criterion is Indicated

exist for some limit cycle parameter values which cause $-1/N_1$ and $G(j\omega)$ to be near the shaded squares. Such local minima either develop into absolute minima or are gradually eliminated as more harmonics are added.

Returning to the main argument, the next step involves the addition of the next higher harmonic, the third in this case. Initially, we will assume that there is no third harmonic component present in the input to the nonlinearity. There will, nevertheless, be some third harmonic present in the output of the nonlinearity. This means that $|-1/N_3|^2 = 0$ (since the third harmonic input to the nonlinearity is zero) and that $\angle -1/N_3$ is arbitrary. The error is redefined so as to include a component due to the difference between $-1/N_3$ and $G(j3\omega)e^{j\Delta}$.

$$e = \left[|-1/N_1|^2 - |G(j\omega)|^2\right]^2 + K^2\left[\angle -1/N_1 - \left(\angle G(j\omega) + \Delta\right)\right]^2 + \left[|-1/N_3|^2 - |G(j3\omega)|^2\right]^2 + K^2\left[\angle -1/N_3 - \left(\angle G(j3\omega) + \Delta\right)\right]^2 \qquad (3\text{-}3)$$

The third harmonic phase component of the error (4th term in the above equation) is initially zero because the phase of $-1/N_3$ may be arbitrarily chosen to equal $\angle G(j3\omega) + \Delta$.

Reducing the error now involves computing the first partial derivatives of the error with respect to the amplitude and frequency of the fundamental and with respect to the amplitude and phase relative to the fundamental of the third harmonic. All parameters are then incremented to reduce the error. This procedure is repeated until the error is brought arbitrarily close to zero.

Next, we will change the system under analysis to make it correspond with the one which is actually of interest. To accomplish this, increment Δ to zero while bringing the error arbitrarily close to zero at each step by the method described above. If the solution does not become trivial when $\Delta = 0$, then what remains will be a second approximation, or dual input describing function determination of the limit cycle parameters.

This procedure can be continued in order to refine the results still further by adding the effect of other higher harmonics. The result would then be a multiple harmonically related sine wave input describing function determination of the limit cycle parameters. Each additional higher harmonic can be added in exactly the same way as the third harmonic.

The generalized describing function for the satellite attitude control problem was computed* using the following values for the control system parameters:

$$a = 2.0 \qquad d = 1.0 \qquad \tau = 0.5 \qquad T_E = 1.0 \qquad K_1K_2 = 1.777$$

No limit cycle is indicated by the first approximation sinusoidal input describing function for these parameter values. The weighting of the phase angle errors (in degrees) relative to amplitude ratio squared errors in the error criterion was 5 to 1.

The generalized describing function computation including the first and third harmonics resulted in a local minimum; that is, the error criterion could not be reduced to zero after the arbitrary phase shift was removed. Attempts to locate other minima which might be absolute minima were unsuccessful. The "limit cycle" frequency at the local minimum was:

$$\omega = 0.767 \text{ rad/sec.}$$

The limit cycle frequency from the (exact) phase plane solution was:

$$\omega_{\text{phase plane}} = 0.546 \text{ rad/sec.}$$

The fact that the error criterion could not be reduced to zero indicated that simultaneous satisfaction of Eq. 3-1 for the fundamental and third harmonic only was not possible. In fact, this situation is a precise analogy, in higher order geometry, to the situation encountered with the first approximation sinusoidal input describing function when the describing function locus approaches the frequency response locus and then diverges from it.

*Programming and computing were done by David H. Weir.

Rather than to embark on the computational orgy of adding more harmonics without adding insight, we decided to explore expected results for the satellite attitude control problem using the Tsypkin locus technique (Refs. 18 and 3) in order to gain insight as to our difficulty with the apparently less than satisfactory answer produced by the generalized describing function technique.

Observing that the effects of truncating after the n^{th} harmonic in the generalized describing function technique are equivalent to placing an ideal low pass filter with a cut-off frequency, ω_{co},

$$n\omega < \omega_{co} < (n + 1)\omega$$

in the satellite attitude control loop, it is clear that truncation in the generalized describing function analysis corresponds on a term to term basis with truncation of the infinite series of the Tsypkin locus approach. The exact answers we would expect to obtain (including the effects of truncation) from the generalized describing function are obtainable in principle from the Tsypkin approach, in this problem, since the infinite series contains only a finite number of non-zero terms. In practice, of course, only numerical answers are available because transcendental functions are involved. The equations for this computation are summarized in Appendix B.

The Tsypkin locus formulation results in a simpler treatment of this problem since only a two parameter optimization is required regardless of the number of harmonics included. The generalized describing function formulation requires a 2n parameter optimization where n is the number of harmonics included. However, application of the Tsypkin locus is limited to systems with an off-on nonlinearity; whereas there is no such restriction on the generalized describing function.

Performance of this computation for several values of the gain yielded the results summarized in Table 3-1.

Table 3-1

Limit Cycle Frequencies Predicted by Two Methods of Analysis

Gain, K_1K_2	$\omega_{\text{phase plane}}$	ω_{Tsypkin}	No. of Terms (Harmonics) in Tsypkin Locus Calc.
6.8	2.382	2.34*	1 (min. no.)**
5.33	1.792	1.1381	2 (min. no.)
4.5	1.482	1.1707	2 (min. no.)
4.0	1.30	1.3488	3 (min. no.)
1.777	0.546	0.570	8, $5 <$ (min. no.) ≤ 8

*Result also obtainable from first approximation sinusoidal input describing function analysis.
**(min. no.) indicates that the number stated is the minimum number of harmonics that must be included in order that a limit cycle (intersection) be indicated.

Notice that as the gain, K_1K_2, is decreased below the minimum for which the first approximation describing function gives an answer, (approximately $K_1K_2 = 6.79$) a steadily increasing minimum number of harmonics is required to obtain an indication of the limit cycle. For the problem posed initially, K_1K_2, = 1.777, somewhere between the 9th through 15th harmonics (or from 5 to 8 terms in Tsypkin locus calculation not counting the even numbered harmonics which have zero amplitudes for this example) must be included.

With this knowledge in hand, it was then apparent that a more appropriate value of K_1K_2 to use for demonstrating the two harmonic version of the generalized describing function technique was 4.5. Computation using this value yielded $\omega = 1.1707$ rad/sec in comparison to $\omega_{\text{phase plane}} = 1.482$ rad/sec and $\omega_{\text{Tsypkin}} = 1.1707$ rad/sec. The two harmonic approximation to the input wave to the nonlinearity was.

$$\psi(t) \doteq 1.9105 \sin 1.1707\, t + 0.44433 \sin (3.5121\, t + 1.8433) \qquad (3\text{-}4)$$

This is compared with the actual waveform in normalized time in Figure 3-6.

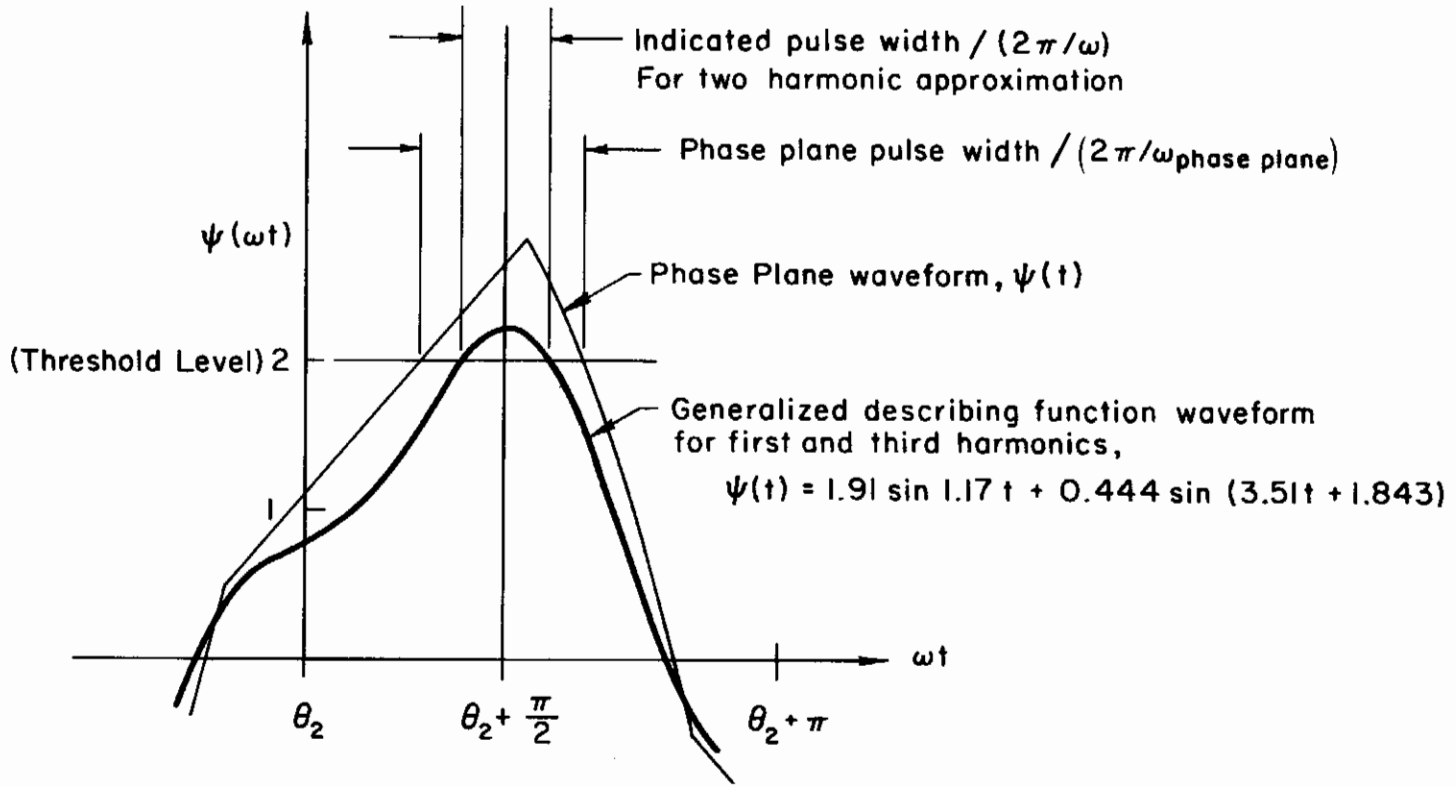

Note: Waveforms aligned such that pulses are symmetrical about $\theta_2 + \frac{\pi}{2}$

Figure 3-6. Comparison of Exact and Approximate Waveforms

Comparison of the Generalized Describing Function with Other Methods and Conclusions

A summary of results for other methods of analyzing the satellite attitude control problem is given in Appendix C. These results are compared with those for the generalized describing function in Table 3-2. The assumptions necessary for the application of each method and the different aspects of the extendability of each method for more complex systems than our satellite attitude example are also contained in the table. The third line item in Table 3-2 pertains only to the satellite attitude control example. The remainder of the line items apply as general comments as well.

Comparison of the limit cycle frequencies shows the generalized describing function underestimates the actual limit cycle frequency by approximately the same amount as the nonsinusoidal describing function overestimates the limit cycle frequency. It is possible to refine the generalized describing function result by including more harmonics. An analogous procedure can be followed in general for the nonsinusoidal describing function only with the addition of more detailed information about one waveform in the loop.

In conclusion, let us note that the generalized describing function technique provides another approximate method for discovering periodic solutions to unforced closed-loop systems containing a single isolated nonlinear element. The method becomes practical or useful only when digital computation is employed for calculation and when other techniques such as the phase plane or the Tsypkin approach are impractical to apply. This implies that the problem of interest will involve a system of order three or more which has a nonlinear elemer[illegible]ch is not of the off-on variety amenable to treatment with the Tsy[illegible]us technique.

The generalized describing function, like the Tsypkin approach, yields more precise results as more harmonics are included, becoming exact as infinitely many are included. It provides one way to get started with higher (better) approximation describing functions when the curves representing the negative inverse of the first approximation sinusoidal input describing function and the frequency response locus of the linear elements do not intersect.

Table 3-2

Summary of Results and General Characteristics for the Several Describing Functions

Comparison Item \ Analysis Method	Generalized Describing Function	Tsypkin Locus	Phase Plane	Rate Diagram	Nonsinusoidal Describing Function	Sinusoidal Describing Function
Limit Cycle Frequency predicted for satellite attitude problem for $K_1K_2 = 4.5$	1.1707 r/s	1.1707 r/s	1.482 r/s	1.482 r/s	1.768 r/s	Does not predict a limit cycle
Results of method are:	Approximate	Approximate	Exact	Exact for satellite attitude problem. In general, method is approximate.	Approximate, can be exact if waveform is known exactly.	Approximate
Basic Assumption of Method	Effects of some higher harmonics are negligible	Off-on nonlinearity	None	Off-on nonlinearity. Off time is long with respect to transient of linear element	Approximate shape of limit cycle waveform at one point in loop must be known	Effects of all higher harmonics is negligible
Method extendable to higher order systems	Yes	Yes	In principle	Yes	Yes	Yes
Method extendable to obtain better approximations	Yes	Yes	Not applicable	Not extendable when method is approximate	Yes, but requires more accurate knowledge of one system waveform	No
Method applicable for all piecewise continuous nonlinear characteristics with a finite number of segments	Yes	No, applies to off-on nonlinear elements only	In principle	No, applies to off-on nonlinear elements only	Yes	Yes
Computational Approach	Digital Computation Required	Graphical or Digital Computation	Analytical solution often possible	Analytical solution often possible	Usually a combination of analytical and digital computation	Graphical solution

The major disadvantages of its use are:

1. Increasing dimensionality of the parameter space in which the error criterion must be minimized. Dimension is double the number of harmonics included.
2. The problem of determining when all minima of the error criterion have been located.

CHAPTER IV

ANALYSIS WITH THE RANDOM INPUT DESCRIBING FUNCTION FOR HYSTERESIS

Some model tests of tilt-wing VTOL aircraft have revealed hysteresis in plots of longitudinal force and pitching moment as a function of forward velocity. Evaluation of the hovering performance of a pilot-tilt-wing VTOL system in gusty air including the effects of hysteresis in the X_u and M_u stability derivatives constitutes an example of a problem containing two complex nonlinearities amenable to quasi-linearization through the use of the random input describing function for a simple nonlinear element, the deadzone.

Now, by and large there are few examples of important aerodynamic nonlinearities, but hysteresis in X_u and M_u would certainly seem to be such nonlinearities if the width of the hysteresis loops were at all large.

In view of the erratic motions which VTOL machines undergo in hover close to the ground, (which are usually attributed to the impingement of the reflected slipstream on the fuselage and tail and to ingestion of the reflected slipstream through the propeller disc) it is interesting to conjecture that the measured nonlinearities may be responsible in part for the observed motions when the vehicle is under the control of the pilot. As a plausible indication of the results to be expected, consider the following.

The longitudinal equations of motion for u and θ (vide Eq. 4-4 below), in the absence of pilot loop closure, and considering only the M_u derivative to display the hysteresis characteristic are shown in block diagram form in Figure 4-1. Following the suggestions of either Leland (Ref. 19) or Brown

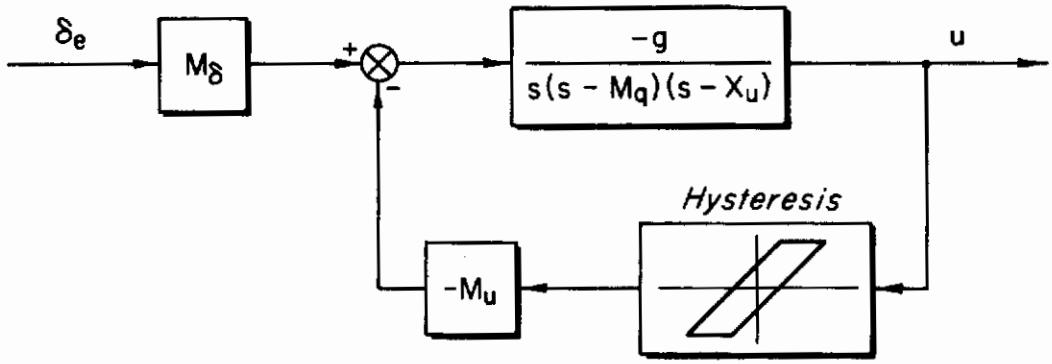

$M_{\delta_e}, g, M_u > 0 \qquad M_q < X_u < 0$

Figure 4-1. Block Diagram Representation of u and θ Equations of Motion

(Ref. 20) the random input describing function for hysteresis with unity slopes can be taken as a first order lag with unity DC gain and break frequency, A:

$$DF = \frac{A}{s + A} \tag{4-1}$$

Qualitatively the bandwidth of the describing function approaches zero as the RMS of its input signal becomes very small with respect to the hysteresis loop width, and approaches infinity as the RMS of its input signal becomes very large with respect to the hysteresis loop width. Thus A can be expected to range from zero to infinity. The characteristic equation of the quasi-linear system may now be written

$$1 + \frac{gM_u\, A}{s(s - M_q)\,(s - X_u)\,(s + A)} = 0 \tag{4-2}$$

and this equation may be rearranged so as to make A the variable parameter along the root locus.

$$1 + \frac{A\left[s(s - M_q)\,(s - X_u) + gM_u\right]}{s^2(s - M_q)\,(s - X_u)} = 0 \tag{4-3}$$

Now the plot of the numerator roots of the open-loop function in Eq. 4-3 as M_u is increased yields a locus of zeros for a new plot, based upon Eq. 4-3, that shows the effect of hysteresis. These plots are shown in Figure 4-2. There it can be appreciated that for a given value of M_u which would make the hovering mode unstable, the inclusion of the quasi-linear representation of hysteresis will lower the frequency and increase the negative damping ratio of the hovering mode for any but the very smallest values of the RMS variation in forward speed. With the inevitable contribution of pilot control action and wind gusts to the variability of the forward speed, it might be expected that this destabilizing effect would be very marked, and that this might show up in an analysis including pilot loop closures as an inability to stabilize the closed-loop pilot-vehicle system with a quasi-linear controller function within the capabilities of actual pilots.

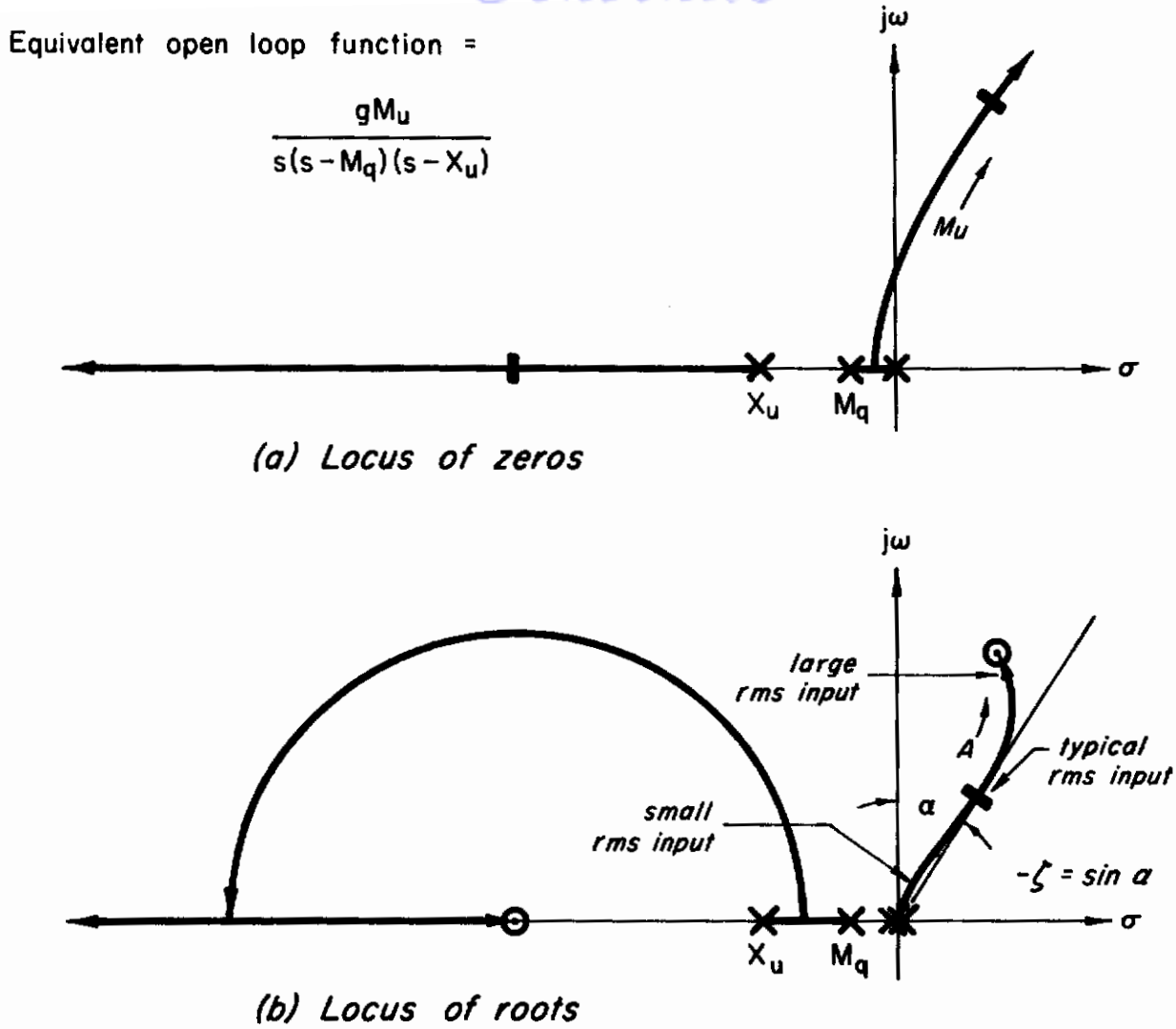

Figure 4-2. Root Loci Showing the Influence of Hysteresis in M_u

Stating this from a slightly different viewpoint, we might consider the consequences of a suddenly changed gust environment such as might result when a hovering VTOL encounters the downwash of another aircraft. A situation such as this might require the pilot to suddenly generate greater leading phase angles and to alter his operating gains. This could be a particularly unfavorable situation if a pilot developed only the minimum lead necessary to stabilize the vehicle against very small disturbances. (The implication here is that small disturbance effects will fall within the hysteresis loop width.) In the presence of larger gusts, not only the input environment would be changed but also the apparent controlled element transfer function would be altered. This situation might possibly necessitate a rapid change in the

pilot's control technique. Observations indicate that pilots cannot adapt rapidly to changes in the controlled element transfer function other than to changes in gain; therefore, this limitation might significantly affect the hovering performance of the pilot-tilt-wing VTOL system.

Analysis

The approximate longitudinal equations of motion for a hovering tilt-wing VTOL given below are adapted from Ref. 21. The notation employed is that of Ref. 22.

$$\begin{bmatrix} (s-X_u) & 0 & g \\ -Z_u & (s-Z_w) & 0 \\ -M_u & 0 & (s^2-M_q s) \end{bmatrix} \begin{Bmatrix} u \\ w \\ \theta \end{Bmatrix} = \begin{bmatrix} 0 \\ Z_{\delta_e} \\ M_{\delta_e} \end{bmatrix} \delta_e + \begin{bmatrix} 0 \\ Z_{\delta_c} \\ M_{\delta_c} \end{bmatrix} \delta_c + \begin{bmatrix} X_u \\ Z_u \\ M_u \end{bmatrix} u_g + \begin{bmatrix} 0 \\ Z_w \\ 0 \end{bmatrix} w_g \quad (4\text{-}4)$$

Control of vertical velocity is accomplished with propeller thrust through δ_c and control of pitch attitude through what effectively is elevator control, δ_e. Gust effects are assumed one-dimensional and gust gradient effects are neglected.

Numerators and denominators of the resulting transfer functions are listed below in Table 4-1.

Inspection of the various transfer functions indicates that vertical motions do not couple into the u and θ motions and that forward velocity and pitch attitude motions couple only slightly into the w motion. The pitching moment resulting from δ_e can produce substantial pitch angles which force the u motion via the $g\theta$ term. The control deflections, in the case of δ_e, can be considered to produce large X and Z forces and pitching moment, and for δ_c, only a large Z force is produced. Gust inputs in the x direction force u and θ motions strongly and the w motion slightly. Gust inputs in the z direction force only the w motion.

In view of the above considerations, the problem can be partitioned into two parts; one considering u and θ motions in response to the δ_e control and u_g disturbances, and another considering essentially the w motions in response

Table 4-1

Numerators and Denominators, Hovering Tilt-Wing VTOL

$$\Delta = (s - Z_w)\left|s(s - X_u)(s - M_q) + gM_u\right|$$

$$N_\delta^u = -M_\delta\, g(s - Z_w)$$

$$N_\delta^w = Z_\delta\left|s(s - X_u)(s - M_q) + gM_u - gZ_u\frac{M_\delta}{Z_\delta}\right|;\ \text{note } M_{\delta_c} \doteq 0$$

$$N_\delta^\theta = M_\delta\,(s - X_u)(s - Z_w)$$

$$N_{u_g}^u = (s - Z_w)\left|X_u\, s(s - M_q) - gM_u\right| \qquad (4\text{-}5)$$

$$N_{u_g}^w = s^2(s - M_q)\, Z_u$$

$$N_{u_g}^\theta = s(s - Z_w)\, M_u$$

$$N_{w_g}^u = 0$$

$$N_{w_g}^w = Z_w\left|s(s - X_u)(s - M_q) + gM_u\right|$$

$$N_{w_g}^\theta = 0$$

to the δ_c and δ_e control deflections and u_g and w_g disturbances. Notice that the second part is essentially a continuation of the first when pilot loop closures are considered. This is because of the significant influence of δ_e on the w motion.

Our attention here, however, will be confined to the first part of the problem for two reasons.

1. This is the only part of the problem where the nonlinear stability derivatives of interest, X_u and M_u, appear in the open-loop transfer function of loops closed by the pilot since the pilot does not find a $w \rightarrow \delta_e$ closure advantageous. Only in a closed loop do nonlinearities cause us to be uncertain about system stability.
2. The second part of the problem is concerned with a controlled element which has received a great deal of attention from a handling qualities viewpoint. Pilots are capable of making high gain loop closures around this type of controlled element with relative ease and pilot-vehicle system performance can be predicted accurately in this situation.

In the work following, numerical data from XC-142 model tests will be used. It is impossible to conduct this work in literal rather than numerical terms because of extreme algebraic complexity.

XC-142 Longitudinal Derivatives (Ref. 23)

Princeton Track Data for Level Flight, U_0 = 1 ft/sec

$$X_u = -0.43,\ X_w = X_q = X_{\delta_c}{}^{\dagger} = X_{\delta_e}{}^{\dagger} = 0$$

$$Z_u = 0.045,\ Z_w = -0.05,\ Z_q = 0,\ Z_{\delta_c}{}^{\dagger} = 1.00,\ Z_{\delta_e}{}^{\dagger} = 3.20$$

$$M_u = 0.0175,\ M_w = 0.002,\ M_q = -0.19,\ M_{\delta_c}{}^{\dagger} \doteq 0,\ M_{\delta_e}{}^{\dagger} = 1.00$$

$(\ )^{\dagger}$ Indicates δ_e inputs are normalized with respect to M_{δ_e}, and δ_c inputs are normalized with respect to Z_{δ_c}.

Handling qualities theory (Refs. 21, 24) and multiloop analysis (Refs. 24, 25, 26) has been applied to estimate the loop closures that the pilot would make to stabilize and control the u and θ motions of the XC-142. These calculations were performed using the above linear experimentally determined stability derivatives in the equations of motion. The necessity for estimating the pilot loop closures in this manner was dictated by the requirement to keep the problem within manageable proportions.

The resulting pilot transfer functions are:

$\theta \rightarrow \delta_e$ closure

$$Y_{p_\theta} = \frac{K_\theta}{M_{\delta_e}} e^{-0.2s} (s + 1/T_{I_\theta}) \doteq - \frac{K_\theta}{M_{\delta_e}} \frac{(s + 1/T_{I_\theta})(s - 10)}{(s + 10)} \qquad (4\text{-}6)$$

$u \rightarrow \delta_e$ closure

$$Y_{p_u} = \frac{K_u}{M_{\delta_e}} e^{-0.2s} \doteq - \frac{K_u}{M_{\delta_e}} \frac{(s - 10)}{(s + 10)} \qquad (4\text{-}7)$$

with $K_\theta = 6.01$, $1/T_{I_\theta} = 1.05$ and $K_u = -0.675$ or -0.0575. The resulting closed-loop pilot-XC-142 system transfer function, $u_c \rightarrow u$, where u_c is the reference or commanded value of u, for $K_u = -0.675$ is:

$$\left.\frac{u}{u_c}\right|_{\substack{\theta \rightarrow \delta_e \\ u \rightarrow \delta_e}} = \frac{0.868 \left(1 - \frac{s}{10}\right)}{\left[\left(\frac{s}{2.25}\right)^2 + \frac{2(.2)s}{2.25} + 1\right]\left[\left(\frac{s}{6.9}\right)^2 + \frac{2(.28)s}{6.9} + 1\right]} \qquad (4\text{-}8)$$

These pilot loop closures result in a 25° phase margin for the first (θ) loop closure and a 28° phase margin for the second (u) loop closure. The value for K_u used above results in unrealistically large θ excursions in response to gust disturbances, so a smaller value of K_u was also used.

For $K_u = -0.0575$:

$$\left.\frac{u}{u_c}\right|_{\substack{\theta \to \delta_e \\ u \to \delta_e}} = \frac{0.360\left(1 - \frac{s}{10}\right)}{\left[\left(\frac{s}{1.0}\right)^2 + \frac{2(.8)s}{1.0} + 1\right]\left[\left(\frac{s}{7.15}\right)^2 + \frac{2(.22)s}{7.15} + 1\right]} \qquad (4\text{-}9)$$

In both cases, the system bandwidth is increased and a significant amount of system damping is supplied by the pilot.

The next step is to rearrange the equations of motion plus the pilot loop closures so that the signal paths containing the X_u and M_u stability derivatives appear as outer loops in the development of the (u/u_g)"* transfer function with pilot loops closed. This will enable us to consider the effects of hysteresis in these stability derivatives.

$$\begin{bmatrix} (s - X_u) & g \\ -M_u & (s^2 - M_q s) \end{bmatrix} \begin{Bmatrix} u \\ \theta \end{Bmatrix} = \begin{bmatrix} 0 \\ M_{\delta_e} \end{bmatrix} \left(-Y_{p_\theta}\,\theta - Y_{p_u}\,u\right) + \begin{bmatrix} X_u \\ M_u \end{bmatrix} u_g \qquad (4\text{-}10)$$

Rearranging:

$$\begin{bmatrix} s & g \\ Y_{p_u} M_{\delta_e} & (s^2 - M_q s) + Y_{p_\theta} M_{\delta_e} \end{bmatrix} \begin{Bmatrix} u \\ \theta \end{Bmatrix} = \begin{bmatrix} X_u \\ M_u \end{bmatrix} (u + u_g) \qquad (4\text{-}11)$$

The open-loop transfer function for (u/u_g)" wherein X_u and M_u operate on the input, $(u + u_g)$ is:

$$\left(\frac{u}{u + u_g}\right)'' = \frac{-(-X_u)\left\{s(s - M_q) + Y_{p_\theta} M_{\delta_e}\right\} - g\,M_u}{s\left\{s(s - M_q) + Y_{p_\theta} M_{\delta_e}\right\} - g\,Y_{p_u} M_{\delta_e}} \qquad (4\text{-}12)$$

*The double prime on transfer functions indicates that two pilot loop closures are included.

A block diagram for the quasi-linear closed-loop system may then be constructed as shown below.

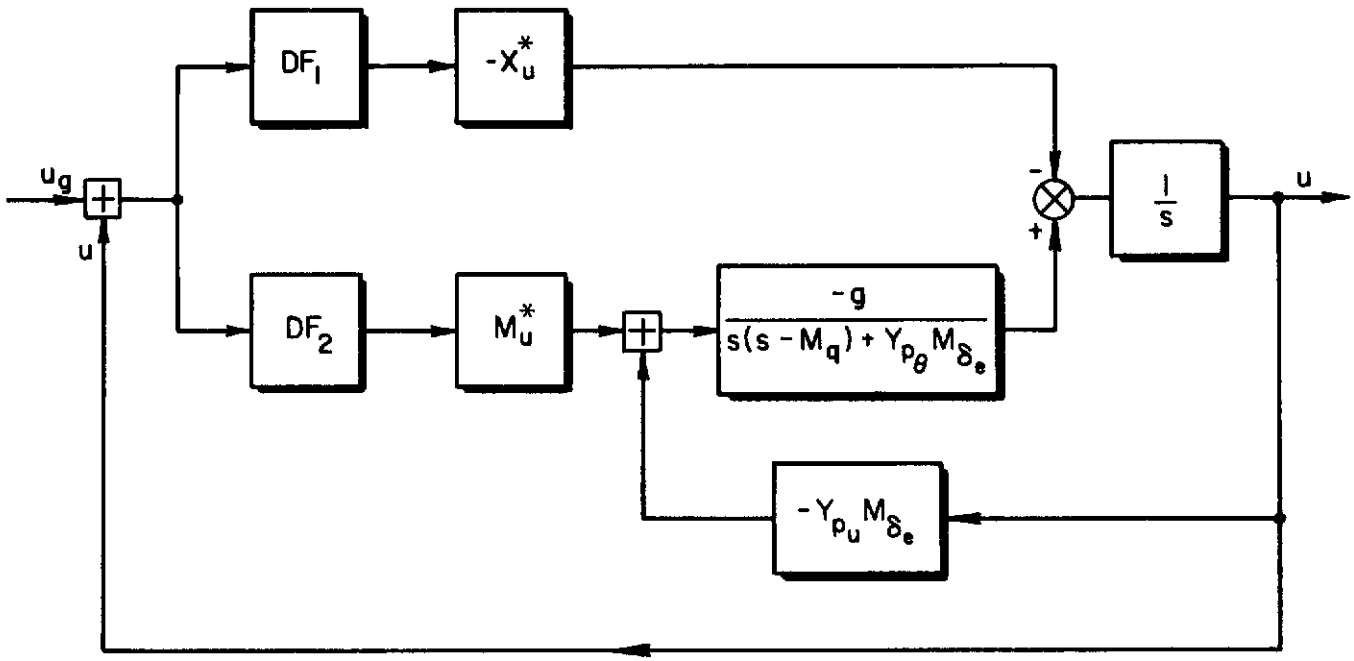

Figure 4-3. Block Diagram of the Quasi-linear Pilot–XC-142 VTOL System in Hover

X_u^* and M_u^* denote linear gains scaling the outputs of hysteresis describing functions with unity slope characteristics. If DF_1 and DF_2 are replaced by unity slope hysteresis characteristics with the proper loop widths, then the operations on the $(u + u_g)$ signal represent the nonlinear stability derivatives X_u and M_u.

Random input describing functions for the hysteresis nonlinearity are required for analysis of this problem. Two describing functions which are likely to be useful have been developed by Leland (Ref. 19) and Brown (Ref. 20).

Leland's analytical method proceeds parallel to the synthesis of hysteresis with analog computer components wherein a deadzone and a high gain integrator are contained in a unity gain feedback loop. This representation of hysteresis is used in the system under analysis with the deadzone element replaced by its random input describing function, a gain. The applicable value of this gain

(for a given gain of the integrator) is that value which produces the RMS value of the input to the describing function for which that value of the gain is also the random input describing function for the deadzone. An extension of this procedure can be employed for the case wherein two nonlinear elements are present in the system. Vide Ref. 19.

The random input describing function for hysteresis developed by Brown (Ref. 20) has the form of a unity gain first order lag as does the form ultimately used by Leland. However, Brown proceeds by empirically determining the lag break frequency as a function of the ratio of RMS value of the hysteresis input to the loop width and the half-power frequency of the input spectrum. The value of the lag break frequency is adjusted for minimum RMS error between the lag and actual hysteresis element outputs.

The half-power frequency, ω_0, of a low-pass spectrum is defined by

$$\int_0^{\omega_0} \Phi(\omega)d\omega = \frac{1}{2}\int_0^{\infty} \Phi(\omega)d\omega \qquad (4\text{-}13)$$

where $\Phi(\omega)$ is the power spectral density. Brown has shown that the break frequency of the lag is directly dependent upon the half-power frequency of the input to the nonlinearity, and as a consequence of this fact, the break frequency is nondimensionalized by ω_0.

When this random input describing function is used in a system, the applicable value of the lag break frequency is that value which produces the RMS value and half-power frequency of the input to the describing function for which that value of the break frequency is also the "optimum" random input describing function for the hysteresis. This procedure can also be extended to cases wherein two hysteresis elements are present in the system, but the calculation involved is very extensive.

Brown has also shown by example that the half-power frequency and RMS value of the nonlinearity input adequately characterize any lowpass input spectrum to this describing function. (Spectra which are obtained by shaping white noise with a lowpass first order filter are completely specified by these two parameters.)

From Refs. 27 and 28 the one-dimensional gust spectrum in the x axis direction, assuming isotropic turbulence, is

$$\Phi_{u_g u_g}(\omega) = \frac{\sigma^2 L}{\pi U_0} \frac{1}{1 + \left(\frac{\omega L}{U_0}\right)^2} \quad \text{where } \sigma^2 = \int_{-\infty}^{\infty} \Phi_{u_g u_g}(\omega)\, d\omega \qquad (4\text{-}14)$$

where σ is the RMS level of the gust velocity, L is the scale length of the turbulence, ω is the frequency of a particular spectral component and U_0 is the mean velocity of the air mass with respect to the aircraft. Since we are dealing with a hovering vehicle, it is necessary to assume a headwind component with magnitude U_0 in order for gusts to exist when using this representation. There is no theoretical model for gusts occurring at a fixed point over the ground in the absence of a mean wind. This lack is explainable by the fact that observations seem to indicate that the existence of longitudinal gusts is dependent on the existence of a mean wind.

The actual gust velocity may be considered to be produced by passing unit white noise through a filter having the transfer function:

$$\frac{\sigma \sqrt{U_0/L}\sqrt{\pi}}{s + U_0/L}$$

Now the mean square value of any system variable can be evaluated by cascading the appropirate transfer function with the above filter and evaluating the Phillip's integral (Ref. 29).

Experimental data assembled to date indicates that the hysteresis loop width, when it exists, is nearly the same for X_u and M_u, indicating that the same physical effect is producing the major portions of the force and moment due to u. The maximum value of the hysteresis loop half-width observed so far is approximately 10 ft./sec.* For this problem, we will use a half-width, a, of 8 ft./sec.*

*These are scaled to full-scale velocities.

Sufficient information is now assembled for quantitative evaluation of the hysteresis effects.

The first approach to the problem will assume that the hysteresis loop width is the same for X_u and M_u. This is approximately true as mentioned previously. Under this assumption, the X force and pitching moment due to u may be generated as shown in the sketch below instead of as shown in Figure 4-3.

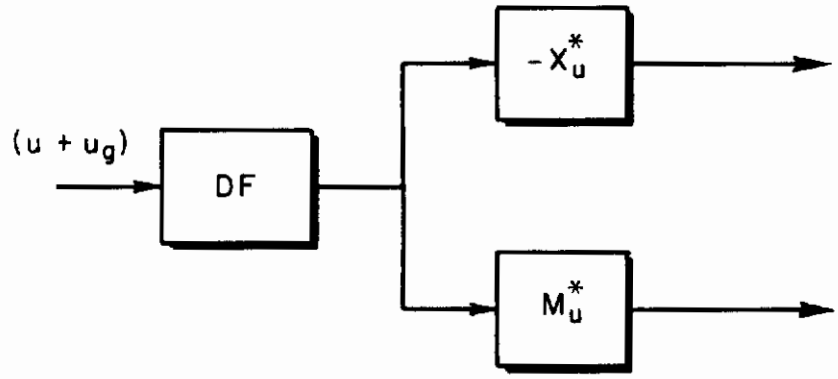

The describing function (Leland's or Brown's) is a simple lag.

$$DF = \frac{A}{s + A} \tag{4-15}$$

The open-loop transfer function for the quasi-linear system is then (from Eq. 4-12)

$$\left(\frac{u}{u + u_g}\right)'' = \frac{A}{s + A} \frac{-(-X_u^*)\{s(s - M_q) + Y_{p_\theta} M_{\delta_e}\} - g M_u^*}{s\{s(s - M_q) + Y_{p_\theta} M_{\delta_e}\} - g Y_{P_u} M_{\delta_e}} \tag{4-16}$$

$$\left(\frac{u}{u + u_g}\right)'' = \frac{A}{s + A} U \tag{4-17}$$

The closed-loop transfer function is:

$$\left(\frac{u}{u_g}\right)'' = \left(\frac{u}{u_g}\right)''(A) = \frac{AU}{s + A(1 - U)} \tag{4-18}$$

When $A \to \infty$ the system approaches the one which would exist if X_u and M_u were linear.

$$\left(\frac{u}{u_g}\right)''(\infty) = \frac{U}{1 - U} = H \tag{4-19}$$

When $A \to 0$ the X_u and M_u signal paths are open, therefore the u_g disturbance input never exceeds the hysteresis loop width and:

$$\left(\frac{u}{u_g}\right)''(0) = 0 \tag{4-20}$$

Equation 4-18 can be normalized to reflect only the changes in the u spectrum due to the nonlinear effect by dividing through by Eq. 4-19.

$$\frac{1}{H}\left(\frac{u}{u_g}\right)''(A) = \frac{AU/H}{s + AU/H} \tag{4-21}$$

Inasmuch as the power spectral density of u arising from u_g can be obtained by multiplying $\Phi_{u_g u_g}(\omega)$, $|H(j\omega)|^2$, and $\left|\frac{1}{H(j\omega)}\left(\frac{u}{u_g}\right)''(j\omega,A)\right|^2$, Eq. 4-21 gives an assessment of the potential significance of the nonlinearity. $\frac{1}{H}\left(\frac{u}{u_g}\right)''(A)$ may be developed as a function of A, the characteristic parameter of the hysteresis describing function, using root locus techniques. The roots of $\frac{1}{H}\left(\frac{u}{u_g}\right)''(A)$ for the pilot-XC-142 system are very closely approximated by those shown in Figure 4-4. The open-loop transfer function used to obtain Figure 4-4 is a low frequency approximation. There, a moderately well damped second order dipole pair occurring at a high frequency relative to the bandwidth of the input and the dominant system dynamics has been approximated by its low frequency equivalent. That is, for our example

$$\frac{s^2 + 2(2.72)\ 6.90s + (6.90)^2}{s^2 + 2(2.72)\ 6.95s + (6.95)^2} \doteq \frac{(6.90)^2}{(6.95)^2} = 0.983$$

for $|s| < 6.90$. The open-loop root locus gain in the approximation is $K = 0.983A$. Since it is $\left|\frac{1}{H}\left(\frac{u}{u_g}\right)''(A)\right|^2$ which is of interest, this has

been plotted as a function of A in Figure 4-5 for the pilot-XC-142 system. Note that the parameter A is, as yet, unrelated to the parameters of the gust environment and the hysteresis loop width, 2a. These relations can be determined using either Leland's or Brown's random input describing function for hysteresis. We shall use Leland's representation here because it requires considerably less computation.

The steps in implementing Leland's method are as follows:

1. The gain, C, of the high-gain integrator in the describing function is selected so that the ratio of the deadzone half-width to the RMS of the deadzone input, a/σ_ϵ, is $\mathbf{0}(1)$* or greater. It is usually best to select a value for C and then verify that this condition exists.
2. The quasi-linear system is solved for the RMS level of the input to the quasi-linearized deadzone element, σ_ϵ, as a function of K_{dz}, the equivalent gain of the deadzone element.
3. If the above function of K_{dz} is plotted with the Gaussian random input describing function for the deadzone element on K_{dz} versus ratio of deadzone size to RMS deadzone input coordinates, the curves intersect for some value of K_{dz}. At this value, the RMS value of the input to K_{dz} in the quasi-linear system is the same RMS value for which K_{dz} is the random input describing function for the deadzone element.
4. The above value of K_{dz} is used in a straight-forward linear analysis to compute the RMS levels of the variables of interest, u and θ.

Denoting input to K_{dz} by ϵ

$$\frac{\epsilon}{u_g}(A) = \frac{sH}{sH + AU} \tag{4-22}$$

where $A = K_{dz}\, C$, and:

$$\epsilon(A) = \frac{sH\sigma\sqrt{U_0/L}\sqrt{\pi}}{(sH + AU)\,(s + U_0/L)} \tag{4-23}$$

*$\mathbf{0}(\ )$ indicates the order of magnitude of whatever number is placed within the parentheses.

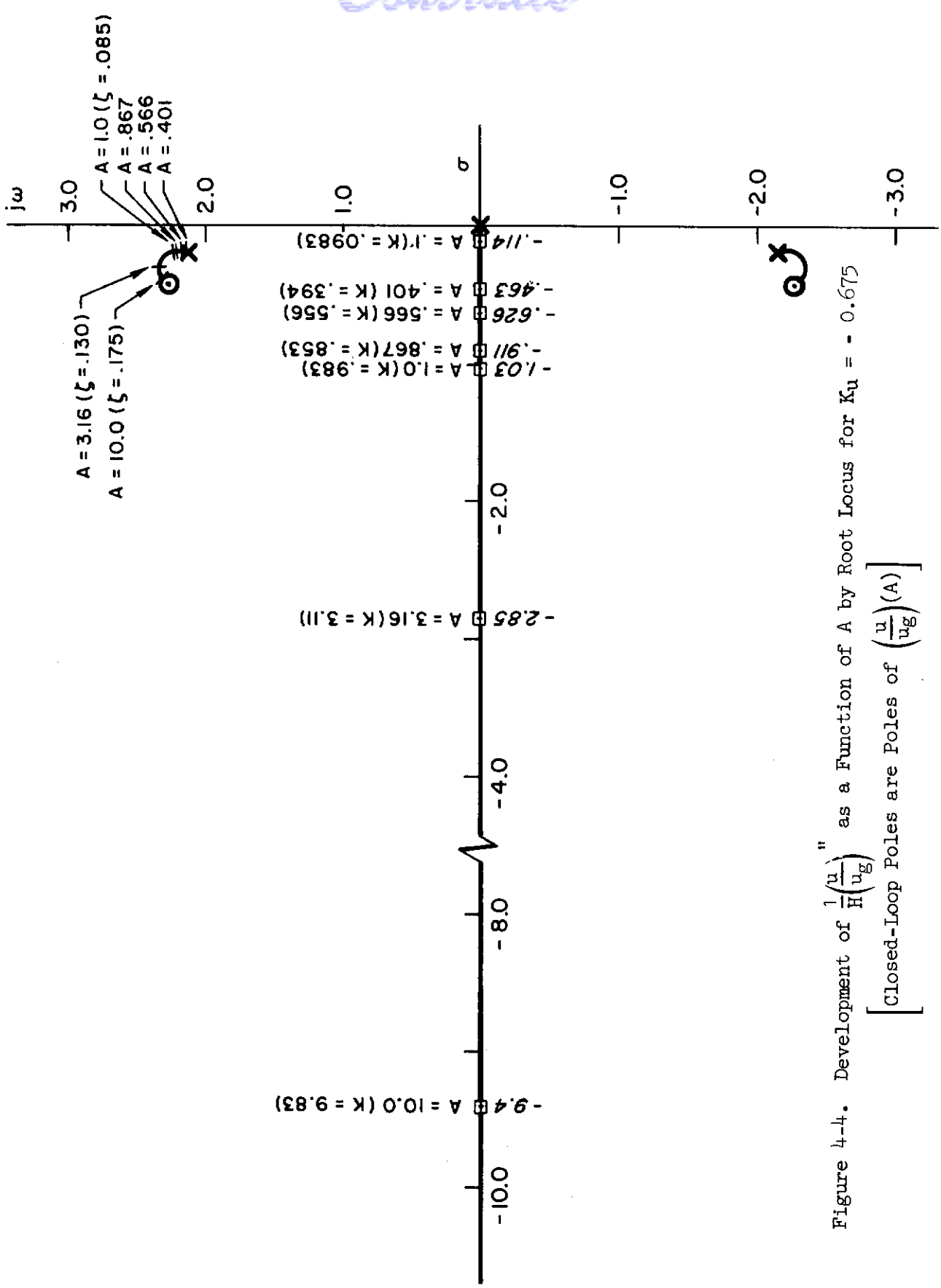

Figure 4-4. Development of $\frac{1}{H\left(\frac{u}{u_g}\right)}$ as a Function of A by Root Locus for $K_u = -0.675$

$$\left[\text{Closed-Loop Poles are Poles of } \left(\frac{u}{u_g}\right)(A)\right]$$

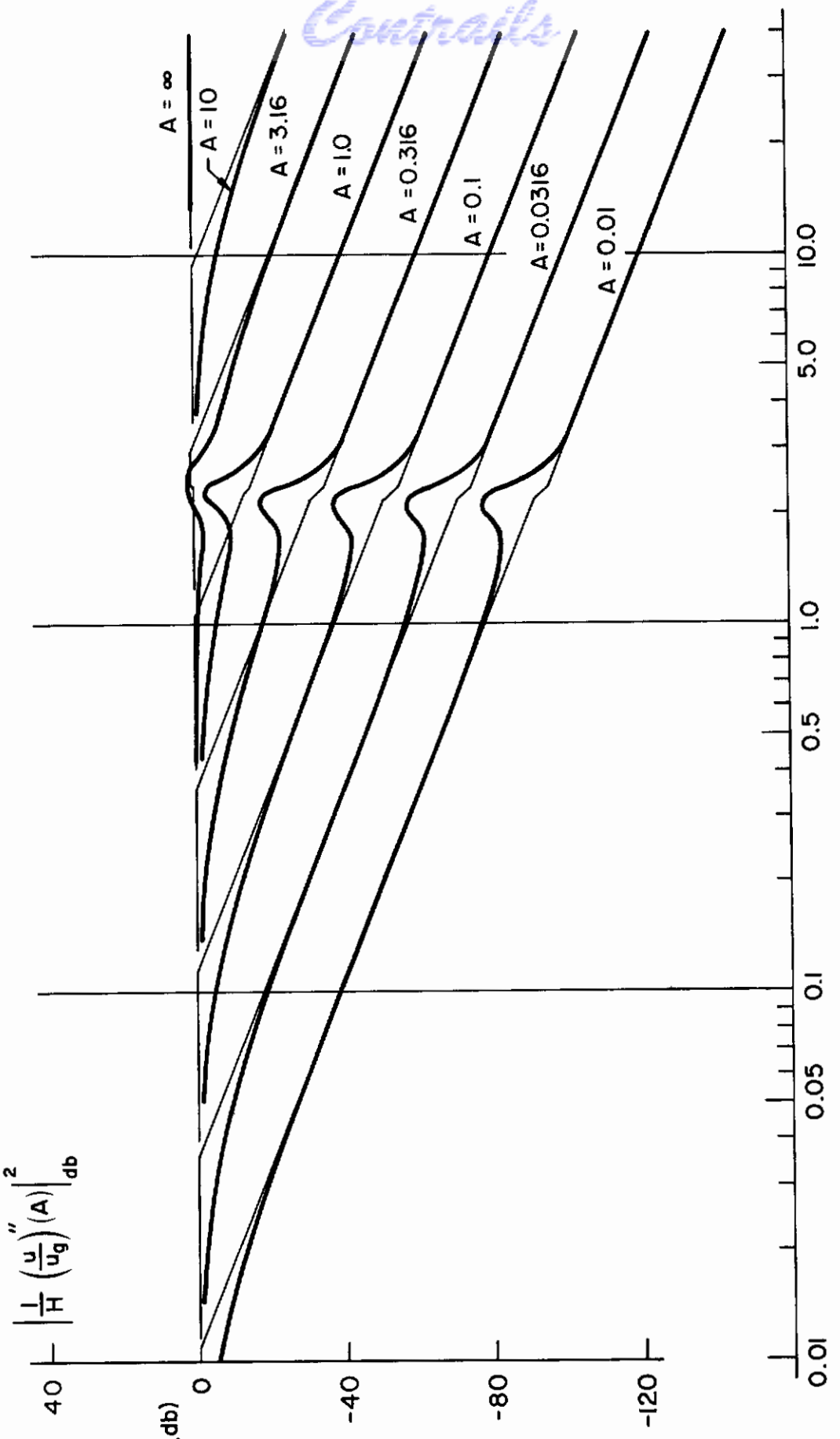

Figure 4-5. Modification Factor for u Spectrum Arising from Nonlinear Effect for $K_u = -0.675$

Consider a hysteresis half-loop width, a, of 8.0 ft./sec., an RMS gust level of 10 ft./sec. = σ, a head or tail wind of 10 ft./sec = U_0, and a turbulence scale length, L, of 100 ft.* (Since only the ratio of U_0/L enters the computation, we will actually be considering all U_0 and L (or h) such that $U_0/L = 0.1$, $L = 0.93h$.)

Then for $K_u = -0.675$

$$\epsilon(A) = \frac{10\sqrt{0.1/\pi}}{\left[1 + F(s)\right](s + 0.1)} \tag{4-24}$$

where

$$F(s) = \frac{A}{s} \frac{s^2 + 2(.19)\,2.31s + (2.31)^2}{s^2 + 2(.093)\,(2.155)s + (2.155)^2} \frac{s^2 + 2(.272)\,(6.90)s + (6.90)^2}{s^2 + 2(.272)\,(6.95)s + (6.95)^2}$$

$$\doteq \frac{A}{s} \frac{(2.31)^2}{(2.155)^2} \frac{(6.90)^2}{(6.95)^2} \doteq 1.13 \frac{A}{s}$$

for $|s| < 2.155$.

$$\epsilon(A) \doteq \frac{10\sqrt{0.1/\pi}\, s}{(s + 1.13A)(s + 0.1)} = \frac{10\sqrt{0.1/\pi}\, s}{(s + 20K_{dz})(s + 0.1)} \tag{4-25}$$

where $1.13\,C = 20$. $\overline{\epsilon^2}$ as a function of K_{dz} may be obtained by evaluating the following integral. (See Ref. 29).

$$\overline{\epsilon^2} \doteq \frac{20}{2\pi j} \int_{-j\infty}^{+j\infty} \frac{s}{(s + 20\,K_{dz})(s + 0.1)} \frac{(-s)}{(-s + 20\,K_{dz})(-s + 0.1)}\, ds \tag{4-26}$$

*The turbulence scale length is taken to be proportional to altitude for altitudes less than 1000 ft. See Refs. 27 and 28. $L = 0.93h$, $h < 1000$ ft.

$$\overline{\epsilon^2} \doteq \frac{0.5}{K_{dz} + 0.005} \doteq \sigma_\epsilon^2 \qquad (4\text{-}27)$$

Computation of other cases for different values of U_0/L and K_u are carried out in a similar manner although the computations are more complex because approximations such as in Eq. 4-25 for the case shown cannot then be made. Results for $U_0/L = 0.1, 0.2$ and $K_u = -0.675, -0.0575$ are summarized in the following table and Figure 4-6 along with the values of K_{dz} for which $\sigma_\epsilon(K_{dz})$ intersects the deadzone describing function curve.

We need not consider various σ values because of the quasi-linear nature of the ultimate system model. What is of main importance is covering the range in A from U_0/L to the frequency of the dominant system mode.

C	K_u	U_0/L $(sec)^{-1}$	K_{dz}	a/σ_ϵ $(sec)^2$	K_{dz} intersect.
20/1.13	-.675	0.1	0.01	1.39	
			0.03	2.12	
			0.05	2.65	0.032
20/1.13	-.675	0.2	0.03	1.60	
			0.05	1.96	
			0.07	2.26	0.049
0.5/0.994	-.0575	0.1	.15	1.205	
			.20	1.283	
			.25	1.357	0.200
2.0/0.994	-.0575	0.2	.15	1.28	
			.20	1.39	0.181

Notice that $a/\sigma_\epsilon \geq 0(1)$ indicating that the values of C used are adequate in magnitude.

The values of K_{dz} at the intersections are used to compute the quasi-linear transfer functions for u/u_g and θ/u_g which are necessary to compute σ_u and σ_θ.

Continuing the sample computation, we find that $A = C\ K_{dz_{intersect.}} =$ (20/1.13) (0.032) = 0.566. The poles of the closed-loop quasi-linear transfer functions can be found from Figure 4-4. The zeros of the $\left(u/u_g\right)''$ and $\left(\theta/u_g\right)''$ transfer functions are not affected by the nonlinearity. Therefore the zeros

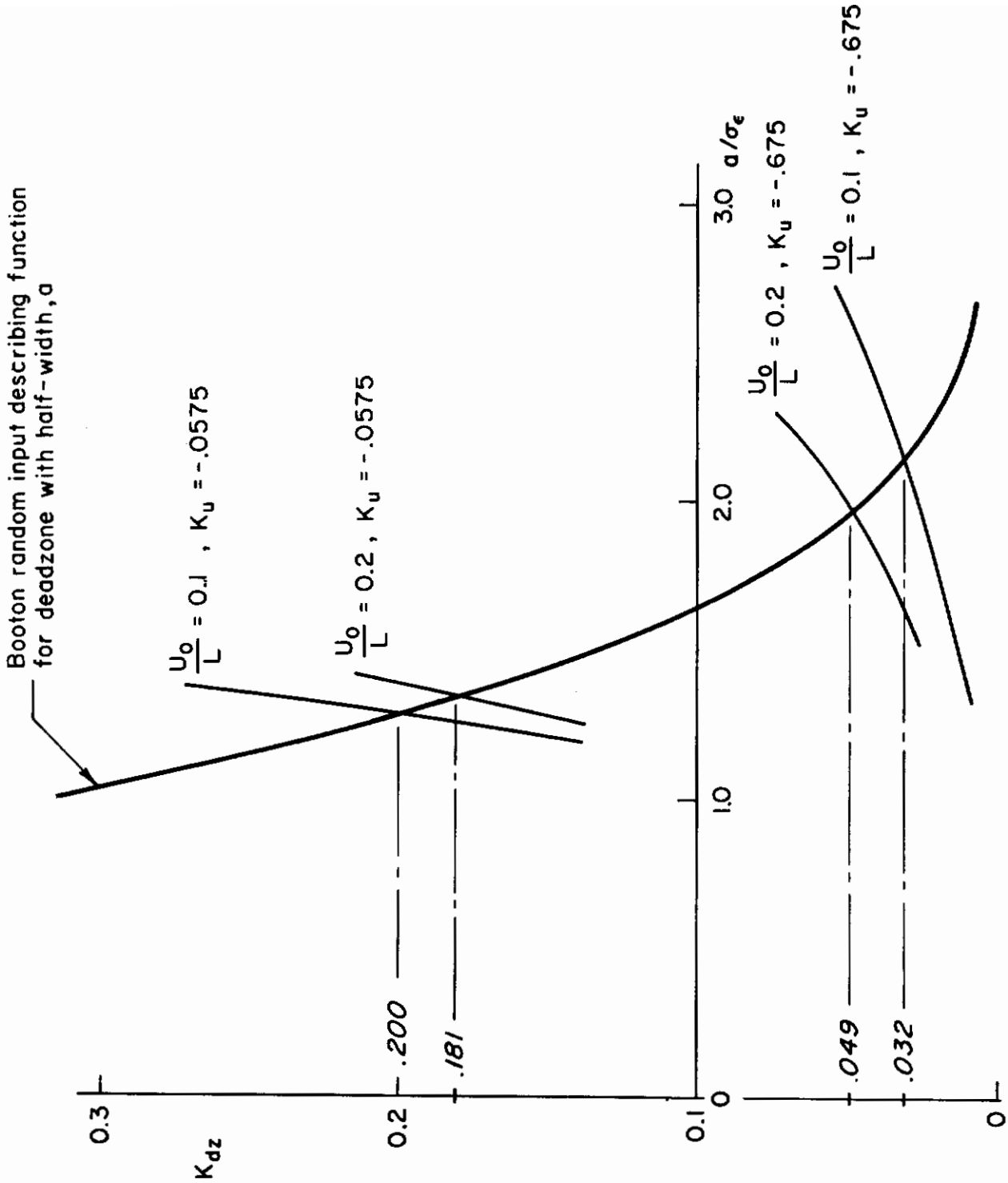

Figure 4-6. Describing Function Curve and System Function Curves for Pilot-XC-142 System

of the $\left(u/u_g\right)''$ transfer function are those of H.

$$\left(\frac{u}{u_g}\right)''(A) = \frac{-A(.43)\ (s + 1.45)\ (s^2 + 2(.19)\ 7.25s + (7.25)^2)}{s(s^2 + 2(.093)\ 2.155s + (2.155)^2)\ (s^2 + 2(.272)\ 6.95s + (6.95)^2)}$$

$$+ A(s^2 + 2(.19)\ 2.31s + (2.31)^2)\ (s^2 + 2(2.72)\ 6.90s + (6.90)^2) \quad (4\text{-}28)$$

Dividing through by $(s^2 + 2(.272)\ 6.95s + (6.95)^2)$ and using a previous low frequency approximation plus the approximation

$$- A(.43)\ (s + 1.45)\ \frac{s^2 + 2(.19)\ 7.25s + (7.25)^2}{s^2 + 2(.272)\ 6.95s + (6.95)^2}$$

$$\doteq - A(.43)\ (s + 1.45)\ \frac{(7.25)^2}{(6.95)^2} = - .468A\ (s + 1.45)$$

for $|s| \leq 6.95$ gives:

$$\left(\frac{u}{u_g}\right)''(A) = \frac{A\ (-.468)\ (s + 1.45)}{s(s^2 + 2\ (.093)(2.155)\ s + (2.155)^2)} \quad (4\text{-}29)$$

$$+ 0.983A\ (s^2 + 2\ (.19)\ 2.31\ s + (2.31)^2)$$

$$\left(\frac{u}{u_g}\right)''(.566) = \frac{(.566)\ (-.468)\ (s + 1.45)}{(s + .626)\ (s^2 + 2\ (.09)\ (2.21)\ s + (2.21)^2)} \quad (4\text{-}30)$$

$$u''(.566) = \frac{10\sqrt{0.1/\pi}\ (.566)\ (-.468)\ (s + 1.45)}{(s + .1)\ (s + .626)\ (s^2 + 2\ (.09)\ 2.21\ s + (2.21)^2)} \quad (4\text{-}31)$$

The evaluation of Phillip's integrals in Ref. 29 may again be used to calculate σ_u and σ_θ.

In order to calculate σ_θ, the $(\theta/u)''$ quasi-linear transfer function is required.

$$(\theta/u)'' = \frac{M_u^*\ s + Y_{p_u}\ M_{\delta_e}\ (-X_u^*)}{-(-X_u^*)\ \left\{s(s - M_q) + Y_{p_\theta}\ M_{\delta_e}\right\} - gM_u^*} \quad (4\text{-}32)$$

The results of these computations are summarized in the following table.

U_0/L $(sec)^{-1}$	K_u	$A(sec)^{-1}$	$\sigma_u\left(\frac{ft}{sec}\right)$	σ_θ(deg)
0.1	-.675	∞	1.59	7.13
		.566	1.26	6.38
0.2		∞	1.72	7.53
		.867	1.06	6.40
0.1	-.0575	∞	6.20	2.70
		.1006	5.76	2.55
0.2		∞	5.97	2.61
		.401	6.275	2.74

Results

Calculated values for σ_u and σ_θ indicate that the break frequency of the describing function, A, has little effect upon σ_u and σ_θ when $A \geq U_0/L$ and the pilot is providing a reasonable amount of attitude stabilization. Of course, as $A \rightarrow 0$ σ_u and σ_θ will approach zero also. More important by far in determining system performance, is the pilot's velocity loop closure gain, K_u. The results indicate that in all likelihood, the pilot will adjust this gain to achieve a tradeoff between σ_u and σ_θ to his liking.

The above results arise from the fact that the hysteresis nonlinearity is in the forward portion of a closed loop with respect to u_g inputs, and this closed loop has low open-loop gain. This, combined with the high-gain loop closure the pilot supplies for attitude stabilization, makes the effect of the nonlinear loop closure quite unimportant on a comparative basis. Hence the effect of the non-linearity is essentially open-loop in nature. That is, the damping and frequency of the $UA/(s + A)$ transfer function poles are nearly the same as the poles of $(u/u_g)"(A)$. Handling qualities theory has enabled us to show that dominant mode damping ratios on the order of 0.1 and greater, and bandwidths on the order of 1.0 rad./sec. and greater are achievable in the case of the XC-142 through pilot control, and assures us, therefore, that the nonlinear effects will not significantly alter the pole positions of the closed-loop pilot-vehicle system.

In fact, considering Figure 4-5 it is quite evident that decreasing values of A (increasing ratio of hysteresis loop width to RMS input) will be beneficial, rendering the pilot-hovering tilt-wing VTOL system relatively less sensitive to gusts in relatively calm air than it would otherwise be if X_u and M_u were linear.

Because the effects of X_u and M_u are so nearly open-loop in nature, it would be uninteresting to pursue the case of separate treatment of the individual nonlinear characteristics further. It is inevitable that the parameters for each nonlinearity will be nearly identical and the results would not shed new light on the problem.

Finally, when comparisons of our end results are made with our initial expectations based upon the vehicle characteristics alone, the discrepancy between them should serve as a strong reminder that it is most often foolish to predict pilot-vehicle system performance on the basis of vehicle characteristics alone.

REFERENCES

1. Graham, Dunstan, Duane McRuer, Analysis of Nonlinear Control Systems, John Wiley, New York, 1961.

2. Ergin, E. I., V. D. Norum, T. G. Windeknecht, Techniques for Analysis of Nonlinear Attitude Control Systems for Space Vehicles, Vols. I-IV, TDR-62-208, Aeronautical Systems Division, Wright-Patterson Air Force Base, Ohio, June 1962.

3. Gibson, J. E., Nonlinear Automatic Control, McGraw-Hill, New York, 1963.

4. Chen, K., "Quasi-Linearization Techniques for Transient Study of Nonlinear Feedback Control Systems," Trans. AIEE, Vol. 75, Pt II, (1956).

5. Smith, H. K., "The Applicability of Quasi-linear Methods to Non-linear Feedback Systems with Random Inputs," to be published in the 1963 IFAC Congress Proceedings.

6. Ogata, K., "An Analytic Method for Finding the Closed Loop Frequency Response of Nonlinear Feedback Control Systems," Trans. AIEE, Vol. 76, Pt. II, (1957).

7. Glenn, J. E., "Manual Flight Control System Functional Characteristics," IEEE Trans. on Human Factors in Electronics, Vol. HFE-4, No. 1, (Sept. 1963), pp. 29-37.

8. Ashkenas, I. L., H. R. Jex, D. T. McRuer, Pilot-Induced Oscillations: Their Cause and Analysis, TR-239-2, Systems Technology, Inc., Inglewood, Calif., and NOR-64-143, Norair Division, Northrop Corp., Hawthorne, Calif., 20 June 1964.

9. Crane, H. L., "Analog-Computer Investigation of Effects of Friction and Preload on the Dynamic Longitudinal Characteristics of a Pilot-Airplane Combination," TN D-884, NASA, Washington, D. C., 1961.

10. Ashkenas, I. L., Valve Friction in Fully-Powered Hydraulic Systems, unpublished notes, 17 September 1959.

11. McRuer, D. T. (ed.), The Hydraulic System, BuAer Report AE-61-4IV, Bureau of Aeronautics, Navy Department, March 1953.

12. Den Hartog, J. P., Mechanical Vibrations (2nd Edition), McGraw-Hill Book Co., Inc., New York, N. Y., 1940.

13. Gardner, M. F. and J. L. Barnes, Transients in Linear Systems, John Wiley and Sons, Inc., New York, N. Y., 1942.

14. McRuer, D. T. (ed.), Methods of Analysis and Synthesis of Piloted Aircraft Flight Control Systems, BuAer Report AE-61-4I, Bureau of Aeronautics, Navy Department, March 1952.

15. West, J. C., Analytical Techniques for Non-linear Control Sytems, English Universities Press, London 1960.

16. Peters, R. A., V. J. Kovacevich, Dunstan Graham, Single-Axis Attitude Regulation of Extra-Atmospheric Vehicles, TR 61-129, Aeronautical Systems Division, Wright-Patterson Air Force Base, Ohio, February 1962.

17. Patapoff, H., Rate Diagram Method of Analysis of an On-Off Control System, TR-60-0000-19323, Space Technology Laboratories, Inc., Los Angeles, California, July 1960.

18. Tsypkin, J. A., Theorie der Relaissysteme der automatischen Regelung (a translation of the Russian edition of 1955), R. Oldenbourg Verlag, Munich 1958.

19. Leland, H. R., "Input-Output Cross-Correlation Functions for Some Memory Type Nonlinear Systems with Gaussian Input ," Applications and Industry, AIEE, No. 49, July 1960.

20. Brown, W. A., "Linearisation of Backlash in Control Systems with Random Inputs," Proc. IEE, Vol. III, No. 2, February 1964.

21. Wolkovitch, J. and R. P. Walton, VTOL and Helicopter Approximate Transfer Functions and Closed-Loop Handling Qualities, BuWeps TR 128-1, September 1963.

22. McRuer, D. T., C. L. Bates, I. L. Ashkenas (Eds.), Dynamics of the Airframe, Bu Aer Report AE-61-4 II, Bureau of Aeronautics, Navy Department, September, 1952.

23. Walton, R. P., Transfer Function Description of XC-142 and X-22A VTOL Configurations in Transition Flight, Systems Technology, Inc., TM 135-I-1, April 1964.

24. Ashkenas, I. L. and D. T. McRuer, "A Theory of Handling Qualities Derived from Pilot-Vehicle System Considerations," Aerospace Engineering, Vol. 21, No. 2, February 1962.

25. McRuer, D. T., I. L. Ashkenas and H. R. Pass, Analysis of Multiloop Vehicular Control Systems, ASD-TDR-62-1014, March 1964.

26. Clark, L. G. and D. Graham, Summary of Analyses of Closed-Loop VTOL Aircraft Flight, Systems Technology, Inc., TM 135-II-2, February 1964.

27. Etkin, B., Theory of the Flight of Airplanes in Isotropic Turbulence: Review and Extension, UTIA Report No. 72, February 1961.

28. Etkin, B., A Simple Method for the Analogue Computation of the Mean-Square Response of Airplanes to Atmospheric Turbulence, UTIA Technical Note No. 32, January 1960.

29. Newton, G. C. Jr., Gould, L. A. and Kaiser, J. F., Analytical Design of Linear Feedback Controls, John Wiley, New York, 1957.

30. McRuer, Duane T., Unified Analysis of Linear Feedback Systems, ASD TR 61-118, July 1961.

APPENDIX A

EQUATIONS FOR GENERALIZED PERIODIC INPUT DESCRIBING FUNCTION CALCULATION

The equations given below are applicable when a single isolated nonlinear element is contained in a closed loop which otherwise contains only constant coefficient linear elements. The nonlinearity must be describable piecewise by algebraic functions of the nonlinearity input. Simple and complex (e.g. hysteresis) nonlinearities are included although the latter may require some small amount of logical description in addition to the piecewise algebraic description.

Cascaded linear elements contained in the loop are given by $G(jm\omega)$, the complex gain of the linear elements at the m^{th} harmonic of the fundamental frequency, ω. The amplitude ratio squared and phase angle of a general $G(jm\omega)$, using the notation of Ref. 30, is given by Eqs. A-1 and A-2. An arbitrary constant phase shift, $e^{j\Delta}$, has been included in these equations to assist in obtaining an initial solution to the problem (see Chapter III).

1. Frequency Response and Sensitivity for Linear Portion of the Open-loop.

   a. Amplitude ratio squared

$$|G(jm\omega)|^2 = \frac{K^2 \prod_{j=1}^{w} \left[\left(1 - \left\{\frac{m\omega}{\omega_j}\right\}^2\right)^2 + \left(\frac{2\zeta_j m\omega}{\omega_j}\right)^2\right]}{(m\omega)^{2k} \prod_{i=1}^{v} \left[\left(1 - \left\{\frac{m\omega}{\omega_i}\right\}^2\right)^2 + \left(\frac{2\zeta_i m\omega}{\omega_i}\right)^2\right]}$$

$$\frac{\prod_{j=2w}^{n} \left[1 + (T_j m\omega)^2\right]}{\prod_{i=2v}^{m+n-k} \left[1 + (T_i m\omega)^2\right]} \quad * \qquad \text{(A-1)}$$

*In following the notational precedent set in Ref. 30 we must pay special attention to the fact that the product over i refers to a different set of roots than the product over j. Despite the apparent similarity of the numerator and denominator roots in the generalized notational form used, cancellations will not occur to the extent that the two sets of roots are numerically different.

b. Phase angle

$$\measuredangle G(jm\omega) + \Delta = \sum_{j=1}^{w} \tan^{-1}\left[\frac{\frac{2\zeta_j m\omega}{\omega_j}}{1 - \left\{\frac{m\omega}{\omega_j}\right\}^2}\right] + \sum_{j=2w}^{n} \tan^{-1}\left|T_j m\omega\right| + \text{logic} + \text{logic}$$

$$- \sum_{i=1}^{v} \tan^{-1}\left[\frac{\frac{2\zeta_i m\omega}{\omega_i}}{1 - \left\{\frac{m\omega}{\omega_i}\right\}^2}\right] - \sum_{i=2v}^{m+n-k} \tan^{-1}\left|T_i m\omega\right| - \frac{k\pi}{2} - m\omega\tau + \Delta + \text{logic} + \text{logic} \qquad \text{(A-2)}$$

Logic function for inverse trig. function arguments

Numerator Sign of Argument	Denominator Sign of Argument	Relation of Actual Angle to Principle Value
+	+	(PV)
-	+	- (PV)
-	-	π + (PV)
+	-	π - (PV)

The principal value, (PV), is assumed to range from 0 to $\pi/2$.

c. Amplitude ratio squared sensitivity to frequency

$$\frac{\partial\left(\left|G(jm\omega)\right|^2\right)}{\partial\omega} = \frac{2}{\omega}\left|G(jm\omega)\right|^2$$

$$\left\{-k + \sum_{j=1}^{w} \frac{\left[\left(\frac{2\zeta_j m\omega}{\omega_j}\right)^2 - 2\left(1 - \left\{\frac{m\omega}{\omega_j}\right\}^2\right)\left[\frac{m\omega}{\omega_j}\right]^2\right]}{\left[\left(1 - \left\{\frac{m\omega}{\omega_j}\right\}^2\right)^2 + \left(\frac{2\zeta_j m\omega}{\omega_j}\right)^2\right]}\right.$$

$$+\sum_{j=2w}^{n}\frac{(T_j m\omega)^2}{\left[1+(T_j m\omega)^2\right]}$$

$$-\sum_{i=1}^{v}\frac{\left[\left(\frac{2\zeta_i m\omega}{\omega_i}\right)^2-2\left(1-\left\{\frac{m\omega}{\omega_i}\right\}^2\right)\left[\frac{m\omega}{\omega_i}\right]^2\right]}{\left[\left(1-\left\{\frac{m\omega}{\omega_i}\right\}^2\right)^2+\left(\frac{2\zeta_i m\omega}{\omega_i}\right)^2\right]}$$

$$-\sum_{i=2v}^{m+n-k}\frac{(T_i m\omega)^2}{\left[1+(T_i m\omega)^2\right]}\Bigg\} \qquad \text{(A-3)}$$

d. Phase angle sensitivity to frequency

$$\frac{\partial(\angle G(jm\omega)+\Delta)}{\partial\omega}=\frac{\partial\angle G(jm\omega)}{\partial\omega}=-m\tau$$

$$+\frac{1}{\omega}\Bigg\{\sum_{j=1}^{w}\frac{\left(\frac{2\zeta_j m\omega}{\omega_j}\right)\left(1+\left\{\frac{m\omega}{\omega_j}\right\}^2\right)}{\left[\left(1-\left\{\frac{m\omega}{\omega_j}\right\}^2\right)^2+\left(\frac{2\zeta_j m\omega}{\omega_j}\right)^2\right]}+\sum_{j=2w}^{n}\frac{(T_j m\omega)}{\left[1+(T_j m\omega)^2\right]} \qquad \text{(A-4)}$$

$$-\sum_{i=1}^{v}\frac{\left(\frac{2\zeta_i m\omega}{\omega_i}\right)\left(1+\left\{\frac{m\omega}{\omega_i}\right\}^2\right)}{\left[\left(1-\left\{\frac{m\omega}{\omega_i}\right\}^2\right)^2+\left(\frac{2\zeta_i m\omega}{\omega_i}\right)^2\right]}-\sum_{i=2v}^{m+n-k}\frac{(T_i m\omega)}{\left[1+(T_i m\omega)^2\right]}\Bigg\}$$

2. Generalized Describing Function and its Sensitivity for the Isolated Nonlinear Element of the Open Loop.

a. Definition of nonlinear element input-output characteristics

$$x_0'=f(x_i) \qquad \text{(A-5)}$$

where x_0' is the output of the nonlinear element

x_i is the input to the nonlinear element

The function f relates the input, x_i, to the output, x_o'. In application, the function f may be composed of several algebraic functions, f_r, each of which obtains over some interval in x_i.

b. Definition and composition of the x_i and x_o signals.

$$x_i \triangleq \sum_{m=1}^{M} c_m \sin (m\theta + \psi_m) \qquad \text{(A-6)}$$

$$\psi_1 \triangleq 0 \qquad \theta \triangleq \omega t$$

$$x_o \triangleq \sum_{m=1}^{M'} C_m \sin (m\theta + \varphi_m) \doteq x_o' \qquad \text{(A-7)}$$

x_o is a truncated series approximation to x_o'. The truncation is performed such that M' = M or M' = M + 1; the latter case is an alternate statement of one special case of interest wherein M' = M with $c_M = 0$.

c. Definition of the generalized describing function.

For the m^{th} harmonic the negative inverse describing function amplitude ratio squared is:

$$\left|-1/N_m\right|^2 = \frac{c_m^2}{C_m^2} = \frac{c_m^2}{A_m^2 + B_m^2} \qquad \text{(A-8)}$$

The negative inverse describing function phase angle is:

$$\measuredangle\,(-1/N_m) = \psi_m - \varphi_m - \pi = \psi_m - \tan^{-1}\left[\frac{A_m}{B_m}\right] - \pi \qquad \text{(A-9)}$$

$$+ \text{ logic}$$

A_m and B_m are given by the following equations:

$$A_m = \frac{1}{\pi}\int_0^{2\pi} f(\theta;\, c_1, c_2, \ldots, c_M;\, \psi_2, \psi_3, \ldots, \psi_M) \cos m\theta\, d\theta \qquad \text{(A-10)}$$

$$B_m = \frac{1}{\pi}\int_0^{2\pi} f(\theta;\ c_1,\ c_2,\ \ldots,\ c_M;\ \psi_2,\ \psi_3,\ \ldots,\ \psi_M)\ \sin m\theta d\theta \qquad \text{(A-11)}$$

In these equations, the integral over θ must be considered in parts corresponding to intervals in θ (or x_i) over which a single algebraic function, f_r, represents the function, f. The end points of these intervals will be denoted by θ_r. The equations for A_m and B_m may then be written explicitly in terms of these intervals in θ over a range from 0 to 2π.

$$A_m = \frac{1}{\pi}\sum_{r=1}^{R}\int_{\theta_{r-1}}^{\theta_r} f_r(\theta;\ c_1,\ c_2,\ \ldots,\ c_M;\ \psi_2,\ \psi_3,\ \ldots,\ \psi_M)\ \cos m\theta d\theta \qquad \text{(A-12)}$$

$$B_m = \frac{1}{\pi}\sum_{r=1}^{R}\int_{\theta_{r-1}}^{\theta_r} f_r(\theta;\ c_1,\ c_2,\ \ldots,\ c_M;\ \psi_2,\ \psi_3,\ \ldots,\ \psi_M)\ \sin m\theta d\theta \qquad \text{(A-13)}$$

$$\theta_0 \triangleq 0 \text{ and } \theta_R \triangleq 2\pi.$$

The intermediate intervals are determined by the solutions to a set of transition point equations which are assumed to be of the form

$$F_r(x_i) = 0\ , \quad r = 1,\ 2,\ \ldots,\ R \qquad \text{(A-14)}$$

which is adequate to describe relay, dead zone, saturation, etc., characteristics. (A more complex description is required for complex nonlinearities.)

Transition point equations express the transition from one algebraic equation describing the nonlinear characteristic to another algebraic equation describing the nonlinear characteristic. This may be diagramed as shown:

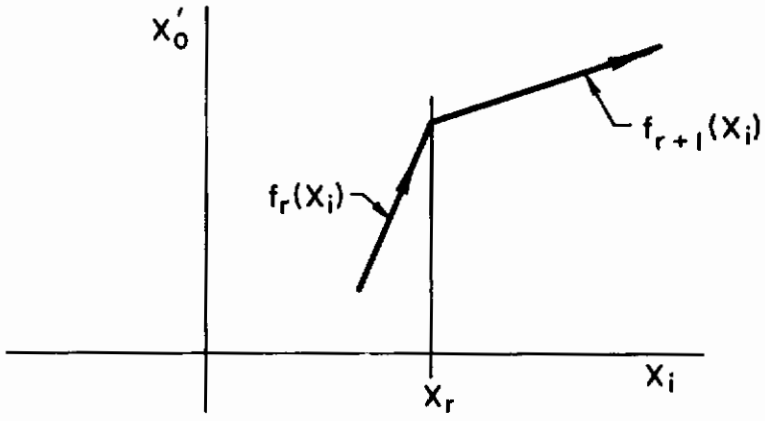

The transition point equation for the case shown above is:

$$F_r(x_i) = x_i - x_r = 0 \tag{A-15}$$

or

$$\left[\sum_{m=1}^{M} c_m \sin(m\theta + \psi_m)\right] - x_r = 0 \tag{A-16}$$

A solution to this equation is $\theta = \theta_r$. The r index is incremented every time x_i passes through a transition point such as x_r shown. As x_i executes a single period, i.e., as θ ranges from 0 to 2π, certain transition point equations may be repeated because some transition point equations will have multiple solutions in θ. For the purpose of this problem, the transition points are most easily considered in order of increasing θ in the interval $0 < \theta < 2\pi$. The reason for this is obvious upon considering the equation for A_m and B_m since successive values of the transition points, θ_r, are required for these calculations.

In practice, the transition points, θ_r, would be found by incrementing through the θ variable in the 0 to 2π interval and noting those values of θ for which a transition point equation is satisfied.

a. Sensitivity of the generalized describing function to α_g where α_g represents one member of the set of problem parameters $c_1, c_2, \ldots, c_M; \psi_2, \psi_3, \ldots, \psi_M$.

Sensitivity of the m^{th} harmonic negative inverse describing function squared to α_g.

$$\frac{\partial(|-1/N_m|^2)}{\partial\alpha_g} = 2\left(\frac{c_m C_m \frac{\partial c_m}{\partial\alpha_g} - c_m^2 \frac{\partial C_m}{\partial\alpha_g}}{c_m^3}\right) \tag{A-17}$$

Sensitivity of the m^{th} harmonic negative inverse describing function phase to α_g.

$$\frac{\partial(\measuredangle - 1/N_m)}{\partial\alpha_g} = \frac{\partial\psi_m}{\partial\alpha_g} - \frac{\partial\varphi_m}{\partial\alpha_g} \tag{A-18}$$

$$\frac{\partial\varphi_m}{\partial\alpha_g} = \frac{1}{A_m^2 + B_m^2}\left\{B_m \frac{\partial A_m}{\partial\alpha_g} - A_m \frac{\partial B_m}{\partial\alpha_g}\right\} \tag{A-19}$$

Recall that α_g is a dummy parameter that may represent any <u>one</u> of the parameters, $c_1, c_2, \ldots, c_M; \psi_2, \psi_3, \ldots, \psi_M$. Eqs. A-20 through A-23 follow directly from this fact. The introduction of a dummy parameter enables the equations to be written in a form which is considerably more compact than would be possible otherwise.

$$\frac{\partial c_m}{\partial\alpha_g} = 1.0 \qquad \text{for } \alpha_g = c_m \tag{A-20}$$

$$\frac{\partial c_m}{\partial\alpha_g} = 0 \qquad \text{for } \alpha_g \neq c_m \tag{A-21}$$

$$\frac{\partial\psi_m}{\partial\alpha_g} = 1.0 \qquad \text{for } \alpha_g = \psi_m \tag{A-22}$$

$$\frac{\partial\psi_m}{\partial\alpha_g} = 0 \qquad \text{for } \alpha_g \neq \psi_m \tag{A-23}$$

$$\frac{\partial C_m}{\partial\alpha_g} = \frac{1}{(A_m^2 + B_m^2)^{1/2}}\left\{A_m \frac{\partial A_m}{\partial\alpha_g} + B_m \frac{\partial B_m}{\partial\alpha_g}\right\} \tag{A-24}$$

$$\frac{\partial A_m}{\partial\alpha_g} = \frac{1}{\pi}\sum_{r=1}^{R}\left\{\int_{\theta_{r-1}}^{\theta_r} \frac{\partial f_r}{\partial x_i}\left[\frac{\partial c_m}{\partial\alpha_g}\sin(m\theta + \psi_m)\right.\right.$$

$$+ \frac{\partial \psi_m}{\partial \alpha_g} c_m \cos(m\theta + \psi_m) \Bigg] \cos m\theta \, d\theta$$

$$+ f_r(\theta_r) \frac{\partial \theta_r}{\partial \alpha_g} \cos m\theta_r - f_r(\theta_{r-1}) \frac{\partial \theta_{r-1}}{\partial \alpha_g} \cos m\theta_{r-1} \Bigg\} \qquad \text{(A-25)}$$

$$\frac{\partial B_m}{\partial \alpha_g} = \frac{1}{\pi} \sum_{r=1}^{R} \Bigg\{ \int_{\theta_{r-1}}^{\theta_r} \frac{\partial f_r}{\partial x_i} \Bigg[\frac{\partial c_m}{\partial \alpha_g} \sin(m\theta + \psi_m)$$

$$+ \frac{\partial \psi_m}{\partial \alpha_g} c_m \cos(m\theta + \psi_m) \Bigg] \sin m\theta \, d\theta \qquad \text{(A-26)}$$

$$+ f_r(\theta_r) \frac{\partial \theta_r}{\partial \alpha_g} \sin m\theta_r - f_r(\theta_{r-1}) \frac{\partial \theta_{r-1}}{\partial \alpha_g} \sin m\theta_{r-1} \Bigg\}$$

The $\partial f_r / \partial x_i$ may usually be hand computed (algebraically). Note that the last two terms in the braces in Eqs. A-25 and A-26 result from the fact that the limits of integration in Eqs. A-12 and A-13 are functions of $c_1, c_2, \ldots, c_M; \psi_2, \psi_3, \ldots, \psi_M$. The last two terms in the braces of Eqs. A-25 and A-26 are cancelled by negative counterparts in the summation over r <u>if</u> f is a continuous function. That is, if $f_r(\theta_{r-1}) = f_{r-1}(\theta_{r-1})$ over all r. $f_r(\theta_r)$ and $f_r(\theta_{r-1})$ are constants which are the nonlinearity output signal levels at the transition points r and r-1 respectively in r.

Transition point sensitivity to α_g.

To calculate $\partial \theta_r / \partial \alpha_g$, consider the equation defining θ_r.

$$F_r(x_i) = \sum_{m=1}^{M} c_m \sin(m\theta_r + \psi_m) - x_r = 0 \qquad \text{(A-27)}$$

If we regard x_i as a function of the intermediate variable, θ_r, and of the independent variables, $c_1, c_2, \ldots, c_M; \psi_2, \psi_3, \ldots, \psi_M$, then

$$\left(\frac{\partial F_r}{\partial \alpha_h}\right)_{\substack{\alpha_g \neq \alpha_h \\ \text{const.}}} = 0 \qquad \text{(A-28)}$$

for $\alpha_h = c_1, c_2, \cdots, c_M$. That is, α_h is a dummy parameter that may represent any one of the parameters, $c_1, c_2, \cdots, c_M$.

$$\left(\frac{\partial F_r}{\partial c_m}\right)_{\substack{\alpha_g \neq c_m \\ \text{const.}}} = 0 = \sin(m\theta_r + \psi_m) + \frac{\partial \theta_r}{\partial c_m} \sum_{m=1}^{M} m\, c_m \cos(m\theta_r + \psi_m) \qquad \text{(A-29)}$$

and:

$$\frac{\partial \theta_r}{\partial c_m} = \frac{-\sin(m\theta_r + \psi_m)}{\sum_{m=1}^{M} m\, c_m \cos(m\theta_r + \psi_m)} \qquad \text{(A-30)}$$

For $\alpha_h = \psi_2, \psi_3, \cdots, \psi_M$ (again α_h is a dummy parameter)

$$\left(\frac{\partial F_r}{\partial \psi_m}\right)_{\substack{\alpha_g \neq \psi_m \\ \text{const.}}} = 0 = c_m \cos(m\theta_r + \psi_m) + \frac{\partial \theta_r}{\partial \psi_m} \sum_{m=1}^{M} m\, c_m \cos(m\theta_r + \psi_m) \qquad \text{(A-31)}$$

and

$$\frac{\partial \theta_r}{\partial \psi_m} = \frac{-c_m \cos(m\theta_r + \psi_m)}{\sum_{m=1}^{M} m\, c_m \cos(m\theta_r + \psi_m)} \qquad \text{(A-32)}$$

3. Definition of a Positive Definite Criterion Function, Its Sensitivity to Δ, ω and α_g and Parameter Up-dating Equations.

$$e = \sum_{m=1}^{M} \beta_m^2 + \sum_{m=1}^{M'} \gamma_m^2 \qquad \text{(A-33)}$$

$$\beta_m \triangleq K_0 \left\{ \angle G(jm\omega) + \Delta - \angle - 1/N_m \right\} \qquad \text{(A-34)}$$

$$\gamma_m \triangleq \left\{ |G(jm\omega)|^2 - | - 1/N_m|^2 \right\} \qquad \text{(A-35)}$$

$$\frac{\partial \beta_m}{\partial \omega} = K_0 \frac{\partial(\angle G(jm\omega))}{\partial \omega} \qquad \text{(A-36)}$$

$$\frac{\partial \gamma_m}{\partial \omega} = \frac{\partial(|G(jm\omega)|^2)}{\partial \omega} \qquad \text{(A-37)}$$

$$\frac{\partial \beta_m}{\partial \alpha_g} = - K_0 \frac{\partial(\angle - 1/N_m)}{\partial \alpha_g} \qquad \text{(A-38)}$$

$$\frac{\partial \gamma_m}{\partial \alpha_g} = - \frac{\partial(| - 1/N_m|^2)}{\partial \alpha_g} \qquad \text{(A-39)}$$

where $\alpha_g = c_1, c_2, \ldots, c_M; \psi_2, \psi_3, \ldots, \psi_M$

Parameter up-dating equations using Newton's iterative method. The parameter changes are obtained by solution of Eq. A-40.

$$\begin{bmatrix} \frac{\partial\beta_1}{\partial\omega} & \frac{\partial\beta_1}{\partial c_1} & \cdots & \frac{\partial\beta_1}{\partial c_M} & \frac{\partial\beta_1}{\partial\psi_2} & \cdots & \frac{\partial\beta_1}{\partial\psi_M} \\ \vdots & \vdots & & \vdots & \vdots & & \vdots \\ \frac{\partial\beta_M}{\partial\omega} & \frac{\partial\beta_M}{\partial c_1} & \cdots & \frac{\partial\beta_M}{\partial c_M} & \frac{\partial\beta_M}{\partial\psi_2} & \cdots & \frac{\partial\beta_M}{\partial\psi_M} \\ \frac{\partial\gamma_1}{\partial\omega} & \frac{\partial\gamma_1}{\partial c_1} & \cdots & \frac{\partial\gamma_1}{\partial c_M} & \frac{\partial\gamma_1}{\partial\psi_2} & \cdots & \frac{\partial\gamma_1}{\partial\psi_M} \\ \vdots & \vdots & & \vdots & \vdots & & \vdots \\ \frac{\partial\gamma_{M'}}{\partial\omega} & \frac{\partial\gamma_{M'}}{\partial c_1} & \cdots & \frac{\partial\gamma_{M'}}{\partial c_M} & \frac{\partial\gamma_{M'}}{\partial\psi_2} & \cdots & \frac{\partial\gamma_{M'}}{\partial\psi_M} \end{bmatrix} \begin{Bmatrix} \delta\omega \\ \delta c_1 \\ \delta c_M \\ \delta\psi_2 \\ \vdots \\ \delta\psi_M \end{Bmatrix} = - \begin{Bmatrix} \beta_1 \\ \vdots \\ \beta_M \\ \gamma_1 \\ \vdots \\ \gamma_{M'} \end{Bmatrix} \quad \text{(A-40)}$$

APPENDIX B

ALGEBRAIC MODIFICATION OF THE TSYPKIN LOCUS TECHNIQUE FOR THE SATELLITE ATTITUDE CONTROL PROBLEM*

Two of the four necessary and sufficient conditions (often displayed by means of the Tsypkin locus) for a periodic solution of a system containing one off-on nonlinear element in a closed loop have been arranged into an algebraic form suitable for digital computation and specialized to treat the system shown in Fig. B-1.

Switching times of the off-on nonlinearity are computed to satisfy harmonic balance around the control loop. The fundamental frequency of the periodic oscillation and the amplitudes and phases of the harmonics are determined as by-products of the switching time calculations.

The remaining two necessary conditions are that the input to the nonlinearity has a negative first derivative with respect to time when switching off the positive torque pulse and when switching on the negative torque pulse. Satisfaction of these conditions is best verified by direct calculation after the switching times, frequencies, amplitudes and phase have been found.

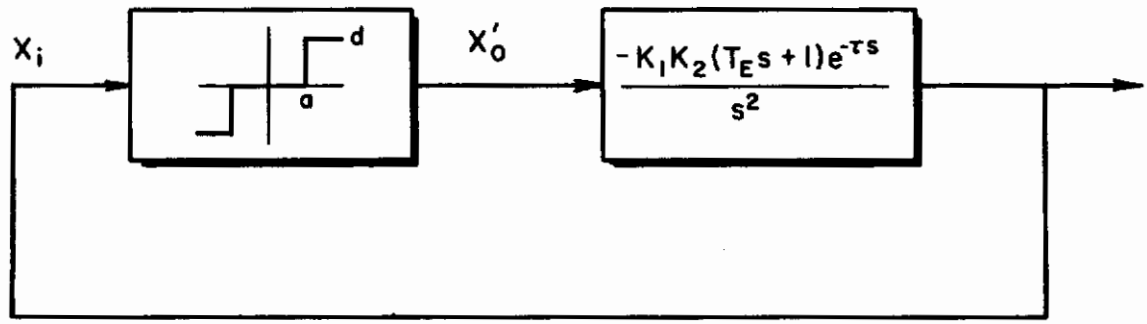

Figure B-1. Satellite Attitude Control System

Assume for the two harmonic case:

$$\psi(t) \doteq x_1 = c_1 \sin \omega t + c_3 \sin (3\omega t + \psi_3) \qquad \text{(B-1)}$$

$$x_0' \doteq x_0 \doteq y(t) \qquad \text{(B-2)}$$

$$x_0 = B_1 \sin \omega t + A_1 \cos \omega t + B_3 \sin 3\omega t + A_3 \cos 3\omega t \qquad \text{(B-3)}$$

*Developed by Robert L. Stapleford for the express purpose of resolving the apparent paradox encountered in applying the generalized periodic input describing function to the satellite attitude control problem.

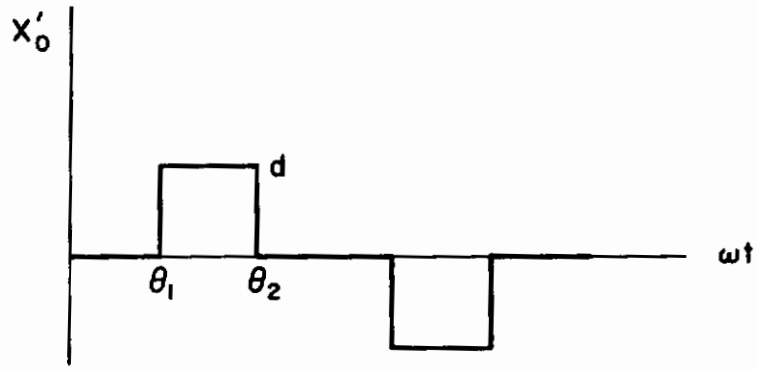

Figure B-2. Output of Nonlinear Element

Solution for the two harmonic case:

1. Estimate θ_1 and θ_2

2. Compute B_1 and A_1

$$B_1 = \frac{2d}{\pi} (\cos \theta_1 - \cos \theta_2) \tag{B-4}$$

$$A_1 = \frac{2d}{\pi} (\sin \theta_2 - \sin \theta_1) \tag{B-5}$$

3. Solve for ω to balance phase of 1st harmonic

$$0 = \tan^{-1} \frac{A_1}{B_1} + \tan^{-1} \omega T_E - \omega\tau \tag{B-6}$$

Use Newton's method to iterate for ω, i.e. $h(\omega) = 0$

$$h = \tan^{-1} \frac{A_1}{B_1} + \tan^{-1} \omega T_E - \omega\tau \tag{B-7}$$

$$\frac{dh}{d\omega} = \frac{T_E}{1 + \omega^2 T_E^2} - \tau \tag{B-8}$$

$$\omega_{i+1} = \omega_i - \frac{\tan^{-1} \frac{A_1}{B_1} + \tan^{-1} \omega_i T_E - \omega_i \tau}{\frac{T_E}{1 + \omega_i^2 T_E^2} - \tau} \tag{B-9}$$

with $\omega_0 = 0$

4. Solve for c_1 to balance amplitude of 1st harmonic

$$c_1 = \frac{K_1 K_2}{\omega^2} \sqrt{(B_1^2 + A_1^2)\ (1 + \omega^2 T_E^2)} \tag{B-10}$$

5. Compute B_3 and A_3

$$B_3 = \frac{2d}{3\pi} (\cos 3\theta_1 - \cos 3\theta_2)$$

$$A_3 = \frac{2d}{3\pi} (\sin 3\theta_2 - \sin 3\theta_1) \tag{B-11}$$

6. Solve for c_3 to balance amplitude of 3rd harmonic

$$c_3 = \frac{K_1 K_2}{9\omega^2} \sqrt{(B_3^2 + A_3^2)\ (1 + 9\omega^2 T_E^2)} \tag{B-12}$$

7. Solve for ψ_3 to balance phase of 3rd harmonic

$$\psi_3 = \tan^{-1} \frac{A_3}{B_3} + \tan^{-1} 3\omega T_E - 3\omega\tau \tag{B-13}$$

8. Compute errors in magnitude of x_i at θ_1 and θ_2

$$-\epsilon_1 = a - c_1 \sin \theta_1 - c_3 \sin (3\theta_1 + \psi_3) \tag{B-14}$$

$$-\epsilon_2 = a - c_1 \sin \theta_2 - c_3 \sin (3\theta_2 + \psi_3) \tag{B-15}$$

9. Iterate θ_1 and θ_2 until ϵ_1 and $\epsilon_2 = 0$ or at least $\left|\frac{\epsilon_i}{a}\right| \ll 1$, $i = 1, 2$

Notes:

a. Include 2π resolution in $\tan^{-1}$

b. A_1 should always be negative or $\sin \theta_1 > \sin \theta_2$, or

$$\left|\frac{\pi}{2} - \theta_1\right| < \left|\frac{\pi}{2} - \theta_2\right| \tag{B-16}$$

to obtain solution frequencies which are less than the frequency for which

$$\angle \frac{- K_1 K_2 \left(T_E j\omega + 1\right) e^{-j\omega\tau}}{\omega^2} = - \pi,$$

but greater than zero.

Additional harmonics are treated in precisely the same manner as was the third harmonic. The derivatives which follow were calculated for the n^{th} harmonic

Derivatives

$$\frac{\partial B_n}{\partial \theta_1} = - \frac{2d}{\pi} \sin n\theta_1 \qquad \frac{\partial B_n}{\partial \theta_2} = \frac{2d}{\pi} \sin n\theta_2 \qquad \text{(B-17, 18)}$$

$$\frac{\partial A_n}{\partial \theta_1} = - \frac{2d}{\pi} \cos n\theta_1 \qquad \frac{\partial A_n}{\partial \theta_2} = \frac{2d}{\pi} \cos n\theta_2 \qquad \text{(B-19, 20)}$$

$$\frac{\partial \omega}{\partial \theta_i} = \frac{A_1 \dfrac{\partial B_1}{\partial \theta_i} - B_1 \dfrac{\partial A_1}{\partial \theta_i}}{\left(B_1^2 + A_1^2\right)\left(\dfrac{T_E}{1 + \omega^2 T_E^2} - \tau\right)} \qquad \text{(B-21)}$$

$$\frac{\partial c_n}{\partial \theta_i} = n c_n \left[\frac{- \left(2 + n^2 \omega^2 T_E^2\right)}{n\omega \left(1 + n^2 \omega^2 T_E^2\right)} \frac{\partial \omega}{\partial \theta_i} + \frac{B_1 \dfrac{\partial B_1}{\partial \theta_i} + A_1 \dfrac{\partial A_1}{\partial \theta_i}}{B_1^2 + A_1^2} \right] \qquad \text{(B-22)}$$

$$\frac{\partial \psi_n}{\partial \theta_i} = \frac{B_n \dfrac{\partial A_n}{\partial \theta_i} - A_n \dfrac{\partial B_n}{\partial \theta_i}}{B_n^2 + A_n^2} + n \left(\frac{T_E}{1 + n^2 \omega^2 T_E^2} - \tau \right) \frac{\partial \omega}{\partial \theta_i} \qquad \text{(B-23)}$$

$$\frac{\partial \epsilon_i}{\partial \theta_j} = \frac{\partial c_1}{\partial \theta_j} \sin \theta_i + \delta_{ij} c_1 \cos \theta_i \qquad \text{(B-24)}$$

$$+ \sum_n \left[\frac{\partial c_n}{\partial \theta_j} \sin (n\theta_i + \psi_n) + c_n \left(n\delta_{ij} + \frac{\partial \psi_n}{\partial \theta_j} \right) \cos (n\theta_1 + \psi_n) \right]$$

Iteration Increments

$$\begin{bmatrix} \dfrac{\partial \epsilon_1}{\partial \theta_1} & \dfrac{\partial \epsilon_1}{\partial \theta_2} \\ \dfrac{\partial \epsilon_2}{\partial \theta_1} & \dfrac{\partial \epsilon_2}{\partial \theta_2} \end{bmatrix} \begin{Bmatrix} \Delta\theta_1 \\ \Delta\theta_2 \end{Bmatrix} = - \begin{Bmatrix} \epsilon_1 \\ \epsilon_2 \end{Bmatrix} \qquad \text{(B-25)}$$

$$\Delta\theta_1 = \frac{\epsilon_2 \dfrac{\partial \epsilon_1}{\partial \theta_2} - \epsilon_1 \dfrac{\partial \epsilon_2}{\partial \theta_2}}{\dfrac{\partial \epsilon_1}{\partial \theta_1} \dfrac{\partial \epsilon_2}{\partial \theta_2} - \dfrac{\partial \epsilon_1}{\partial \theta_2} \dfrac{\partial \epsilon_2}{\partial \theta_1}} \qquad \text{(B-26)}$$

$$\Delta\theta_2 = \frac{\epsilon_1 \dfrac{\partial \epsilon_2}{\partial \theta_1} - \epsilon_2 \dfrac{\partial \epsilon_1}{\partial \theta_1}}{\dfrac{\partial \epsilon_1}{\partial \theta_1} \dfrac{\partial \epsilon_2}{\partial \theta_2} - \dfrac{\partial \epsilon_1}{\partial \theta_2} \dfrac{\partial \epsilon_2}{\partial \theta_1}} \qquad \text{(B-27)}$$

APPENDIX C

RESULTS OF SATELLITE ATTITUDE CONTROL PROBLEM ANALYSES

The results of analyzing the satellite attitude control system shown in Figure C-1 by four methods are summarized in this Appendix. The phase plane, rate diagram, nonsinusoidal describing function and sinusoidal input describing function are the four methods used. Of these, the first two methods yield exact results, and the last two methods yield approximate results for this problem.

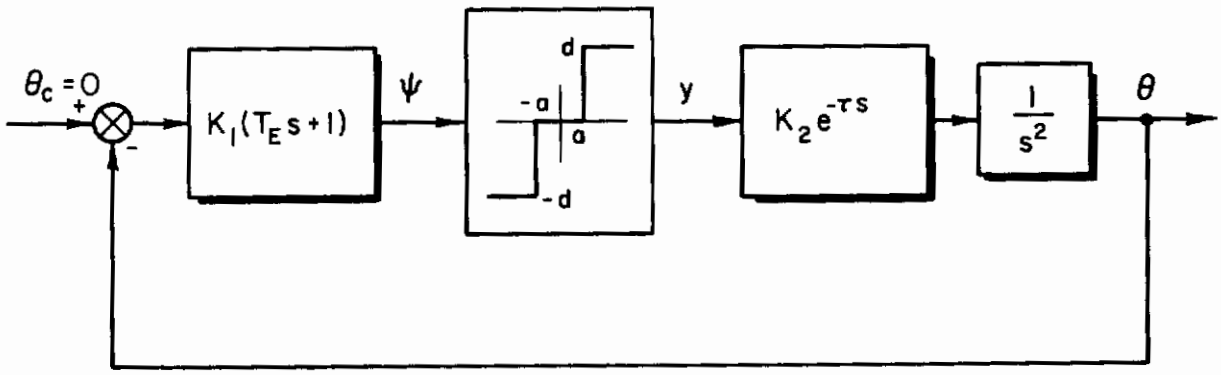

Figure C-1. Single-Axis Attitude Control System for a Satellite

Phase Plane Analysis

When we analyze this problem for the existence of a limit cycle by means of the phase plane method, for $\tau = 0$ no limit cycle exists, for values of τ less than T_E and $K_1K_2 < \frac{4a}{\tau d(2T_E-\tau)}$ a limit cycle exists, and for values of τ greater than T_E the system is unstable. (See pages 128-133 of Ref. 16.) The phase plane method of analysis yields the exact answers to this problem. The phase plane diagram for the system of Figure C-1 with deadtime is illustrated in Figure C-2.

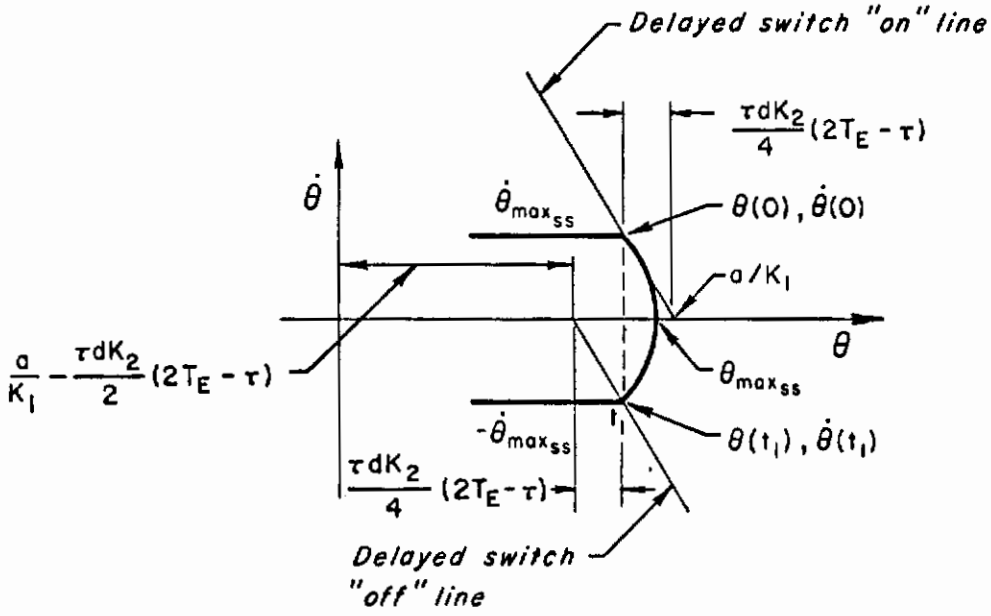

Figure C-2. Phase Plane Diagram for Satellite Attitude Control Limit Cycle

Expressions for the limit cycle pulse width, period, maximum attitude rate and maximum attitude excursion are:

$$\Delta t = \tau \left[\frac{1-\tau/2T_E}{1-\tau/T_E}\right] \tag{C-1}$$

$$T = 2\tau \left[\frac{1-\tau/2T_E}{1-\tau/T_E}\right] + 4(T_E-\tau) \left[\frac{4a}{K_1 \tau dK_2 (2T_E-\tau)} - 1\right] \tag{C-2}$$

$$\dot{\theta}_{max_{ss}} = \frac{\tau dK_2}{2} \left[\frac{1-\tau/2T_E}{1-\tau/T_E}\right] \tag{C-3}$$

$$\theta_{max_{ss}} = \frac{a}{K_1} + \frac{\tau dK_2}{4} (2T_E-\tau) \left[\frac{\tau(2T_E-\tau)}{8(T_E-\tau)^2} - 1\right] \tag{C-4}$$

Rate Diagram Analysis

Patapoff's rate diagram method (Ref. 17) essentially involves a graphical solution for the on-time of an off-on controller which would be necessary to sustain the oscillation. The fundamental assumption of the rate diagram method is that transient behavior of the input to the nonlinearity dies out between torque pulses. When $G(s) = K_1K_2\ e^{-\tau s}\ (T_E\ s + 1)/s^2$, as in this satellite attitude control example, the assumption is satisfied identically. It is not always necessary to construct the rate diagram itself. In many cases, the conditions for the existence of a limit cycle can be displayed as the result of an algebraic treatment. For the situation of Figures C-1 and C-2, the (unknown) output velocity, $\dot{\theta}_o$, at the beginning of a torque pulse can be expressed in terms of the time duration of the pulse, t_1, before the torque is shut off. This is accomplished by obtaining the time history of the input to the nonlinearity starting at the crossing of a delayed switch "on" line in the phase plane. (Vide Figure C-2.) For the portion of the phase plane shown, the torque pulse is negative and of magnitude d. Initial conditions on the input to the nonlinearity, ψ, are:

$$\begin{aligned} \psi(0) &= -\ K_1(\theta(0) + T_E\dot{\theta}(0)) = -\ a \\ \dot{\psi}(0) &= -\ K_1\dot{\theta}(0) \end{aligned} \qquad \text{(C-5)}$$

The Laplace transform of the input to the nonlinearity during the torque pulse is:

$$\Psi(s) = \frac{dK_1K_2e^{-\tau s}(T_E\ s + 1)}{s^3} - \frac{a}{s} - \frac{K_1\dot{\theta}(0)}{s^2} \qquad \text{(C-6)}$$

When $\psi(t)$ is next again equal to the switching value, $(-\ a)$, at time, $t = t_1$, we may solve for $\dot{\theta}(0)$.

$$\dot{\theta}(0) = \frac{dK_2}{t_1}\ \mathcal{L}^{-1}\left[\frac{e^{-\tau s}(T_E\ s + 1)}{s^3}\right] \qquad \text{(C-7)}$$

Then:

$$\dot{\theta}(0) = \frac{dK_2}{t_1}\left[T_E(t_1 - \tau) + \frac{1}{2}\ (t_1 - \tau)^2\right] \qquad \text{(C-8)}$$

By conservation of momentum:

$$\dot{\theta}(t_1) = \dot{\theta}(0) - dK_2 t_1 \qquad (C\text{-}9)$$

Inspection of Figure C-2 shows that the condition for a limit cycle is:

$$\dot{\theta}(t_1) = -\dot{\theta}(0) \qquad (C\text{-}10)$$

Combining Eqs. C-8, C-9, C-10 enables us to solve for the pulse width, $t_1 = \Delta t$, and maximum attitude rate, $\dot{\theta}(0) = \dot{\theta}_{max_{ss}}$.

$$\Delta t = \tau \left[\frac{1 - \tau/2T_E}{1 - \tau/T_E}\right] \qquad (C\text{-}11)$$

$$\dot{\theta}_{max_{ss}} = \frac{\tau dK_2}{2} \left[\frac{1 - \tau/2T_E}{1 - \tau/T_E}\right] \qquad (C\text{-}12)$$

The period is obtained by computing the ratio of $4\theta(0)$ to $\theta_{max_{ss}}$ and adding $2\Delta t$. All these relations are, of course, identical to the phase plane results because there are no transient producing elements in our choice for $G(s)$, and so the rate diagram method, in this case, is exact.

Nonsinusoidal Describing Function Analysis

Ordinarily, we might be tempted to use the first approximation sinusoidal input describing function to represent the nonlinearity. However, let us observe that since the output of the nonlinearity is a train of narrow alternately positive and negative pulses, the representation of this function by its first Fourier component does seem to stretch the truth of the matter a bit (Vide Fig. C-3c). This suggests that other waveform approximations be used in formulating a describing function for the nonlinearity.

In the present instance we know from examination of the phase plane diagram (Fig. C-2) that if the limit cycle exists at all, the attitude waveform will be very closely approximated by a triangular wave.

The Fourier series for the triangular wave with a peak amplitude, A, illustrated in Figure C-3a is

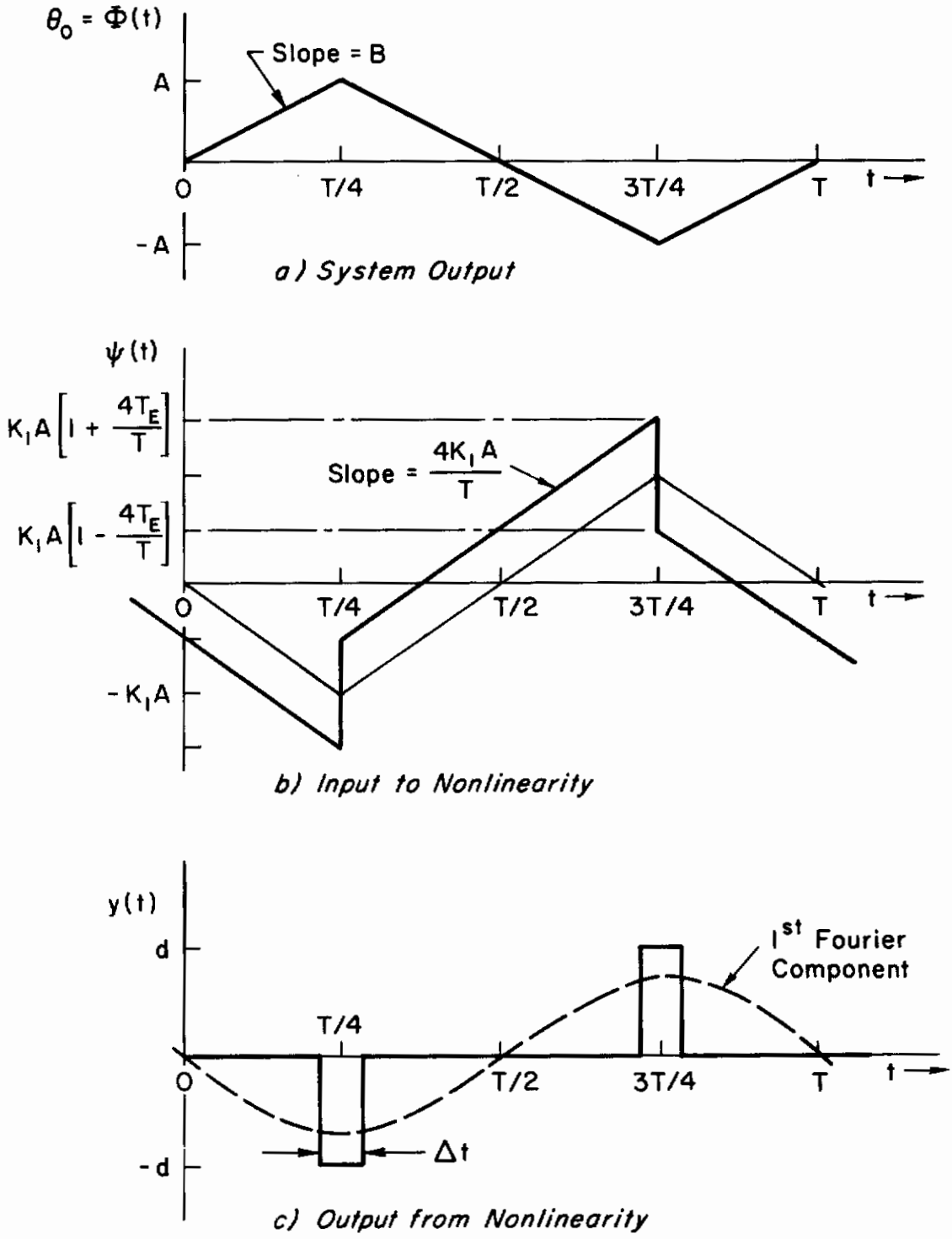

Figure C-3. Approximate Waveforms in Satellite Attitude Control System Output

$$\Phi(t) = \frac{8A}{\pi^2} \sum_{n=1}^{\infty} \frac{(-1)^{n+1}}{(2n-1)^2} \sin \frac{2\pi(2n-1)t}{T} \qquad (C-13)$$

and the Fourier series for the square wave which is the first time derivative of the triangular wave is:

$$\dot{\Phi}(t) = \frac{16A}{\pi T} \sum_{n=1}^{\infty} \frac{(-1)^{n+1}}{(2n-1)} \cos \frac{2\pi(2n-1)t}{T} \qquad (C-14)$$

For an assumed triangular wave output of the system of Figure C-1, the output of the equalizer and input to the nonlinearity, $\psi(t)$, is the sum of these two waves weighted by the appropriate gains of the system. The input to the nonlinearity is shown in Figure C-3b and is expressed in Fourier series by Eq. C-15.

$$\psi(t) = -K_1 \left[\Phi(t) + T_E \dot{\Phi}(t) \right]$$

$$\psi(t) = -K_1 \left[\frac{8A}{\pi^2} \sum_{n=1}^{\infty} \frac{(-1)^{n+1}}{(2n-1)^2} \sin \frac{2\pi(2n-1)t}{T} \right. \qquad (C-15)$$

$$\left. + \frac{16AT_E}{\pi T} \sum_{n=1}^{\infty} \frac{(-1)^{n+1}}{(2n-1)} \cos \frac{2\pi(2n-1)t}{T} \right]$$

As an approximation, let us assume that the output of the nonlinearity is a train of very narrow, alternately positive and negative pulses, centered at the points in time, T/4 and 3T/4, as shown in Figure C-3c. Then, the output of the nonlinearity is an odd function of time and $f(t) = -f(t + T/2)$, and therefore, there are no cosine terms or even harmonics in its Fourier series. Note that for the waveform given by Eq. C-15 and the nonlinearity of interest, the trailing edges of the pulses would actually occur at the T/4 and 3T/4 points in time. The supposition of a small, constant, phase shift either before or after the nonlinearity is ultimately necessary to make the waveform conform to our assumption.

The coefficients of the Fourier series of the pulse train are

$$B_m = \frac{2}{T}\int_0^T f(t)\,\sin\frac{2\pi mt}{T}\,dt$$

$$= \frac{-4d}{T}\int_{\frac{T}{4}-\frac{\Delta t}{2}}^{\frac{T}{4}+\frac{\Delta t}{2}} \sin\frac{2\pi mt}{T}\,dt$$

$$= \frac{2d}{\pi m}\cos\frac{2\pi mt}{T}\Bigg|_{\frac{T}{4}-\frac{\Delta t}{2}}^{\frac{T}{4}+\frac{\Delta t}{2}}$$

$$B_{(2n-1)} = \frac{4d(-1)^n}{\pi(2n-1)}\sin\frac{\pi(2n-1)\Delta t}{T} \doteq \frac{4d\Delta t(-1)^n}{T} \qquad (C\text{-}16)$$

where $m = 2n-1$, and $n = 1, 2, \ldots$. The final approximation in Eq. C-16 becomes inaccurate at high frequencies and/or for $\Delta t/T$ which are not very much less than 1/2.

From Figure C-4, the width of the pulse, Δt, can be expressed in terms of the slope of the input wave and the difference between the peak value of the input wave and the threshold of the nonlinearity. The slope of the input wave is $(-K_1)$ times the first time derivative of the triangular wave, a square wave. The amplitude, B, of this square wave may be expressed in terms of the amplitude and period of the triangular wave by considering the geometrical properties of the waveforms. That is, the area under the positive half cycle of the attitude rate waveform, $\dot{\theta}$, must equal the peak to peak amplitude, (2A), of the attitude waveform, θ.

$$2A = \frac{BT}{2}$$

$$B = \frac{4A}{T} \qquad (C\text{-}17)$$

The slope of the input wave is therefore $\pm 4K_1A/T$, as indicated in Figure C-4, and for thresholds between $K_1A\left[1 + 4T_E/T\right]$ and $K_1A\left[1 - 4T_E/T\right]$ the width of the pulses is given by Eq. C-18.

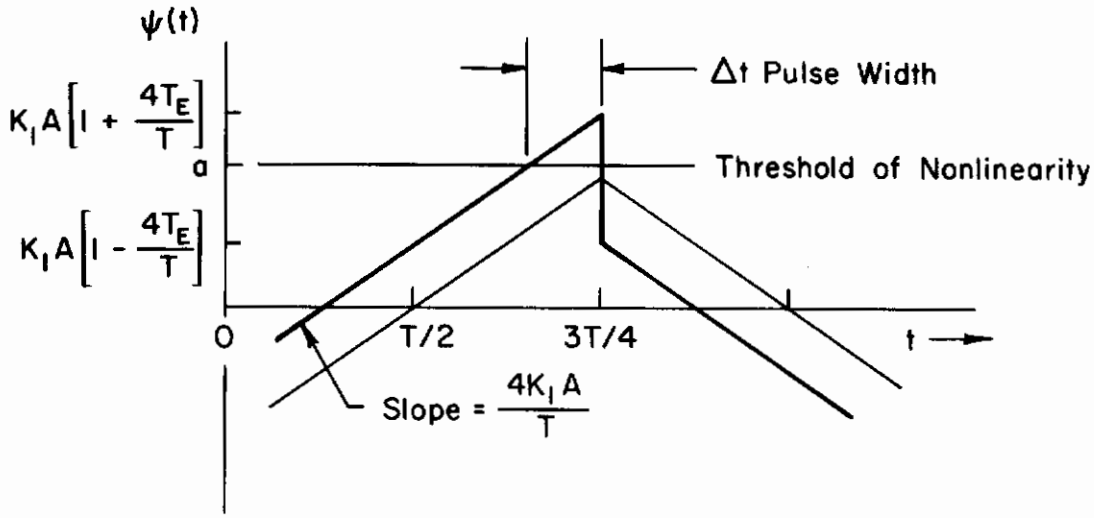

Figure C-4. Geometrical Properties of the Input Wave Used in the Calculation of Pulse Width

$$\Delta t = \frac{K_1 A\left[1 + \frac{4T_E}{T}\right] - a}{\frac{4K_1 A}{T}} \qquad (C\text{-}18)$$

$$\Delta t = \frac{T}{4}\left[1 + \frac{4T_E}{T} - \frac{a}{K_1 A}\right] \leq \frac{T}{2}$$

The inequality restriction arises from the fact that the pulse width cannot exceed one half of the limit cycle period.

The output of the nonlinearity then, expressed as a Fourier series, is:

$$y(t) \doteq d\left[1 + \frac{4T_E}{T} - \frac{a}{K_1 A}\right] \sum_{n=1}^{\infty} (-1)^n \sin \frac{2\pi(2n-1)t}{T} \qquad (C\text{-}19)$$

Now let us introduce a phase lead into the Fourier series expression for y(t), Eq. C-19, to correct for our assumption that the pulses are centered at the quarter period points. The phase lead, α, needed in y(t) to cause the trailing edges of the pulses to occur at T/4 and 3T/4 is:

$$\alpha_{(2n-1)} = (2n-1)\frac{\Delta t}{T}\pi = \frac{\pi(2n-1)}{4}\left[1 + \frac{4T_E}{T} - \frac{a}{K_1 A}\right] \qquad (C\text{-}20)$$

We can now combine the additive series of Eq. C-15 so as to express the sum as a series of sine terms with phase angles.

$$\sum_{n=1}^{\infty} \left[h_{(2n-1)} \cos \varphi_{(2n-1)} \sin \frac{2\pi(2n-1)t}{T} + h_{(2n-1)} \sin \varphi_{(2n-1)} \cos \frac{2\pi(2n-1)t}{T} \right] = \sum_{n=1}^{\infty} h_{(2n-1)} \sin \left[\frac{2\pi(2n-1)t}{T} + \varphi_{(2n-1)} \right] \tag{C-21}$$

For the $(2n-1)^{th}$ harmonic term:

$$h_{(2n-1)} \cos \varphi_{(2n-1)} = \frac{8K_1 A(-1)^n}{\pi^2(2n-1)^2} \tag{C-22}$$

$$h_{(2n-1)} \sin \varphi_{(2n-1)} = \frac{16K_1 AT_E(-1)^n}{\pi(2n-1)T} \tag{C-23}$$

Summing the squares of Eq. C-21 and Eq. C-22, and taking the square root yields $h_{(2n-1)}$.

$$h_{(2n-1)} = \frac{8K_1 A}{\pi^2(2n-1)^2} \sqrt{1 + 4\pi^2(2n-1)^2 T_E^2/T^2} \tag{C-24}$$

The phase angles, $\varphi_{(2n-1)}$, are given by:

$$\varphi_{(2n-1)} = \sin^{-1} \frac{h_{(2n-1)} \sin \varphi_{(2n-1)}}{h_{(2n-1)}} \tag{C-25}$$

$$\varphi_{(2n-1)} = \sin^{-1} \frac{(-1)^n 2\pi(2n-1)T_E/T}{\sqrt{1 + 4\pi^2(2n-1)^2 T_E^2/T^2}} \tag{C-26}$$

Then, using Eqs. C-19, C-20, C-24 and C-26, the describing function for each harmonic of the input wave to the nonlinearity is approximately:

$$\left|N_{(2n-1)}\right| = \left| \frac{\pi^2(2n-1)^2 d \left[1 + \frac{4T_E}{T} - \frac{a}{K_1 A}\right]}{8K_1 A\sqrt{1 + 4\pi^2(2n-1)^2 T_E^2/T^2}} \right| \qquad \text{(C-27)}$$

$$\angle N_{(2n-1)} = \frac{\pi(2n-1)}{4}\left[1 + \frac{4T_E}{T} - \frac{a}{K_1 A}\right] - \sin^{-1} \frac{2\pi(2n-1)T_E/T}{\sqrt{1 + 4\pi^2(2n-1)^2 T_E^2/T^2}} \qquad \text{(C-28)}$$

It is readily appreciated in connection with Eq. C-27 that a lower limit for A is a normalized value of the threshold, $a/K_1\left[1 + 4T_E/T\right]$ so that the gains of the describing functions may be large, but not infinite.

We shall now proceed to solve algebraically for the intersections of $-K_1K_2(1 + j\omega T_E)e^{-j\omega\tau}/\omega^2$ and $-1/N_{(2n-1)}$ by equating the phase angles and amplitude ratios of these functions, then solving the two resulting simultaneous equations for the amplitude, A, and the period, T, of the limit cycle.

Equating the amplitude ratios, and noting that

$$\omega_{(2n-1)} = \frac{2\pi(2n-1)}{T} \qquad \text{(C-29)}$$

we find:

$$\left| \frac{-K_1K_2(1 + jT_E\omega_{(2n-1)})\, e^{-j\omega_{(2n-1)}\tau}}{\omega^2_{(2n-1)}} \right| = \left| \frac{-1}{N_{(2n-1)}} \right|$$

$$\frac{K_1K_2\sqrt{1 + T_E^2\omega^2_{(2n-1)}}}{\omega^2_{(2n-1)}} = \frac{8AK_1\sqrt{1 + T_E^2\omega^2_{(2n-1)}}}{\pi^2(2n-1)^2 d\left[1 + \frac{4T_E}{T} - \frac{a}{K_1A}\right]} \qquad \text{(C-30)}$$

$$\frac{4\pi^2(2n-1)^2}{\omega^2_{(2n-1)}} = T^2 = \frac{32A}{dK_2\left[1 + \frac{4T_E}{T} - \frac{a}{K_1 A}\right]} \tag{C-31}$$

Equating the phase angles, we find:

$$\angle\left(\frac{-K_1K_2(1 + jT_E\omega_{(2n-1)})\, e^{-j\omega_{(2n-1)}\tau}}{\omega^2_{(2n-1)}}\right) = \angle\left(\frac{-1}{N_{(2n-1)}}\right) \tag{C-32}$$

$$\frac{8\tau}{T} = \frac{4\tau\omega_{(2n-1)}}{\pi(2n-1)} = \left[1 + \frac{4T_E}{T} - \frac{a}{K_1 A}\right] \tag{C-33}$$

Substituting this result into Eq. C-31 yields:

$$T = \frac{4A}{\tau dK_2} \tag{C-34}$$

Substituting Eq. C-34 into Eq. C-33 and Eq. C-18 indicates the existence of a limit cycle, and enables us to obtain approximate expressions for the interesting parameters of this limit cycle; Δt, T, $B = \dot{\theta}_{max_{ss}}$ and $A = \theta_{max_{ss}}$.

$$\Delta t \doteq 2\tau \tag{C-35}$$

$$T \doteq 4\left(2\tau + \frac{a}{K_1 \tau dK_2} - T_E\right) \tag{C-36}$$

$$\dot{\theta}_{max_{ss}} \doteq \tau dK_2 \tag{C-37}$$

$$\theta_{max_{ss}} \doteq \tau dK_2\left(2\tau + \frac{a}{K_1 \tau dK_2} - T_E\right) \tag{C-38}$$

The above results are valid when the system parameters satisfy the following inequality:

$$T_E \geq \tau \tag{C-39}$$

This restriction arises from the condition that the threshold of the nonlinearity, a, must be greater than $K_1 A\left[1 - 4T_E/T\right]$. The validity condition requiring the peak of the input wave, $K_1 A\left[1 + 4T_E/T\right]$, to exceed the threshold results in the inequality:

$$\tau > 0 \tag{C-40}$$

In Eq. C-18, it was noted that the pulse width could not exceed one half the limit cycle period. This leads to:

$$\tau \geq T_E - \frac{a}{K_1 \tau d K_2} \tag{C-41}$$

Requiring the period to be positive leads to

$$2\tau \geq T_E - \frac{a}{K_1 \tau d K_2} \tag{C-42}$$

which is compatible with Eq. C-39. Ultimate requirements for validity of this analysis are then (Eqs. C-39 through C-41):

$$T_E \geq \tau \geq T_E - \frac{a}{K_1 \tau d K_2} \tag{C-43}$$

Comparison of the results from the nonsinusoidal describing function analysis with the phase plane results shows that:

1. The limit cycle pulse width and maximum attitude rate predicted by the approximate method are large, compared to the exact results, by a factor of two for $\tau/T_E \rightarrow 0$, are equivalent for $\tau/T_E = 2/3$, and are small by a very large factor for $\tau/T_E \rightarrow 1$.
2. The period tends to reflect the trends of the pulse width, in general. For $\tau/T_E = 2/3$, the period is correctly given by Eq. C-36.
3. Phase plane and nonsinusoidal describing function results agree, as they should, in the limit as the torque pulse approaches being an impulse. These results represent something less than we might have hoped for.

First Approximation Sinusoidal Input Describing Function Analysis

By far the most simple method of predicting a possible limit cycle is with the first approximation sinusoidal describing function technique (Ref. 1). An isolated element sinusoidal describing function for the off-on controller with deadzone is:

$$N = 0,\ A < a\ ;\ N = \frac{4d}{\pi A}\sqrt{1 - \left(\frac{a}{A}\right)^2}\ ,\ A \geq a \qquad (C\text{-}44)$$

where the symbols are defined in Figure C-5.

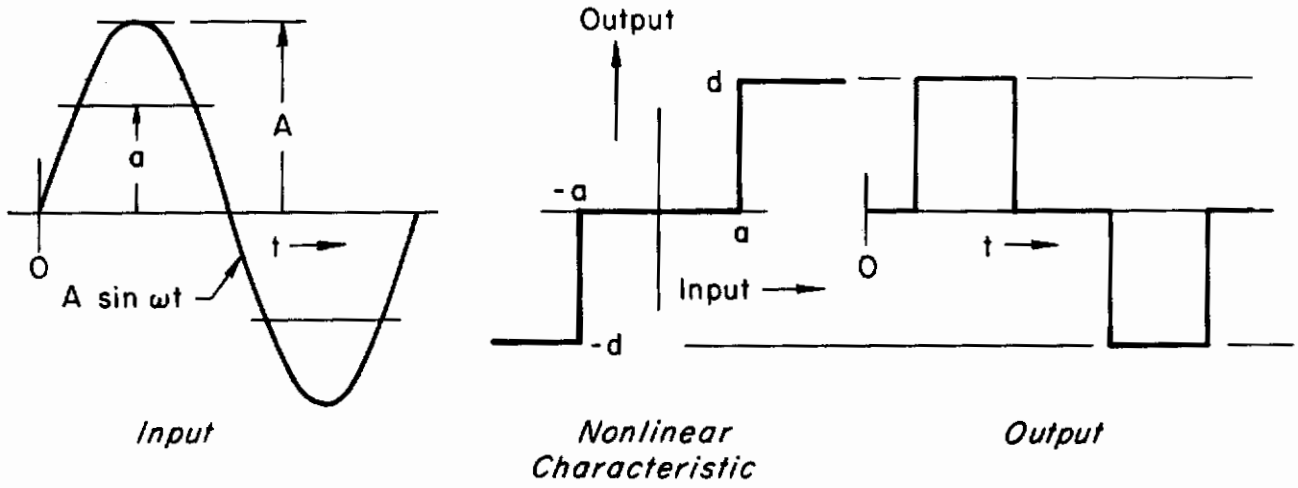

Figure C-5. Input–Output Relationship for the Off-On Nonlinearity

When we apply the first approximation sinusoidal input describing function method to this problem, the results obtained disagree with the results from the phase plane analysis. In particular, if we plot the negative inverse describing function with the frequency response function for the linear elements of the control loop on the gain-phase plane as shown below, we find that for reasonable (low) values of linear element gain, K_1K_2, the curves do not intersect, but are tangent at zero frequency for all positive values of τ.

By reasonable, let us mean those values which satisfy

$$K_1 K_2 < \frac{\pi a}{2d} \frac{\omega^{*2}}{\sqrt{1 + T_E^2 \omega^{*2}}} \qquad \text{(C-45)}$$

where ω^* are the non-zero solutions of:

$$0 \leq \omega\tau = \tan^{-1} \omega T_E \leq \frac{\pi}{2} \qquad \text{(C-46)}$$

This condition indicates those values of the gain, $K_1 K_2$, for which an intersection of the $-1/N$ locus with the frequency response is excluded in the satellite attitude control problem.

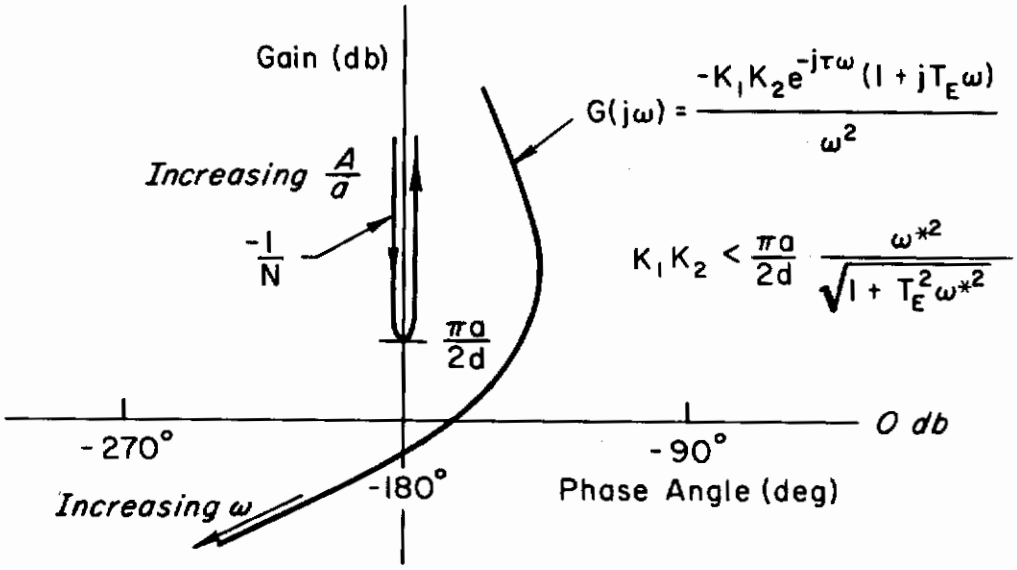

Figure C-6. First Approximation Sinusoidal Describing Function Analysis — Satellite Attitude Control

The situation illustrated in Figure C-6, however, is one in which the analyst has learned to be very cautious. The curves do not intersect, it is true, but they are tangent to each other at zero frequency and approach one another and then diverge at medium frequencies. Any time the curves intersect at a small angle, are tangent, or approach each other and then diverge; the indicated results must be treated with suspicion. A plausible explanation for the failure of the first approximation sinusoidal input describing function to

yield decisive results is that the higher harmonics of the limit cycle waveform are of crucial importance in these cases. In fact, if a small phase lag in the describing function for the fundamental is neglected in the satellite attitude control problem, it is obvious that the results would be significantly different. Presuming that a phase lag has been neglected as a result of using the first approximation sinusoidal input describing function, inclusion of the lag would influence the results in a manner that would bring them into qualitative agreement with the limit cycle predictions obtained from the phase plane analysis which we know to be exact.

UNCLASSIFIED
Security Classification

DOCUMENT CONTROL DATA - R&D
(Security classification of title, body of abstract and indexing annotation must be entered when the overall report is classified)

1. ORIGINATING ACTIVITY (Corporate author)	2a. REPORT SECURITY CLASSIFICATION
Systems Technology, Inc. Hawthorne, California	Unclassified
	2b. GROUP

3. REPORT TITLE

INVESTIGATIONS OF DESCRIBING FUNCTION TECHNIQUE

4. DESCRIPTIVE NOTES (Type of report and inclusive dates)

15 Jan 64 - Nov 64.

5. AUTHOR(S) (Last name, first name, initial)

Graham, Dunstan and Hofmann, Lee Gregor.

6. REPORT DATE	7a. TOTAL NO. OF PAGES	7b. NO. OF REFS
February 1966	101	30

8a. CONTRACT OR GRANT NO.	9a. ORIGINATOR'S REPORT NUMBER(S)
AF 33(615)-1474 b. PROJECT NO. 8219 c. Task No. 821904 d.	9b. OTHER REPORT NO(S) (Any other numbers that may be assigned this report) AFFDL-TR-65-137

10. AVAILABILITY/LIMITATION NOTICES

Qualified requesters may obtain copies of this report from DDC.
Distribution of this document is unlimited.

11. SUPPLEMENTARY NOTES	12. SPONSORING MILITARY ACTIVITY
	Control Criteria Branch Flight Control Division Air Force Flight Dynamics Laboratory

13. ABSTRACT

Three problems were chosen so as to explore some of the apparent limitations of describing function technique for the analysis of nonlinear systems, and to show how the technique might be extended so as to overcome the indicated deficiencies. The problems were a) the effects of stick and valve friction in fully powered, manual aircraft control systems, b) limit cycles in satellite attitude control with off-on jets, and c) the effects of aerodynamic hysteresis in the stability derivatives of tilt-wing VTOL aircraft.

The results indicate that new describing functions can be developed as closed-loop functions provided that specific restrictions are met, that non-sinusoidal, Fourier series describing functions or a generalized periodic input describing function can be successful, but that they are extra-ordinarily difficult to apply, and that the aerodynamic nonlinearities which were considered are of small practical importance.

DD FORM 1 JAN 64 1473

UNCLASSIFIED
Security Classification

Security Classification

14. KEY WORDS	LINK A		LINK B		LINK C	
	ROLE	WT	ROLE	WT	ROLE	WT

INSTRUCTIONS

1. ORIGINATING ACTIVITY: Enter the name and address of the contractor, subcontractor, grantee, Department of Defense activity or other organization *(corporate author)* issuing the report.

2*a*. REPORT SECURITY CLASSIFICATION: Enter the overall security classification of the report. Indicate whether "Restricted Data" is included. Marking is to be in accordance with appropriate security regulations.

2*b*. GROUP: Automatic downgrading is specified in DoD Directive 5200.10 and Armed Forces Industrial Manual. Enter the group number. Also, when applicable, show that optional markings have been used for Group 3 and Group 4 as authorized.

3. REPORT TITLE: Enter the complete report title in all capital letters. Titles in all cases should be unclassified. If a meaningful title cannot be selected without classification, show title classification in all capitals in parenthesis immediately following the title.

4. DESCRIPTIVE NOTES: If appropriate, enter the type of report, e.g., interim, progress, summary, annual, or final. Give the inclusive dates when a specific reporting period is covered.

5. AUTHOR(S): Enter the name(s) of author(s) as shown on or in the report. Enter last name, first name, middle initial. If military, show rank and branch of service. The name of the principal author is an absolute minimum requirement.

6. REPORT DATE: Enter the date of the report as day, month, year, or month, year. If more than one date appears on the report, use date of publication.

7*a*. TOTAL NUMBER OF PAGES: The total page count should follow normal pagination procedures, i.e., enter the number of pages containing information.

7*b*. NUMBER OF REFERENCES: Enter the total number of references cited in the report.

8*a*. CONTRACT OR GRANT NUMBER: If appropriate, enter the applicable number of the contract or grant under which the report was written.

8*b*, 8*c*, & 8*d*. PROJECT NUMBER: Enter the appropriate military department identification, such as project number, subproject number, system numbers, task number, etc.

9*a*. ORIGINATOR'S REPORT NUMBER(S): Enter the official report number by which the document will be identified and controlled by the originating activity. This number must be unique to this report.

9*b*. OTHER REPORT NUMBER(S): If the report has been assigned any other report numbers *(either by the originator or by the sponsor)*, also enter this number(s).

10. AVAILABILITY/LIMITATION NOTICES: Enter any limitations on further dissemination of the report, other than those imposed by security classification, using standard statements such as:

(1) "Qualified requesters may obtain copies of this report from DDC."

(2) "Foreign announcement and dissemination of this report by DDC is not authorized."

(3) "U. S. Government agencies may obtain copies of this report directly from DDC. Other qualified DDC users shall request through _____."

(4) "U. S. military agencies may obtain copies of this report directly from DDC. Other qualified users shall request through _____."

(5) "All distribution of this report is controlled. Qualified DDC users shall request through _____."

If the report has been furnished to the Office of Technical Services, Department of Commerce, for sale to the public, indicate this fact and enter the price, if known.

11. SUPPLEMENTARY NOTES: Use for additional explanatory notes.

12. SPONSORING MILITARY ACTIVITY: Enter the name of the departmental project office or laboratory sponsoring *(paying for)* the research and development. Include address.

13. ABSTRACT: Enter an abstract giving a brief and factual summary of the document indicative of the report, even though it may also appear elsewhere in the body of the technical report. If additional space is required, a continuation sheet shall be attached.

It is highly desirable that the abstract of classified reports be unclassified. Each paragraph of the abstract shall end with an indication of the military security classification of the information in the paragraph, represented as *(TS), (S), (C), or (U)*

There is no limitation on the length of the abstract. However, the suggested length is from 150 to 225 words.

14. KEY WORDS: Key words are technically meaningful terms or short phrases that characterize a report and may be used as index entries for cataloging the report. Key words must be selected so that no security classification is required. Identifiers, such as equipment model designation, trade name, military project code name, geographic location, may be used as key words but will be followed by an indication of technical context. The assignment of links, rules, and weights is optional.

Security Classification